UCRL 10350

# University of California

# Ernest O. Lawrence Radiation Laboratory

TWO-WEEK LOAN COPY

*This is a Library Circulating Copy which may be borrowed for two weeks. For a personal retention copy, call Tech. Info. Division, Ext. 5545*

## BIO-ORGANIC CHEMISTRY QUARTERLY REPORT

March through May 1962

Berkeley, California

## DISCLAIMER

This document was prepared as an account of work sponsored by the United States Government. While this document is believed to contain correct information, neither the United States Government nor any agency thereof, nor the Regents of the University of California, nor any of their employees, makes any warranty, express or implied, or assumes any legal responsibility for the accuracy, completeness, or usefulness of any information, apparatus, product, or process disclosed, or represents that its use would not infringe privately owned rights. Reference herein to any specific commercial product, process, or service by its trade name, trademark, manufacturer, or otherwise, does not necessarily constitute or imply its endorsement, recommendation, or favoring by the United States Government or any agency thereof, or the Regents of the University of California. The views and opinions of authors expressed herein do not necessarily state or reflect those of the United States Government or any agency thereof or the Regents of the University of California.

Research and Development

UCRL-10350
UC-4 Chemistry
TID-4500 (17th Ed.)

UNIVERSITY OF CALIFORNIA
Lawrence Radiation Laboratory
Berkeley, California

Contract No. W-7405-eng-48

# BIO-ORGANIC CHEMISTRY QUARTERLY REPORT
March through May 1962

July 5, 1962

Printed in USA. Price $2.00. Available from the
Office of Technical Services
U. S. Department of Commerce
Washington 25, D.C.

# BIO-ORGANIC CHEMISTRY QUARTERLY REPORT
March through May 1962

## Contents

1. The Interaction Between $Mn^{IV}$ Hematoporphyrin IX and Water (Loach) . . . . . 1

2. The Gas-Liquid Partition Chromatography of the Tetra-O-Acetyl Pentopyranoses (Ferrier) . . . . . 22

3. Structure and Chromatographic Properties of Carbohydrates. The Liquid-Liquid Partition Mobilities of Aldono-γ-Lactones (Ferrier) . . . . . 25

4. Structure and Chromatographic Properties of Carbohydrates. Gas-Liquid Partition Mobilities of Pyranose Derivatives (Ferrier) . . . . . 27

5. The Trimethylsilylation of Xylose and the Nuclear Magnetic Resonance Spectra of the Major Products (Ferrier and Singleton) . . . . . 33

6. Light-Dark Transient Changes in Concentration of Sugar Phosphates Other Than Ribulose Diphosphate in Chlorella (Bassham and Kirk) . . . . . 42

7. The Preparation and Partial Characterization of a Pigment-Protein Complex from the Lamella of Higher Plant Chloroplasts (Biggins and Park) . . . . . 48

8. Chemical Composition and Substructure of Lamellae Isolated from Spinacea Oleracea Chloroplasts (Park and Pon) . . . . . 53

9. Concerning the Occurrence and the Isolation of a Fat-Soluble Fragrant Compound in Petals and Green Leaves of Magnolia Species (Lichtenthaler) . . . . . 69

10. Effect of Environmental Complexity and Training on Cholinesterase Activity, Hexokinase Activity, and Protein Content of Rat Brain (Bennett, Hebert, and Morimoto) 75

11. G Values for the Radiation Decomposition of Nucleic Acid Constituents (Ponnamperuma and Lemmon) . . . . . 81

12. Recovery of Carbon-14 from the Isotope Separator (Ion Accelerator) (Woeller and Lemmon) . . . . . 87

*Preceding Quarterly Reports: UCRL-10156, UCRL-10032.

# BIO-ORGANIC CHEMISTRY QUARTERLY REPORT

March through May 1962

M. Calvin, Director

Lawrence Radiation Laboratory and Department of Chemistry
University of California, Berkeley, California

July 5, 1962

## 1. THE INTERACTION BETWEEN $Mn^{IV}$ HEMATOPORPHYRIN IX AND WATER

Paul A. Loach

### Introduction

The existence of a stable manganese hematoporphyrin IX complex in which the manganese may be considered to be in the 4+ oxidation state is readily demonstrable in aqueous alkaline solution.[1] In the absence of an excess of a stronger oxidant, this complex, $Mn^{IV}H$,[2] acquires an electron to form $Mn^{III}H$ at a rate that depends on a number of factors. This report relates the results of experiments designed to identify the electron donor and to clarify the character of its resultant oxidized form.

### Materials

Hydrogen peroxide (30%, Baker's Analyzed; assay, 8.4 M by permanganate method) and sodium hypochlorite (commercial bleach; assay, 0.35 M) were appropriately diluted for use. Titanium sulfate, potassium ferricyanide, potassium ferrocyanide, sodium hydrosulfite, and the potassium salts of the phosphate buffers employed were used without further purification. Deionized glass-distilled water was used for all solutions. The gases (oxygen, nitrogen, and argon) were acquired from Pacific Oxygen Co., and each was analyzed and found to be 99.99% pure. Each gas had been water-pumped and dried so that no oil vapor contamination was possible.

---

[1] Paul A. Loach, in Bio-Organic Chemistry Quarterly Report, UCRL-10032, Jan. 1962, p. 45.

[2] The following abbreviations are used in this report: $Mn^{III}H$ for $Mn^{III}$hematoporphyrin IX, $Mn^{IV}H$ for $Mn^{IV}$hematoporphyrin IX, $Mn^{III}HdiMe$ for $Mn^{III}$hematoporphyrin IX dimethyl ester, $Mn^{III}H(O\text{-}O)$ for $Mn^{III}$hematoporphyrin IX to which hydrogen peroxide has been added and the pigment then purified as described under "Materials," $Mn^{III}H^{c}$ for $Mn^{III}$hematoporphyrin IX with one equivalent of oxidizing agent, allowed to return to $Mn^{III}$hematoporphyrin IX in strong white light at 15°, and then purified as described under "Materials."

$Mn^{III}H$ and $Mn^{III}HdiMe$ were prepared as described previously.[1] $Mn^{III}H(O-O)$ was prepared by adding 10 ml of $4\times10^{-3}$ M hydrogen peroxide to a 10-ml solution of $2\times10^{-3}$ M $Mn^{III}H$ at pH 13. The pigment was then purified by precipitating it from solution at pH 5 and washing the resuspended solid with water a number of times. The solid was redissolved in $10^{-2}$ M KOH and the precipitation and washings at pH 5 repeated. The residue was dissolved in a minimal amount of base (approximately $10^{-3}$ M KOH) and the resulting solution used for experiments to be described. $Mn^{III}H^c$ was prepared by the addition of one equivalent of sodium hypochlorite to $10^{-3}$ M $Mn^{III}H$ at pH 13. The resulting $Mn^{IV}H$ was converted to $Mn^{III}H^c$ at 15° with the aid of strong white light. $Mn^{III}H^c$ was then further purified by a procedure similar to that given above for $Mn^{III}H(O-O)$.

## Methods

Absorption spectra were recorded with a Cary model 14 M spectrophotometer and a Beckman IR 7 infrared spectrophotometer. A Consolidated Electrodynamics Corporation type 21-130 mass spectrometer was used for analyzing gaseous mixtures. Vessels used for studies conducted in an atmosphere such as argon, nitrogen, or oxygen were patterned after those described by Harbury.[3] Gaseous products emerging from the reaction vessel were analyzed for oxidants by passing the gas through a trap containing $FMNH_2$ (reduced flavin mononucleotide). The trap contained a 1-cm cuvette to take absorption spectra of the contents. It could be sealed off from the system at any time by closing two vacuum stopcocks. During an experiment in which such a trap was being used, the solution in the trap could be changed, without significant introduction of oxygen, by addition of a reagent through a standard taper above the solution while argon was flowing out.

Half-cell potentials for $Mn^{IV}H + e = Mn^{III}H$ were determined by measuring the ratio of $Mn^{IV}H$ to $Mn^{III}H$ spectrophotometrically in the presence of a large excess of potassium ferricyanide and potassium ferrocyanide at known concentrations. The absorption band of $Mn^{III}H$, which occurs at 770 mμ in alkaline solution, was used to determine the ratio of $Mn^{III}H$ to $Mn^{IV}H$. As can be seen in Fig. 1-1, $Mn^{IV}H$ has no absorption maximum in this region. Since this 770-mμ absorption hand is known to shift somewhat with pH,[1] the wavelength used for calculations at a given pH value was that which corresponds to the maximum absorbance at that pH. In each case, the absorbance of fresh $Mn^{III}H$ was noted before addition of solid $K_3Fe(CN)_6$ and $K_4Fe(CN)_6 \cdot 4H_2O$, and this value was assigned to 100% $Mn^{III}H$. At the termination of the experiment, sufficient sodium hypochlorite was added to a portion of the original sample to form 100% $Mn^{IV}H$, and the absorbance was noted. Contributions from different species arising through acid-base equilibria involving either $Mn^{III}H$ or $Mn^{IV}H$ were ignored in the calculation of that potential ($E_m$) at which equal concentrations of $Mn^{IV}H$ and $Mn^{III}H$ were present. Calculations were made by using

[3] H. A. Harbury, J. Biol. Chem. 225, 1009 (1957).

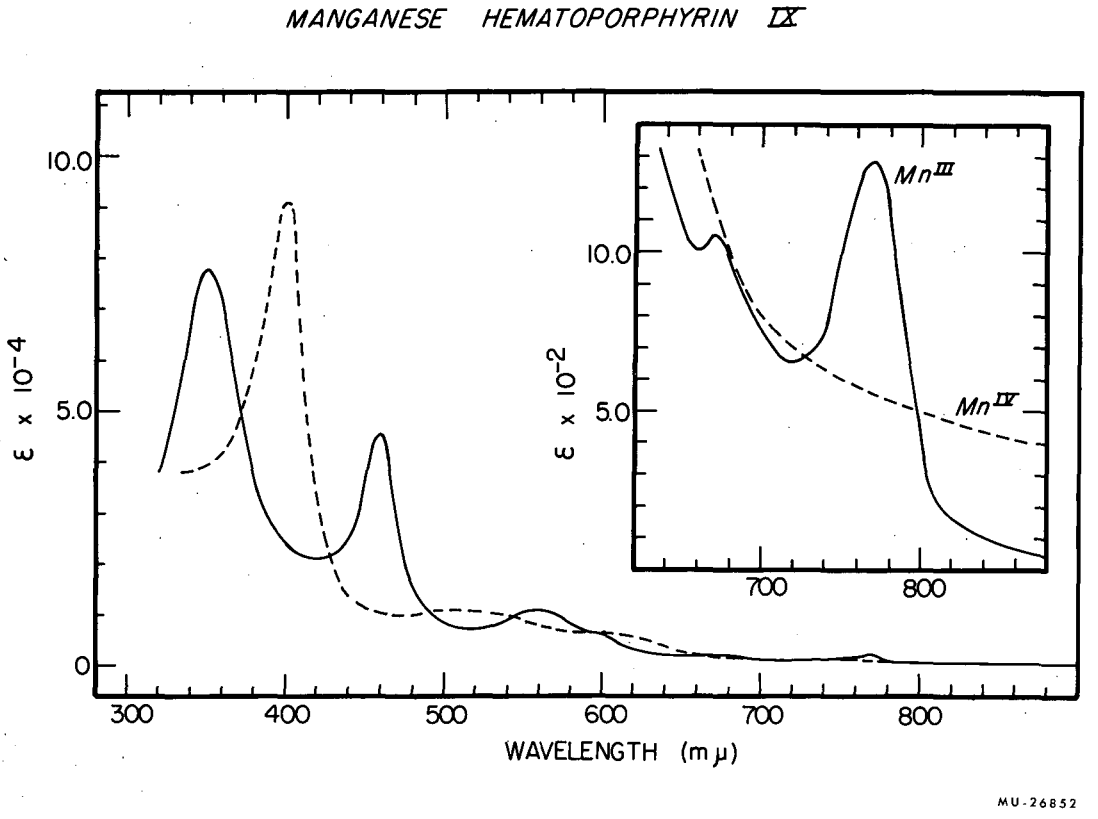


Fig. 1-1. Spectra of $Mn^{III}H$ and $Mn^{IV}H$ in alkaline solution (pH 13, with KOH; 20°).

$$E_h = E_m + \frac{RT}{nF} \ln \frac{(Ox)}{(Red)}, \qquad (1)$$

where $E_h$ = the oxidation-reduction potential at any percentage reduction, referred to the standard hydrogen electrode, $E_m$ = the oxidation-reduction potential at 50% reduction, R - the molar gas constant, T = the absolute temperature, F = the number of coulombs per faraday, n = the number of electrons transferred per equivalent, (Ox) = concentration of the oxidant, and (Red) = concentration of the reductant. For the equilibria involving $Mn^{IV}H$ and $Mn^{III}H$, n = 1, and $E_h$ was established by the known ratio of ferricyanide to ferrocyanide. An independent measurement of the $E_m$ value for this iron couple was made at the concentrations and pH values employed for each individual experiment.

Column chromatography was used in the separation of the complex $Ti^{4+}$-$H_2O_2$ in sulfuric acid from either $Mn^{III}H$ or $Mn^{III}HdiMe$. The resin used was Dowex-AG50W in the hydrogen ion form (50 to 100 mesh) and the eluting solvent was 1.5 N $H_2SO_4$. $Mn^{III}H$ and its dimethyl ester were tightly held by this column while the yellow $Ti^{4+}$-$H_2O_2$ complex easily came off with the eluting solvent.

## Results

The concentration dependence of the rate of conversion of $Mn^{IV}H$ to $Mn^{III}H$ has been studied at pH 13.0 and 20°. The rate was determined by following the increase or decrease in an appropriate absorption band between 330 and 800 mμ (Fig. 1-1). Figure 1-2 shows the results of a typical single experiment and Fig. 1-3 summarizes several such experiments. These data clearly indicate the reaction to be of first order with respect to the concentration of $Mn^{IV}H$. It has been consistently noted that fresh solutions of $Mn^{IV}H$ at first show a more rapid rate for conversion to $Mn^{III}H$, but then the rate decreases. The initial rapid rate results in conversion of 2 to 10% of $Mn^{IV}H$ to $Mn^{III}H$; the rest of the conversion of $Mn^{IV}H$ to $Mn^{III}H$ follows the kinetics indicated in Figs. 1-2 and 1-3. In all experiments reported, this initial phenomenon has been excluded from the data. Both potassium ferricyanide and sodium hypochlorite were used as oxidizing agents with $Mn^{III}H$, and no differences in the rate of reversion of $Mn^{IV}H$ to $Mn^{III}H$ were observed. Hydrogen peroxide, on the other hand, was found to be without spectrophotometric effect in the range 330 to 900 mμ when added to alkaline solutions of $Mn^{III}H$ in stoichiometric amounts or even up to a tenfold excess if the concentration of $Mn^{III}H$ is low ($10^{-5}$ M). This is of interest, since the reduction potential for the process[4, 5]

$$1/2\ H_2O + 1/2\ O_2H^- + e = 3/2\ OH^-\ ;\quad E_{m\ 13} = 0.9\ V \qquad (2)$$

falls between that of sodium hypochlorite and potassium ferricyanide:[5]

[4] The $E_m$ values given with each equation often vary with pH and subscripts are used to signify a particular value of pH; the subscript 13 as used here indicates pH 13. [W. M. Clark, Oxidation-Reduction Potentials of Organic Systems, (The Williams and Wilkins Company, Baltimore, 1960), p. 95 and 527.]

[5] Wendell M. Latimer, The Oxidation States of the Elements and Their Potentials in Aqueous Solution (Prentice-Hall, Inc., New York, 1938).

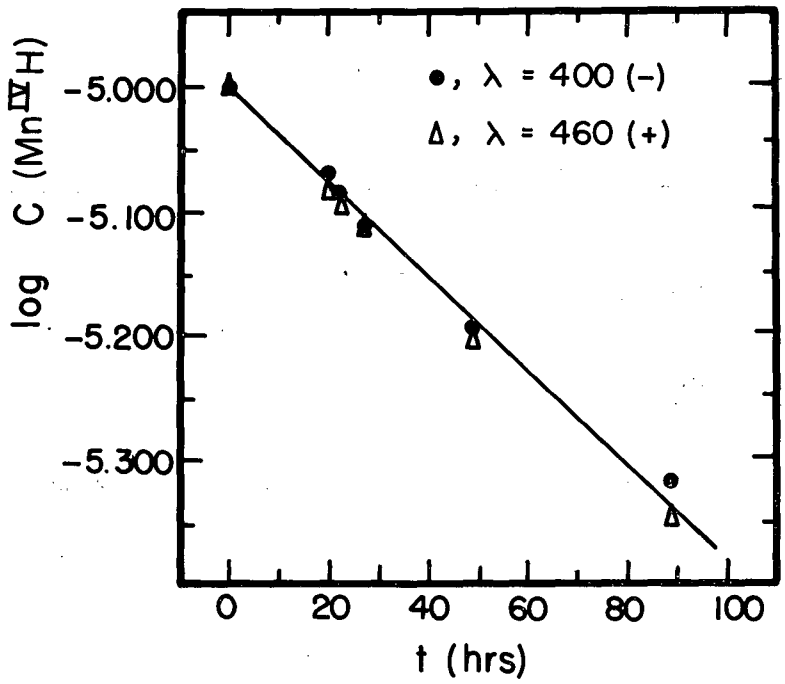


MU-26850

Fig. 1-2. Concentration dependence of the rate of conversion of $Mn^{IV}H$ to $Mn^{III}H$ at pH 13 (with KOH) and 20°. The symbols represent data calculated at the wavelengths given in the figure. Initial concentration of $Mn^{III}H$, $1 \times 10^{-5}$ M; oxidant used to form $Mn^{IV}H$: NaClO; k is the rate constant for the conversion of $Mn^{IV}H$ to $Mn^{III}H$.

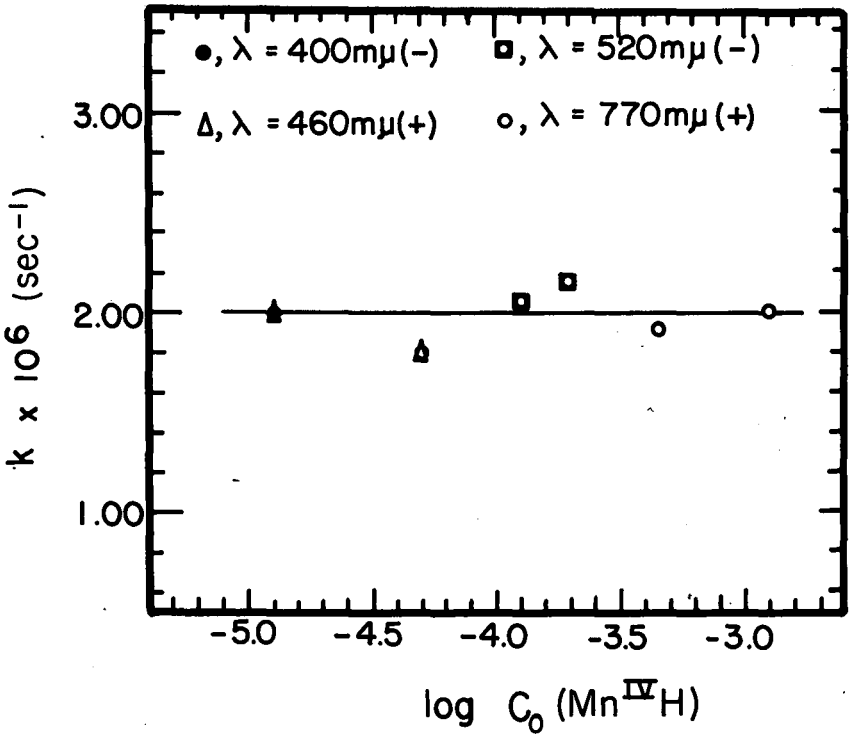


MU-26849

Fig. 1-3. Concentration dependence of the rate for conversion of $Mn^{IV}H$ to $Mn^{III}H$ at pH 13 (with KOH) and 20°. The symbols represent data calculated at the wavelengths given in the figure. $C_o$ is the initial concentration of $Mn^{IV}H$. Oxidant used to form $Mn^{IV}H$, NaClO.

$$Fe(CN)_6^{3-} + e = Fe(CN)_6^{4-}; \quad E_m = 0.4\ V, \tag{3}$$

$$1/2\ ClO^- + 1/2\ H_2O + e = 1/2\ Cl^- + OH^-;\ E_{m\ 13} = 1.0\ V. \tag{4}$$

A difference in rate of interaction between potassium ferricyanide and $Mn^{III}H$ on the one hand and potassium ferricyanide and $Mn^{III}$HdiMe on the other, has also been observed; at concentrations of $10^{-5}$ M, the reaction with the acid is slow whereas that with the ester is quite rapid. The presence of two free carboxylate groups thus appears to cause a significant change in the reactivity of the metalloporphyrin system.

The temperature dependence of the rate of conversion of $Mn^{IV}H$ to $Mn^{III}H$ at pH 13 reveals a linear Arrhenius plot over the range from $2^o$ to $58^o$. The data are given in Fig. 1-4. From Fig. 1-4, an apparent heat of activation of 20 kcal/mole and an entropy of activation of -25 eu may be calculated. This relatively large negative value for the entropy of activation would suggest that the activated state assumes a less probable or more ordered structure.

The pH dependence of the rate of conversion of $Mn^{IV}H$ to $Mn^{III}H$ is shown in Fig. 1-5. The data from each experiment reported in this figure have been subjected to a plot similar to that of Fig. 1-2, and in each case the reaction was found to be of first order with respect to the concentration of $Mn^{IV}H$. From Fig. 1-5 it is apparent that there is little or no pH dependence above pH 12, a fact that rules out direct participation of free hydrogen ion or free hydroxide ion in the reaction.

The presence of up to 0.1 M anions such as $Cl^-$, $CN^-$, $PO_4^{---}$, $H_2BO_3^-$, $CH_3COO^-$, or $HPO_4^{--}$ in the form of their sodium or potassium salts had no effect on the rate of conversion of $Mn^{IV}H$ to $Mn^{III}H$ at pH 13 and $20^o$.

In a previous study[1] it was established that the $Mn^{IV}H$ complex, above pH 10, very likely has the structure

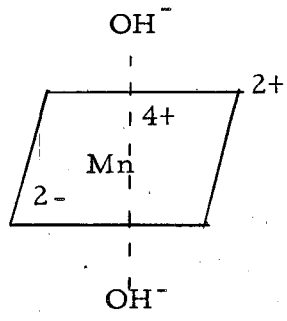


in which the rhombus represents the prophyrin ring and side chains with the exception of the two propionic acid groups (see structure given below). The 2- written inside the rhombus represents the charge distributed on the pyrrole nitrogen atoms of the porphyrin ring and the 4+ indicates the oxidation state of the manganese. The 2+ written outside the ring gives the net charge on the metal-conjugated system only, and does not include those charges on coordinated ligands in positions 5 and 6, which are written above and below the plane of the porphyrin, nor does it include those charges on the propionate side chains (Fig. 1-6).

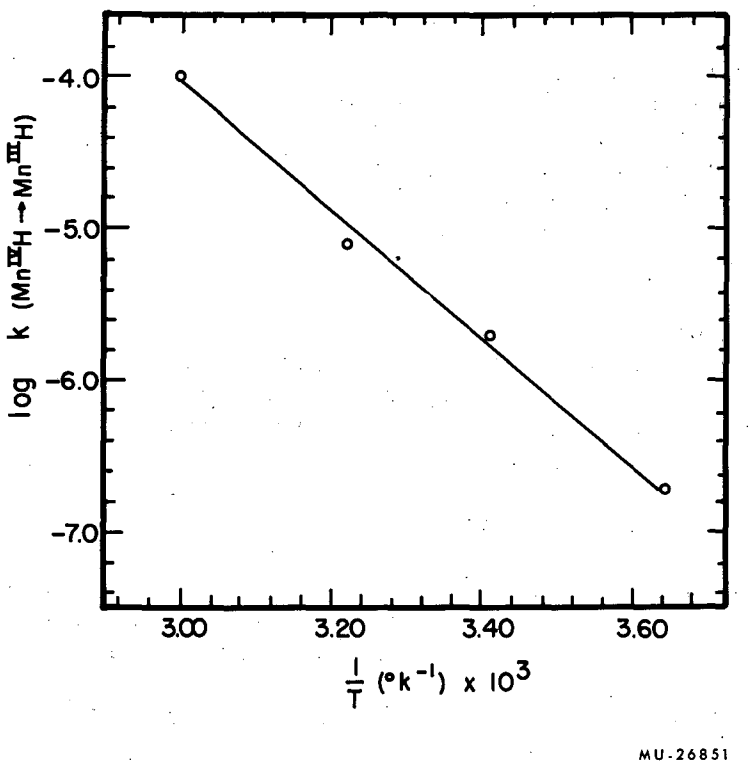


Fig. 1-4. Temperature dependence of the rate for the conversion of $Mn^{IV}H$ to $Mn^{III}H$ at pH 13 (with KOH). The experimental points were calculated from absorbance measurements at 770 mμ. $Mn^{III}H$, $1 \times 10^{-3}$ M; oxidant used, $K_3Fe(CN)_6$.

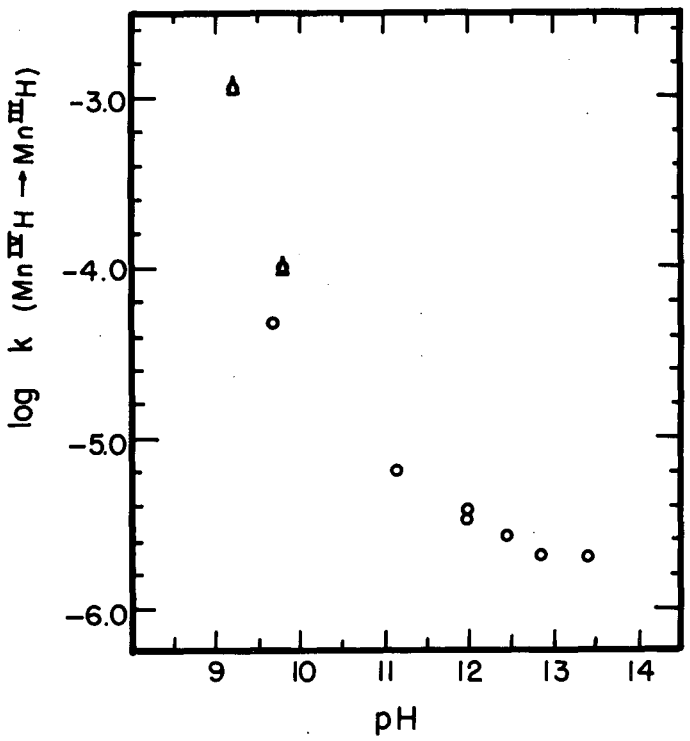


Fig. 1-5. pH dependence of the rate for the conversion of $Mn^{IV}H$ to $Mn^{III}H$ at 20°. Buffers, 0.05 M $H_3BO_3$-$KH_2BO_3$, 0.05 M $K_2HPO_4$-$K_3PO_4$; KOH present.
o, experimental points from absorbance measurements at 770 mμ; initial concentration of $Mn^{III}H$, $1 \times 10^{-3}$ M; oxidants, NaClO and $K_3Fe(CN)_6$.
Δ, experimental points from absorbance measurements at 460 mμ; initial concentration of $Mn^{III}H$, $1 \times 10^{-5}$ M.

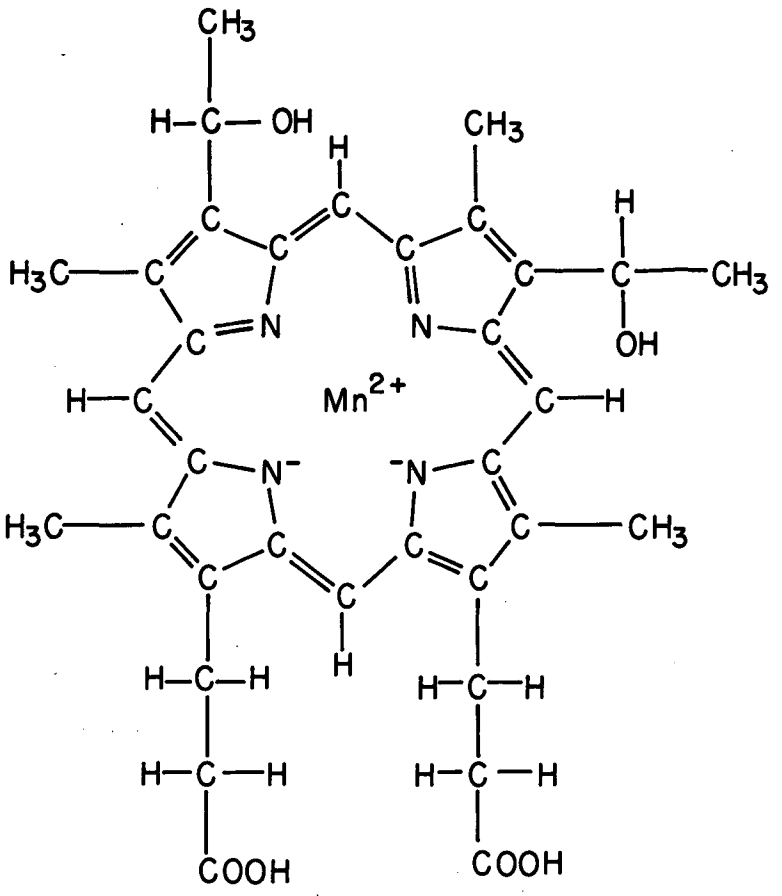


*$Mn^{II}$ HEMATOPORPHYRIN IX*

MU-26946

Fig. 1-6. $Mn^{II}$ hematoporphyrin IX.

The rate studies suggest that the first step of the conversion of $Mn^{IV}H$ to $Mn^{III}H$ may now be more fully written as a dissociation of the complex

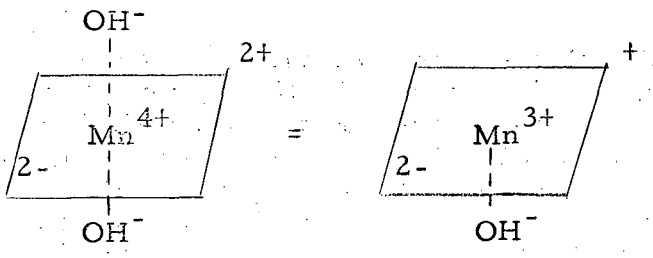


(5)

This process results in the formation of a hydroxyl radical that would quickly oxidize substrates such as the prophyrin ring, side chains of the porphyrin ring, or buffer ions (if present); dimerize to form hydrogen peroxide; or be broken down to oxygen and water. Extensive experiments with high concentrations of $Mn^{III}H$ ($10^{-2}$ M) soon revealed that this pigment is broken down by $10^{-2}$ M hydrogen peroxide to form carbon dioxide along with smaller amounts of other gaseous products. On the other hand, low pigment concentrations and high hydrogen peroxide concentrations resulted in the liberation of oxygen with little or no destruction of $Mn^{III}H$, as observed spectrophotometrically in the region 330 to 900 mμ.

## Evidence for Peroxide Formation

The possibility that hydrogen peroxide may be a stable product of the reaction indicated by Eq. (5) was tested by analyzing for it directly with a relatively specific reagent, titanium sulfate in sulfuric acid.[6, 7, 8] Attempts to sublime the presumed hydrogen peroxide from $Mn^{III}H^{c}$ or to interact $Mn^{III}H^{c}$ with the titanium reagent and separate the products on a Dowex column showed that no free hydrogen peroxide was present. Similar results were obtained with $Mn^{III}H(O\text{-}O)$. Addition of titanium reagent and separation of the products on Dowex-50 failed to reveal the presence of free hydrogen peroxide, nor could the hydrogen peroxide be sublimed from $Mn^{III}H$ even when the solution to which it was added was quickly frozen. In contrast to these results, hydrogen peroxide added to $Mn^{III}HdiMe$ at pH 7 or below was easily recovered by sublimation, or could be complexed with titanium and separated on Dowex-50. No change in absorption spectra in the region of 330 to 900 mμ is observed upon adding hydrogen peroxide to $Mn^{III}H$. Therefore, any chemical combination or interaction between $Mn^{III}H$ and hydrogen peroxide is limited to those groups that are sufficiently far removed from the resonating macrocyclic ring structure so that alteration in their chemical nature is not reflected by a change in light absorption in this region. Only the carboxylate groups of the propionic acid side chains are capable of such interaction, and the possibility of their conversion to a percarboxylic acid or a diacylperoxide is considered here.

---

[6] Klenk, Klepzig's Textil-Z. 42, 549 (1939); CA 34, 1179.

[7] I. M. Kolthoff and E. B. Sandell, Textbook of Quantitative Inorganic Analysis, Revised Ed. (Macmillan Co., New York, 1943), p. 743.

[8] C. N. Satterfield and A. H. Bennell, Anal. Chem. 27, 1174 (1955).

Involvement of carboxyl groups in oxidation processes can lead to the formation of carbon dioxide by oxidative decarboxylation. Upon acidification of $Mn^{III}H^{c}$ to pH 2 with HCl, no significant amount of carbon dioxide was evolved.

Figure 1-7 shows that, unlike the near-uv, visible, and near-ir spectra, the far-infrared spectra of $Mn^{III}H$ and $Mn^{III}H(O\text{-}O)$ reveal significant differences. The difference between the spectra of $Mn^{III}H$ and $Mn^{III}H^{c}$ was also found to have a pattern identical to that shown in Fig. 1-7 for the difference between the $Mn^{III}H$ and $Mn^{III}H(O\text{-}O)$ spectra. Because identical changes occur, the formation of $Mn^{III}H^{c}$ or $Mn^{III}H(O\text{-}O)$ involves a change in the very groups of $Mn^{III}H$ that are the eventual electron donors, and their resultant oxidized form must also be the same. (For the spectra in Fig. 1-7 standardized KBr discs were prepared by weighing out 400 mg of desiccated KBr and 2.3 mg of $Mn^{III}H$ or $Mn^{III}H(O\text{-}O)$, grinding them together, and pressing the mixture into a 1-mm-thick disc of 1 cm diam. The disc was prepared by applying pressure of 25,000 lb/in.$^{2}$ for 30 sec. Before the pressure was applied, the compartment containing the KBr-$Mn^{III}H$ or $Mn^{III}H(O\text{-}O)$ mixture was evacuated for 15 min. Each sample was measured against the same standard KBr disc in the reference cell.)

Minkoff,[9] Davison,[10] and Swern et al.[11] have studied changes in the infrared spectrum of carboxylic acids upon their conversion to percarboxylic acids. In each case there occurred a number of significant changes, and consistent throughout were the following two:

(a) a low-intensity band, assigned to the O-O vibration of aliphatic peracids, that appears between 830 and 890 $cm^{-1}$;

(b) a shift in the carbonyl stretching-vibration band that is on the average 45 $cm^{-1}$ toward higher wave numbers.

Data pertinent to our study are those of Swern et al., in which palmitic and perpalmitic acid were compared in solution and in the solid state. In solutions of perpalmitic acid, a band at 865 $cm^{-1}$ was present, whereas in the solid material there were bands at 879 and 891 $cm^{-1}$. These bands are not present in palmitic acid either in solution or in the solid state. In both solution and solid, the carbonyl frequency is shifted about 40 $cm^{-1}$ to higher wave numbers for the peracid (solution, 1712 → 1748; solid, 1702 → 1747 $cm^{-1}$).

Thus the results of our experiments support the conclusion that a peracid or diacylperoxide of $Mn^{III}H$ is formed when $Mn^{IV}H$ is converted to $Mn^{III}H$. Since a peroxide would be expected to be a strong oxidant, $Mn^{III}H^{c}$ and $Mn^{III}H(O\text{-}O)$ were tested for their oxidizing capabilities and compared with untreated $Mn^{III}H$ as a control. Aniline blue and indigo sulfonic acid were found to be bleached, and iodide ion was oxidized to iodine at pH 6 (as determined by starch-iodide complex) by both $Mn^{III}H^{c}$ and $Mn^{III}H(O\text{-}O)$. Each of these experiments was conducted in both the presence and the absence

[9] G. J. Minkoff, Proc. Roy. Soc. (London) A 224, 176 (1954).

[10] W. T. Davison, J. Chem. Soc. 1951, 2456.

[11] D. Swern, C. R. E. Witnauer, and W. E. Parker, J. Am. Chem. Soc. 77, 5537 (1955).

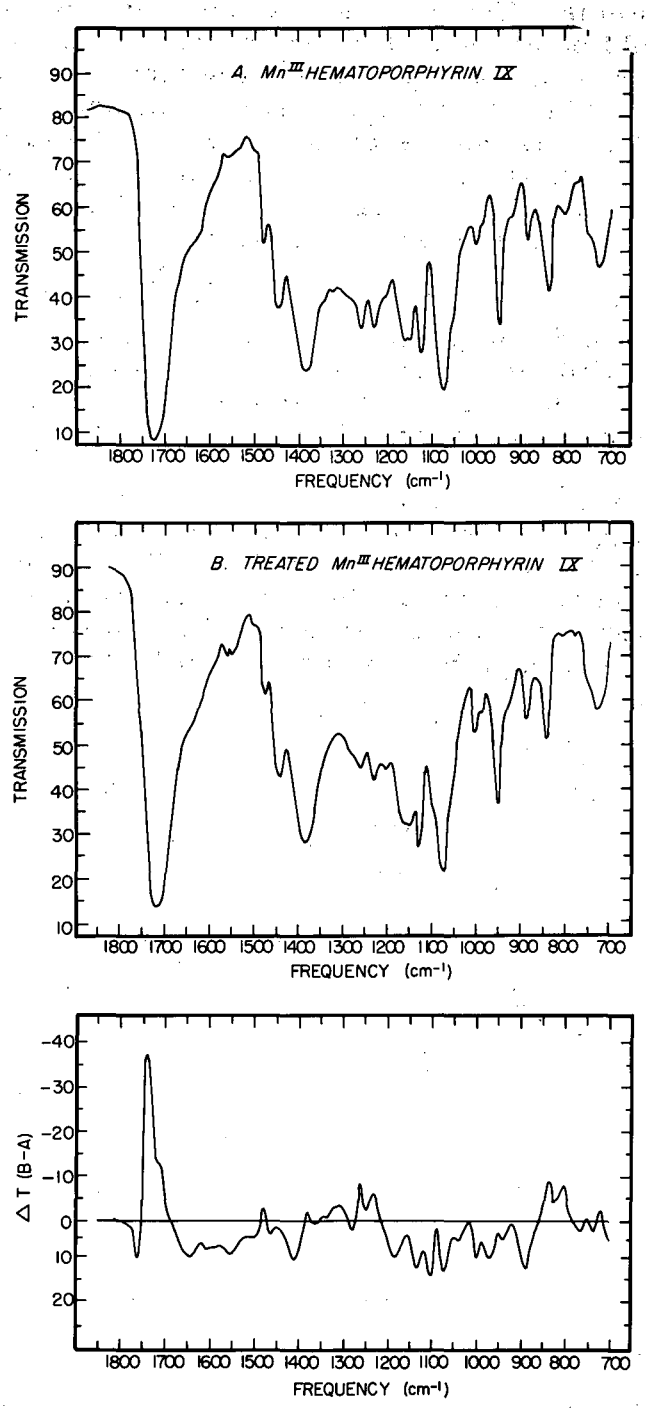


Fig. 1-7. Infrared spectra of $Mn^{III}H$ (A) and $Mn^{III}H(O\text{-}O)$ (B).
A, $Mn^{III}H$ in $10^{-3}$ M KOH brought to pH 2 with the addition of concentrated $HCl$ and the pigment obtained by lyophilizing to dryness;
B, $Mn^{III}H(O\text{-}O)$.
B was handled in the same way as A.

of air, and the control, untreated $Mn^{III}H$, was found to have no effect in any of these systems. The amount of either dye bleached in air was much greater than could be accounted for from the amount of $Mn^{III}H^{c}$ or $Mn^{III}H(O\text{-}O)$ present, possibly indicating that a free radical was being propagated. This kind of oxidation might be initiated by an interaction between the dye and organic peroxide[12] and then be propagated through molecular oxygen. In the absence of air, one molecule of indigo sulfonic acid was bleached at pH 10 for each two molecules of $Mn^{III}H(O\text{-}O)$. This result would indicate either that one molecule of dye undergoes a series of oxidation steps, or that only part of the hydrogen peroxide originally added to $Mn^{III}H$ has been retained as, for example, a diacyl peroxide, while the rest may have been decomposed to oxygen and water. In the test involving the oxidation of iodide ion to iodine at a pH between 5 and 6, only a small amount of iodine could be formed over a 48-h period in the absence of air and in the presence of a starch solution.

The involvement of the propionic acid groups in the formation of a peroxide may provide an explanation for the pH dependence of the rate of conversion of $Mn^{IV}H$ to $Mn^{III}H$ below pH 12 (Fig. 1-5). It would be expected that competition between these negative carboxylate groups and hydroxide ions for coordination positions 5 and 6 would be reflected as a change in rate in the pH range, where the $pK_a'$ value for the reaction indicated in Eq. 6 is operative.[13]

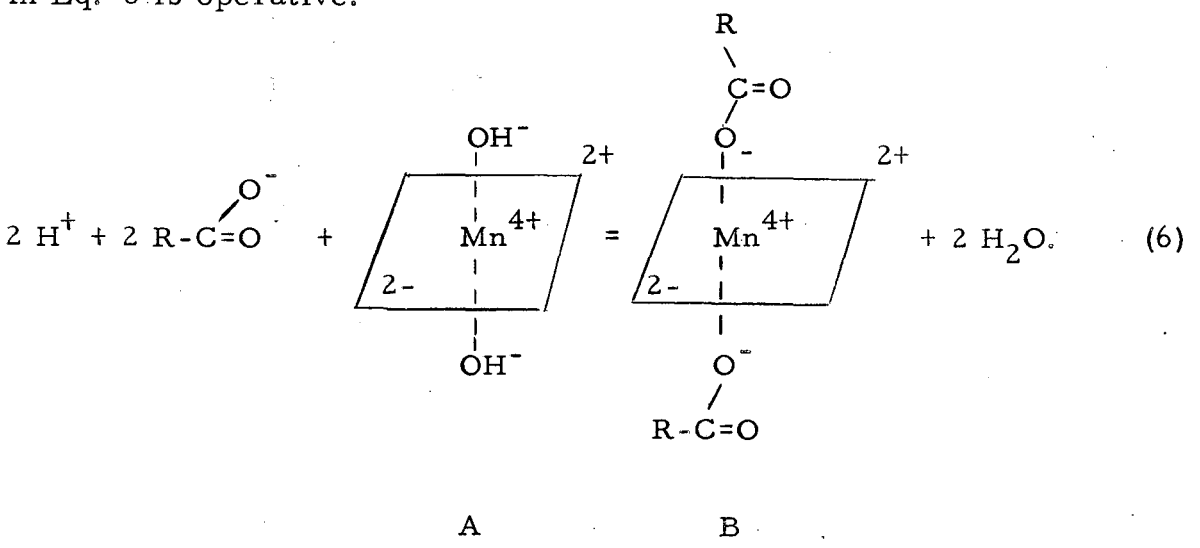


[12] W. C. Schumb, C. N. Satterfield, and R. L. Wentworth, Hydrogen Peroxide (Reinhold Publishing Corp., New York, 1955), p. 381.

[13] The reaction is arbitrarily written as the protonation of both hydroxides. From the present data it could just as well be assumed that only one hydroxide is protonated with a $pK_a'$ near 9.

It is apparent that species B would be favored at low pH and species A at high pH. Thus, if

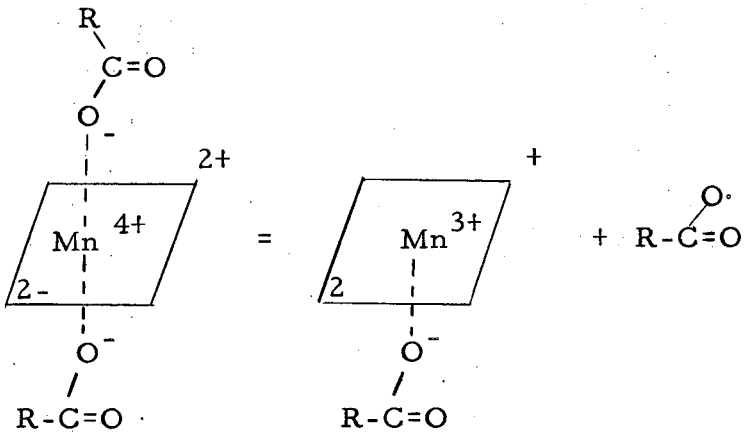


(7)

proceeds to the right at a faster rate than the reaction indicated in Eq. (5), the relationship of log k vs pH observed in Fig. 1-5 would be expected with the addition that, if the data could be extended to sufficiently low pH values, a region should be found where log k is independent of pH.

## Evidence for the Formation of Oxygen

Since the conversion of $Mn^{IV}H$ to $Mn^{III}H$ may be accompanied by the liberation of molecular oxygen, experiments were conducted under argon and nitrogen atmospheres to test the effect of removal of oxygen on the rate of conversion of $Mn^{IV}H$ to $Mn^{III}H$ at pH 13 and at 22°. Table 1-I gives the results. At these low oxygen pressures there was found a tenfold increase in the rate constant for the conversion of $Mn^{IV}H$ to $Mn^{III}H$ over the rate constant determined for a similar experiment conducted under oxygen, or over that rate displayed in air. For each experiment, the rate was of first order with respect to the concentration of $Mn^{IV}H$.

Molecular oxygen has not yet been observed among the gaseous products that were observed in the mass spectrometer. It has been necessary to work at high concentrations (above $10^{-2}$ M) of $Mn^{IV}H$ in order to obtain enough oxygen to permit a decisive measurement, and under these conditions some pigment has always been destroyed. Evidently, the porphyrin is a sufficiently good substrate for the strong-oxidant intermediate that higher concentrations favor porphyrin destruction.

A method used to demonstrate the presence of small amounts of gaseous oxidant issuing from a reaction mixture in which $Mn^{IV}H$ is changing to $Mn^{III}H$ involves passing the argon gas emerging from the reaction vessel through a trap containing a solution of reduced flavin mononucleotide. From the results shown in Table 1-II, about one mole of $FMNH_2$ is oxidized for each two moles of $Mn^{IV}H$ changed to $Mn^{III}H$. Since sublimation experiments have ruled out gaseous hydrogen peroxide as a free product of the reaction, oxygen seems to be a very likely candidate.

Table 1-I. Variation of the rate for the conversion of $Mn^{IV}H$ to $Mn^{III}H$ with different gaseous atmospheres.

| Gaseous phase of system | k ($sec^{-1}$) |
|---|---|
| Air | $2.5 \times 10^{-6}$ |
| Oxygen only | $2.5 \times 10^{-6}$ |
| Nitrogen only | $2.0 \times 10^{-5}$ |
| Argon only | $2.5 \times 10^{-5}$ |
| Cleaned argon[a] | $2.2 \times 10^{-5}$ |

a. The argon was cleaned by passage through a furnace containing fine copper fillings at 350° and then through a solution of 0.1 M $K_3Fe(CN)_6$.

Table 1-II. Measurement of gaseous oxidant.

| System | Time for oxidation of 0.2 μmole of $FMNH_2$ (min) | $\frac{\Delta\ \mu M\ Mn^{IV}H}{\Delta\ \mu M\ FMNH_2}$ |
|---|---|---|
| Argon | 360 | - |
| 6 μmoles NaClO in buffer[a] | 40 | - |
| $Mn^{III}H$ in buffer | 330 | - |
| 1.2 μM NaClO + 2 μM $Mn^{III}H$ | 5 | 2.4 |
| D after standing for 10 min | 12 | 2.2 |
| D after standing for 30 min | 20 | 2.5 |

a. 0.05 M $K_2HPO_4$-$K_3PO_4$, pH 11.

It is apparent that species B would be favored at low pH and species A at high pH. Thus, if

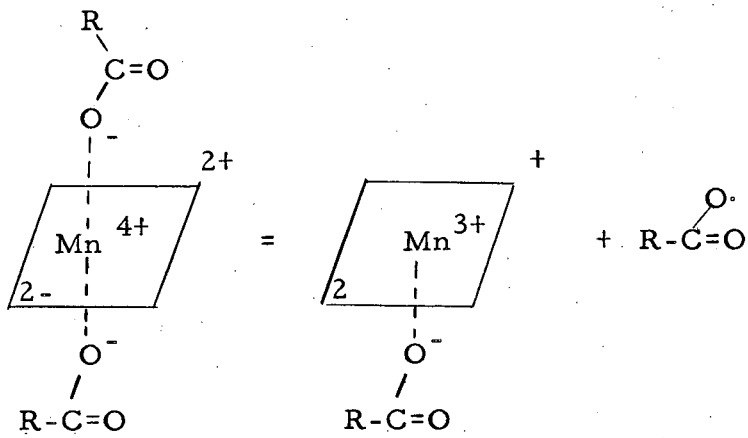


(7)

proceeds to the right at a faster rate than the reaction indicated in Eq. (5), the relationship of log k vs pH observed in Fig. 1-5 would be expected with the addition that, if the data could be extended to sufficiently low pH values, a region should be found where log k is independent of pH.

## Evidence for the Formation of Oxygen

Since the conversion of $Mn^{IV}H$ to $Mn^{III}H$ may be accompanied by the liberation of molecular oxygen, experiments were conducted under argon and nitrogen atmospheres to test the effect of removal of oxygen on the rate of conversion of $Mn^{IV}H$ to $Mn^{III}H$ at pH 13 and at 22°. Table 1-I gives the results. At these low oxygen pressures there was found a tenfold increase in the rate constant for the conversion of $Mn^{IV}H$ to $Mn^{III}H$ over the rate constant determined for a similar experiment conducted under oxygen, or over that rate displayed in air. For each experiment, the rate was of first order with respect to the concentration of $Mn^{IV}H$.

Molecular oxygen has not yet been observed among the gaseous products that were observed in the mass spectrometer. It has been necessary to work at high concentrations (above $10^{-2}$ M) of $Mn^{IV}H$ in order to obtain enough oxygen to permit a decisive measurement, and under these conditions some pigment has always been destroyed. Evidently, the porphyrin is a sufficiently good substrate for the strong-oxidant intermediate that higher concentrations favor porphyrin destruction.

A method used to demonstrate the presence of small amounts of gaseous oxidant issuing from a reaction mixture in which $Mn^{IV}H$ is changing to $Mn^{III}H$ involves passing the argon gas emerging from the reaction vessel through a trap containing a solution of reduced flavin mononucleotide. From the results shown in Table 1-II, about one mole of $FMNH_2$ is oxidized for each two moles of $Mn^{IV}H$ changed to $Mn^{III}H$. Since sublimation experiments have ruled out gaseous hydrogen peroxide as a free product of the reaction, oxygen seems to be a very likely candidate.

Table 1-I. Variation of the rate for the conversion of $Mn^{IV}H$ to $Mn^{III}H$ with different gaseous atmospheres.

| Gaseous phase of system | k ($sec^{-1}$) |
|---|---|
| Air | $2.5 \times 10^{-6}$ |
| Oxygen only | $2.5 \times 10^{-6}$ |
| Nitrogen only | $2.0 \times 10^{-5}$ |
| Argon only | $2.5 \times 10^{-5}$ |
| Cleaned argon[a] | $2.2 \times 10^{-5}$ |

a. The argon was cleaned by passage through a furnace containing fine copper fillings at 350° and then through a solution of 0.1 M $K_3Fe(CN)_6$.

Table 1-II. Measurement of gaseous oxidant.

| System | Time for oxidation of 0.2 μmole of $FMNH_2$ (min) | $\frac{\Delta\ \mu M\ Mn^{IV}H}{\Delta\ \mu M\ FMNH_2}$ |
|---|---|---|
| Argon | 360 | - |
| 6 μmoles NaClO in buffer[a] | 40 | - |
| $Mn^{III}H$ in buffer | 330 | - |
| 1.2 μM NaClO + 2 μM $Mn^{III}H$ | 5 | 2.4 |
| D after standing for 10 min | 12 | 2.2 |
| D after standing for 30 min | 20 | 2.5 |

a. 0.05 M $K_2HPO_4$-$K_3PO_4$, pH 11.

For molecular oxygen to be a product of the conversion of $Mn^{IV}H$ to $Mn^{III}H$, the following half cells must be considered:[1, 4]

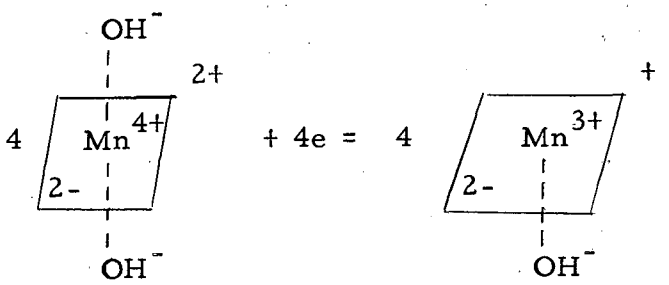


$$+ 4\ OH^-;\ E_{m\ 14} = 0.3\ v, \qquad (8)$$

$$O_2 + 2\ H_2O + 4e = 4\ OH^-;\ E_{m\ 14} = 0.4\ v\ . \qquad (9)$$

From Eqs. (8) and (9), the equilibrium constant may be calculated for the reaction

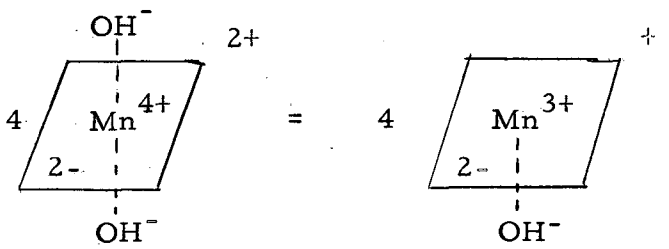


$$+ O_2 + 2H_2O \qquad (10)$$

by using

$$O = E_m\ (\text{for Eq. 8}) - E_m\ (\text{for Eq. 9}) + \frac{RT}{nF}\ \ln K'_{eq}, \qquad (11)$$

where $K'_{eq}$ is the apparent equilibrium constant, because the $E_m$ values are based on concentrations of oxidant and reductant instead of activities. For Eq. (10),

$$K'_{eq} = (Mn^{III}H(OH^-))^4(O_2)/(Mn^{IV}H(OH^-)_2)^4\ .$$

The value of this constant at pH 14 and 20° is $2.2 \times 10^{-2}$ atm. Thus, the equilibrium is shifted toward the right as the oxygen pressure is lowered.

At pH 10, Eq. (10) may be written as

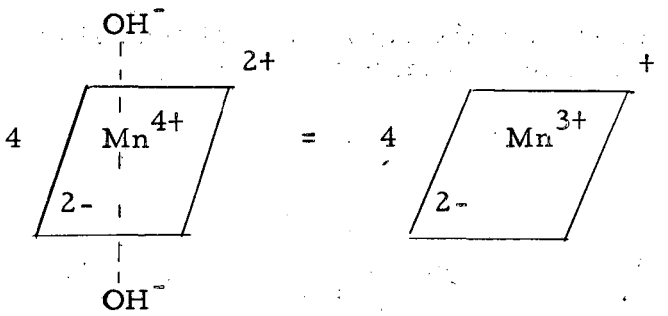


$$+ O_2 + 4\ OH^- + 2H_2O, \qquad (12)$$

because the following equilibrium exists:[1]

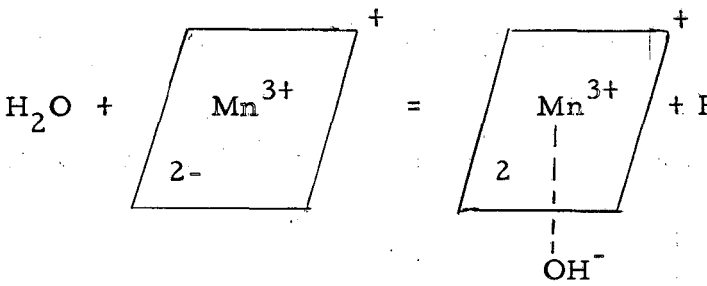


$$+ H^+;\ pK_a = 12\ . \qquad (13)$$

The equilibrium for the reaction represented by Eq. (12) would be dependent upon pH, favoring the products at lower pH values.

## Discussion

The results indicate that $Mn^{IV}H$ is able to produce a peroxide by interacting with water even at very high pH. In addition, molecular oxygen may be formed from water at pH 13 if the concentration of oxygen in the reaction mixture is kept low. At pH 7 the extrapolated value of $E_m$ (Fig. 1-8) for the reaction written in Eq. (8) is appreciably greater than that for the formation of oxygen from water:

$$1/4\ O_2 + H^+ + e = 1/2\ H_2O;\ E_{m\,7} = 0.8\ v. \qquad (14)$$

Thus, a pigment such as a manganese porphyrin complex, in the protective presence of a protein, might be highly efficient in producing molecular oxygen from water, providing it could be oxidized to the 4+ oxidation state by some agent. Among other things, the presence of a protein might function to protect the porphyrin from destruction by strong oxidants, similar to the protection afforded iron protoporphyrin IX by the protein of peroxidases and catalases.

The experimental data bear witness to the fact that the three kinds of reactions to be expected from hydrogen peroxide have been observed--that is, the destructive oxidation of the pigment, formation of another peroxide, or the liberation of oxygen does occur under appropriate conditions. It would seem, then, that the first step of each kind of reaction may involve the formation of a hydroxyl radical or, possibly, a carboxyl radical at lower pH.

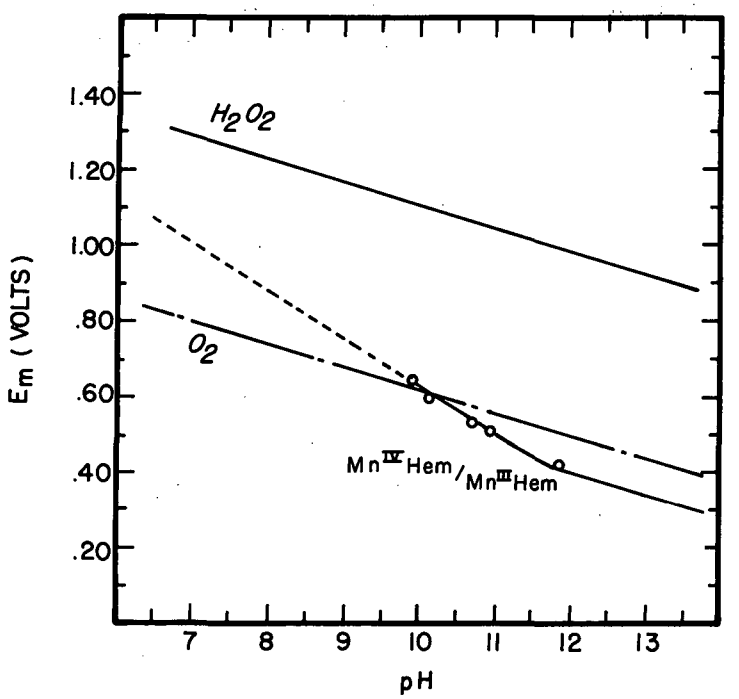


MU-26947

Fig. 1-8. $E_m$ vs pH relationships. The curve labeled $H_2O_2$ represents the half cell $1/2\ H_2O + 1/2\ O_2H^- + e = 3/2\ OH^-$ with 1 M $O_2H^-$; the curve labeled $O_2$ represents the half cell $1/4\ O_2 + 1/2\ H_2O + e = OH^-$ with 1 atm $O_2$; the curve labeled $Mn^{III}H/Mn^{IV}H$ represents the half cell $Mn^{IV}H + e = Mn^{III}H$. o, experimental points for $Mn^{III}H/Mn^{IV}H$.

The characterization of a stable $Mn^{IV}$ complex is the first example of a simple metalloporphyrin system in which such a high oxidation state can be examined under reversible conditions. George[14,15,16] and George and Irvine[17,18,19] have examined higher oxidation states of iron porphyrins complexed with certain proteins. These workers found that one equivalent of a strong oxidant, such as $K_2IrCl_6$, could be added to a solution of an $Fe^{III}$porphyrin complex (for example, metmyoglobin) and the formation of a new species could be observed. Subsequent addition of a reducing agent such as ascorbic acid resulted in the restoration of the $Fe^{III}$ species. This conversion of $Fe^{III}$ to some higher oxidation state was shown to be accompanied by the liberation of two protons at pH 7 and one proton at pH 12. They suggested that the following equilibria

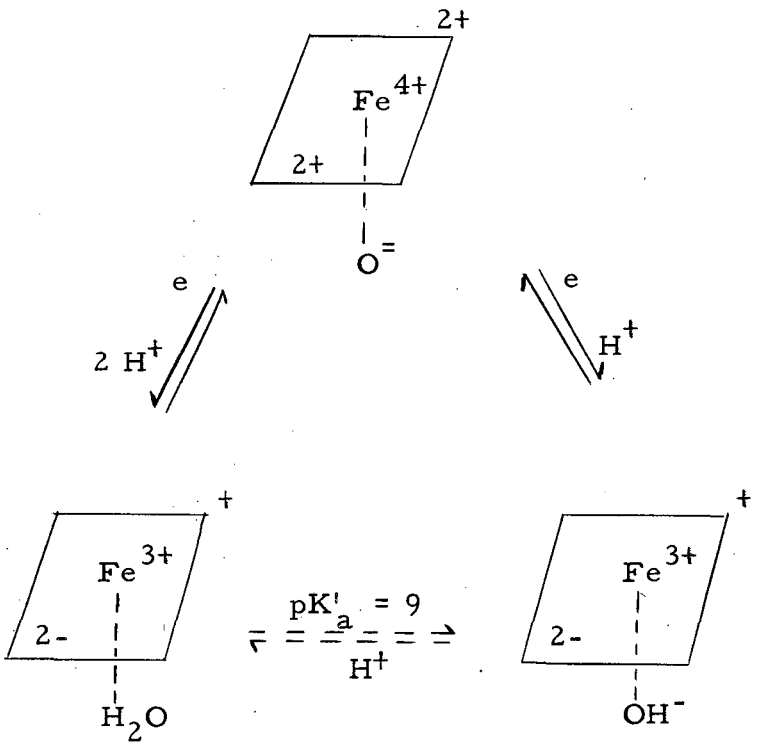


[14] P. George, Science 117, 2201 (1953).

[15] P. George, J. Biol. Chem. 201, 413 (1953).

[16] P. George, Arch. Biochem. Biophys. 45, 21 (1953).

[17] P. George and D. H. Irvine, J. Chem. Soc. (1954), 3142.

[18] P. George and D. H. Irvine, Biochem. J. 58, 188 (1954).

[19] P. George and D. H. Irvine, Biochem. J. 60, 596 (1955).

obtained, where groups of the protein may occupy the 5th coordination position. An $E_m$/pH relationship was shown to be consistent with the above equilibria, the slope of the curve being -0.120 V per pH unit at pH 4 and -0.060 V per pH unit at pH 11. The similarity of these results to our data for manganese porphyrin systems suggests that the general character of higher oxidation states of transition metal-porphyrin complexes may be indicated.

It is of interest that George and Irvine reported instability of $Fe^{IV}$ complexes. Their conclusion was that impurities in, and breakdown of, the strong oxidizing agents employed were responsible. In analogy with our data, the possibility of direct interaction of $Fe^{IV}$ complexes with water to form molecular oxygen or a peroxide must also be considered. The values for the $Fe^{IV}/Fe^{III}$ porphyrin equilibrium for metmyoglobin at alkaline pH are quite close to those determined for the $Mn^{IV}/Mn^{III}$ hematoporphyrin IX equilibrium, so that the two different transition metal-porphyrin complexes may show similarities in their reactions with water.

The results of these experiments with model manganese porphyrin systems should stimulate a more thorough search for compounds that may undergo similar reactions in biological material that is capable of producing molecular oxygen from water.

## Summary

The interaction of $Mn^{IV}H$ with water was shown to result in the destruction of the porphyrin, the formation of an organic peroxide, and (or) the liberation of oxygen depending on the conditions. Rate studies for the conversion of $Mn^{IV}H$ to $Mn^{III}H$ indicated the reaction to be of first order with respect to $Mn^{IV}H$ and independent of the hydrogen ion concentration at high pH values. Each of these facts was consistent with, and suggestive of, a mechanism by which the dihydroxide complex of $Mn^{IV}H$ dissociates to give a hydroxyl radical as a product. The results are discussed with respect to the relationship between the rate of the reaction and pH, the liberation of oxygen from water, and the higher oxidation states of transition-metal porphyrin complexes in general.

## 2. THE GAS-LIQUID PARTITION CHROMATOGRAPHY OF THE TETRA-O-ACETYL PENTOPYRANOSES

Robert J. Ferrier*

O-Methyl[1] and O-trimethylsilyl[2] ethers, O-acetyl esters,[1] and O-isopropylidene ketals[3] of polyhydroxy compounds related to sugars have been subjected successfully to gas-liquid partition chromatography, and many isomeric compounds have been resolved. Until now the acetates of free sugars have not been examined by this technique.[4]

Consideration of results published in the recent literature and others obtained in this Laboratory reveals that retention times and structural features of isomers show a marked interdependence. For example, it can be seen from the results of Gunner, Jones, and Perry[1] that within a series of polyol acetates the retention times of the isomers decrease with increase in the number of erythro-1, 2-diol groupings in the polyols. Thus, e. g., the pentitol acetates are eluted in the order ribitol, arabitol, xylitol. Polyols, and presumably their derivatives, exist in zigzag conformations,[5] so that acetates with shortest retention times are those with greatest number of truly trans-adjacent acetoxy groupings, i. e., those in which intramolecular nonbonded interactions are minimized. Using similar conditions, we have examined the vapor-phase chromatographic behavior of the tetra-O-acetyl pentopyranoses, and have shown likewise that increases in intramolecular steric repulsions apparently result in increases in retention times.

The separations were carried out by using the "Aerograph" gas chromatograph (Wilkens Instrument and Research, Inc.) at 180° on a column (0.6 cm i. d.) packed with Apiezon L grease (20%) on firebrick. The flow rate (helium) was 50 to 70 ml per minute and the retentions were determined by using an internal standard of penta-O-trimethylsilylribitol.

The substances under examination were not isolated in every case, as chromatographic analysis of the mixed products of acetylation of the sugars permitted determination of the retention times of some isomers. It was shown, e. g., that the acetylation products of xylose (acetic anhydride with sodium acetate catalyst) were $X_1$ ($R_T$ 0.85) ($R_T$ = retention time relative to that of crystalline tetra-O-acetyl-β-D-xylopyranose), and $X_2$ ($R_T$ 1.00),

---

*Present address: Chemistry Department, Birkbeck College, University of London.

[1] S. W. Gunner, J. K. N. Jones, and M. B. Perry, Chem. & Ind. (London) 255 (1961), and references contained therein.

[2] E. J. Hedgley and W. G. Overend, Chem. & Ind., (London) 378 (1960).

[3] E. J. Hedgley, O. Mérész, W. G. Overend, and R. Rennie, Chem. & Ind. (London) 938 (1960); M. Calvin, R. J. Ferrier, and E. J. McDonald, unpublished results.

[4] Since this work was completed, W. J. A. Vanden Heuvel and E. C. Horning [Biochem. Biophys. Res. Commun. 4, 399 (1961)] have reported studies on the sugar acetates.

[5] R. J. Ferrier and W. G. Overend, Quart. Rev. (London) 13, 265 (1959).

where $X_2$ predominated. Treatment of the mixture with zinc chloride in acetic anhydride caused only a change in the ratio of the isomers so that $X_1$ predominated. It is therefore the α isomer. The sodium-acetate-catalyzed esterification of β-D-arabinose gave the products $A_1$ ($R_T$ 0.90), $A_2$ ($R_T$ 1.07), and $A_3$ ($R_T$ 1.22), with $A_2$ predominating. $A_2$ has been identified with authentic tetra-O-acetyl-α-D-arabopyranose, and $A_1$ is shown to be its anomer by its being the major component of the mixtures obtained by (a) anomerizing the above mixture with zinc chloride and (b) acetylating the pentose with pyridine as catalyst. In each preparation, all three components were obtained; $A_3$ has not been characterized. The acetylation of β-D-lyxose yielded two products $L_1$ ($R_T$ 0.95) and $L_2$ ($R_T$ 1.10). Since $L_1$ predominated when sodium acetate was used as catalyst and $L_2$ predominated when pyridine was employed, and it is concluded that they are the α and β isomers, respectively. Both crystalline tetra-O-acetyl ribopyranoses were available. The results are summarized in Table 2-I.

Tetra-O-acetyl-β-D-xylopyranose in the Cl conformation[6] has no bulky axial substituents and is believed, therefore, to adopt this chair form. The tetra-O-acetates of α-xylopyranose (Cl), β-lyxopyranose (Cl), β-ribopyranose (Cl), and α-arabopyranose (1C) each have one axial acetoxy grouping [C(1), C(2), C(3), and C(4), respectively] in the indicated conformations and are here assumed to prefer these chair forms. The assumption is borne out by nuclear magnetic resonance studies.[7] The retention times of the lyxose, ribose, and arbinose compounds are strikingly similar (and greater than 1.0), while the figure for tetra-O-acetyl-α-D-xylopyranose is notably smaller. An axial substituent replacing an equatorial one in the all-equatorial compound at any asymmetric carbon other than C(1) thus increases retention time by 0.09 (average value) while inversion at C(1) causes a decrease by 0.15. In Table 2-II are shown the results of applying these values to tetra-acetates that have two axial acetoxy groupings in either chair form and whose conformation would therefore not be readily predicted. (The approximation is arbitrarily made that increase in number of axial substituents affects the retention time linearly.)

The conclusions drawn are in agreement with NMR results[7] except in the case of the α-ribose derivative. The apparently exceptional compound, however, gave an NMR spectrum that did not show conclusively whether it had an equatorial C(1) hydrogen bond, and therefore its conformation remains in doubt. The possibility that the molecules assume different shapes under the dissimilar conditions of examination must be accepted.

We conclude from the regularities noted in the above results that conformation plays an important part in determining retention times and may, in some cases, be assigned on the basis of vapor-phase chromatographic behavior. The dipolar effect (discussed by Edward[8]) that stabilizes many C(1) axial glycosides, acetates, and acetohalogeno-sugars relative to their C(1) equatorial anomers is assumed to be responsible for the anomaly which arises when the stereochemistry is inverted at C(1).

---

[6] R. E. Reeves, Advan. Carbohydrate Chem. 6, 107 (1951).

[7] R. U. Lemieux, R. K. Kullnig, H. J. Bernstein, and W. G. Schneider, J. Am. Chem. Soc. 80, 6098 (1958).

[8] J. T. Edward, Chem. & Ind. 1955, 1102.

Exactly opposite effects have been noted by us in the tetra-O-trimethylsilyl pentose series, i.e., inversion of a bulky grouping from the equatorial to the axial position decreased retention times, and the specific importance of the sterochemistry at C(1) was apparent. This leads to the belief that the effects discussed above may not have simple steric factors as their cause but may arise from alterations in the dipolar properties of the molecules.

Table 2-I. Retention times of the pentose tetra-acetates relative to tetra-O-acetyl-β-D-xylopyranose.

| Tetra-O-acetyl D-pentopyranose | α-isomer | β isomer |
|---|---|---|
| Ribose | 1.23 | 1.09 |
| Arabinose | 1.07 | 0.90 |
| Xylose | 0.85 | 1.00 |
| Lyxose | 0.95 | 1.10 |

Table 2-II. Effects of axial substituents in tetra-acetates

| Tetra-O-acetyl D-pentopyranose | Conformation | Carbon atoms bearing axial substituents | Retention times (relative) Calculated[a] | Retention times (relative) Determined | Deduced conformation |
|---|---|---|---|---|---|
| α-ribose | C1 | C(1), C(3) | 0.94 | 1.23 | 1C |
| | 1C | C(2), C(4) | 1.18 | | |
| β-arabinose | C1 | C(2), C(3) | 1.18 | 0.90 | 1C |
| | 1C | C(1), C(4) | 0.94 | | |
| α-lyxose | C1 | C(1), C(2) | 0.94 | 0.95 | C1 |
| | 1C | C(3), C(4) | 1.18 | | |

a. $0.94 = 1.00 - 0.15 + 0.09$; $1.18 = 1.0 + 2 \times 0.09$.

## 3. STRUCTURE AND CHROMATOGRAPHIC PROPERTIES OF CARBOHYDRATES. THE LIQUID-LIQUID PARTITION MOBILITIES OF ALDONO-γ-LACTONES

Robert J. Ferrier*

It is a simple matter to resolve isomeric carbohydrate substances by partition-chromatographic means. Therefore, the mobilities of compounds depend not only upon fundamental features of the molecules, e.g., molecular weight and "hydrophilic nature" (as determined by the number of unsubstituted hydroxyl groupings present), but also upon subtler factors related to configuration and conformation. Little attention has been paid to the correlation of structure with chromatographic properties or to the study of the detailed physical phenomena upon which the mobilities depend. Some interrelationships between the disposition of the hydroxyl groupings on pyranose sugars and their chromatographic behavior have, however, been noted,[1] and these have lately been reinterpreted in conformational terms.[2] Thus, free sugars that can assume chair conformations having few axial hydroxyls are less mobile than those which have several. We now note some correlations in the γ-lactone series.

All the measurements (see Table 3-I) were made on Whatman No. 1 papers developed with butanol-1:ethanol:water (4:1:5). The members of each group were run together at 25° on one paper, and the mobilities quoted in the table are relative to the fastest in each series.

From erythrono- and threono-γ-lactones it is seen that a C(2)-C(3) cis-diol reduces mobility relative to a trans-diol. The pentono-γ-lactones show that the isomer (lyxo-) with the configuration that has three hydrophilic groupings on one side of the ring travels slowest and that a C(2)-C(3) cis-diol (ribo-) confers lower mobility than a C(3)-C(4) cis-hydroxy-hydroxymethyl system (xylo-).

In the 2-C-hydroxymethylpentono-γ-lactones,[3] in which the situation is complicated by the introduction of another hydrophilic group on the ring, again it is evident that a C(2)-C(3) cis-diol has the effect of reducing the rate of travel and that the isomer with the lyxo- configuration has lowest mobility.

With the hexono-γ-lactones in which simple relationships between structural features and chromatographic properties could be expected to be masked by complexities introduced by the flexible 1,2-dihydroxyethyl grouping at C(4), it is still noticeable that when the three oxygenated substituents are on one side of the five-membered ring (mannono- and gulono-), marked reductions in the rates of travel occur. We were not able to determine the

*Present address: Chemistry Department, Birkbeck College, University of London.

[1] F. R. Isherwood and M. A. Jermyn, Biochem. J. 48, 515 (1951).

[2] R. J. Ferrier and W. G. Overend, Quart. Rev. (London) 13, 265 (1959).

[3] Robert J. Ferrier, unpublished results.

mobilities of the gluco- and talo- isomers directly. The figure given for the former is calculated from the relative mobilities of the gluco- and manno- isomers in this solvent quoted by Abdel-Akher and Smith.[4] The talono-γ-lactone figure is quoted as 0.89, since it was unresolvable from the galacto- isomer. In an acidic solvent it travels 1.06 times as fast as its epimer.[5]

Table 3-I. Mobilities of γ lactones (relative to fastest isomer in each series).

| Tetrono- | | Pentono- | | 2-Hydroxymethyl-pentono- | | Hexono- | |
|---|---|---|---|---|---|---|---|
| Erythrono- | 0.78 | Ribono- | 0.92 | Ribono- | 0.85 | Allono- | 0.94 |
| | | Arabono- | 1.00 | Arabono- | 0.86 | Altrono- | 0.92 |
| Threono- | 1.00 | Xylono- | 0.99 | Xylono- | 1.00 | Glucono- | (0.98)[a] |
| | | Lyxono- | 0.76 | Lyxono- | 0.74 | Mannono- | 0.77 |
| | | | | | | Gulono- | 0.60 |
| | | | | | | Idono- | 1.00 |
| | | | | | | Galactono- | 0.89 |
| | | | | | | Talono- | (0.89)[a] |

a. Calculated values

[4] M. A. Abdel-Akher and F. Smith, J. Am. Chem. Soc. 73, 5859 (1951).

[5] J. D. Smiley and G. Ashwell, J. Biol. Chem. 236, 357 (1961).

# 4. STRUCTURE AND CHROMATOGRAPHIC PROPERTIES OF CARBOHYDRATES. GAS-LIQUID PARTITION MOBILITIES OF PYRANOSE DERIVATIVES

Robert J. Ferrier*

Little attention has been paid to the factors that decide the order in which isomers travel on liquid-liquid paper chromatograms, although correlations between stereochemical features and mobilities have been noted.[1,2] It is becoming evident that corresponding correlations can be made relating retention times on gas-liquid chromatograms and the structures of substituted carbohydrates. Although the physical basis of these correlations is not understood at present, it is hoped that their study will help with the interpretation of other gas-chromatographic data and lead to a more fundamental understanding of the phenomena involved in the application of this technique in sugar chemistry.

Gunner, Jones, and Perry[3] have convincingly shown that in the polyol acetate series, the isomers with the greatest number of ester groupings on one side of the planar zig-zag carbon backbone have the highest column retention times, and that if two isomeric compounds have the same maximum number of substituents on one side, then the member having those groupings closest together will move more slowly. We have independently observed (see Paper 2 in this Quarterly Report) that the introduction of axial ester groupings round the pyranose ring in tetra-O-acetylpentoses increases retention times but that at C(1) an axial substituent has the opposite effect. These two sets of results can be rationalized by noting that in both the cyclic and acyclic series the molecules in which nonbonded steric interactions are at a maximum have the highest retention times, but this may not be the fundamental connecting factor. Indeed, the exceptional behavior of compounds that have axial substituents at C(1) and the differences in the orders in which acetylated and trimethylsilylated derivatives of carbohydrates are eluted (see below) lead us to believe that polar factors are particularly important in determining retention times. Although the methyl ethers of sugars have received most study by this technique, little attention has been given to the order in which they are eluted. Bishop and Cooper[4] have shown, however, that with methyl tri- and tetra-O-methylglucopyranosides the α- isomers are consistently eluted after their anomers,[4] but the results of Kircher[5] and those obtained in this Laboratory indicate that rationalization within the fully methylated pyranose series will be complex.

---

*Present address: Chemistry Department, Birkbeck College, University of London.

[1] F. A. Isherwood and M. A. Jermyn, Biochem. J. 48, 515 (1951).

[2] R. J. Ferrier and W. G. Overend, Quart. Rev. (London) 13, 265 (1959).

[3] S. W. Gunner, J. K. N. Jones, and M. B. Perry, Can. J. Chem. 39, 1892 (1961).

[4] C. T. Bishop and F. P. Cooper, Can. J. Chem. 38, 388 (1960).

[5] H. W. Kircher, Anal. Chem. 32, 1103 (1960).

We now report the results of an examination of some trimethylsilyl ethers of carbohydrates. Hedgley and Overend have prepared volatile trisyl ethers of several nonreducing sugar derivatives and have shown by vapor-phase chromatography that free aldoses give mixed products on treatment with trimethylsilyl chloride in pyridine solution.[6] In mutarotated D-xylose we have demonstrated that four products are obtained, and that the major two (each 47%, minor pair each 3% of total) are the anomeric pyranose ethers (see following report). Trisylation of the crystalline aldose (α-pyranose form) gave products containing 80% tetra-O-trimethylsilyl-α-D-xylopyranose. The retention times [relative to tetra-O-trimethylsilyl-β-D-xylopyranose ($R_T$)] given in Table 4-I for the trisyl ethers of the D-pentopyranoses have been measured -- following the assumption that the major product obtained on etherification of each of the crystalline aldopentoses is the pyranose derivative ($P_1$) having the same anomeric configuration as the parent sugar, and that the major two components ($P_1$ and $P_2$) of the mixtures obtained by trisylation of the mutarotated sugars are the two pyranose forms. For arabinose and lyxose, these assumptions are substantiated by noting the large proportions of the $P_2$ components in the mixtures (see Fig. 4-1) and by comparison of the retention times of the $P_1$ and $P_2$ pairs with those of the corresponding pairs of trisylated methyl pentopyranosides (see Table 4-I). Poor resolution was obtained with the ethers of ribose, so an uncertainty in the $P_2$ retention time must be assumed. This is indicated in Table 4-I.

Table 4-I. Relative retention times of D-pentopyranose derivatives.

| Pentose | | Tetra-acetates (relative to tetra-O-acetyl β-Xylose) | Tetratrisyl ethers | Tritrisyl methylglycosides |
|---|---|---|---|---|
| | | | (relative to tetra-O-trimethylsilyl β-xylose) | |
| D-ribose | α | 1.23 | 0.48[a] | 0.39[a] |
| | β | 1.09 | 0.52 | 0.43 |
| D-arabinose | α | 1.07 | 0.49 | 0.40 |
| | β | 0.90 | 0.41 | 0.38 |
| D-xylose | α | 0.85 | 0.73 | 0.69 |
| | β | 1.00 | 1.00 | 0.77 |
| D-lyxose | α | 0.95 | 0.39 | 0.37 |
| | β | 1.10 | 0.53 | 0.42 |

[a]These figures may contain negative errors of about 0.04.

[6]E. J. Hedgley and W. G. Overend, Chem. & Ind. (London) 378 (1960).

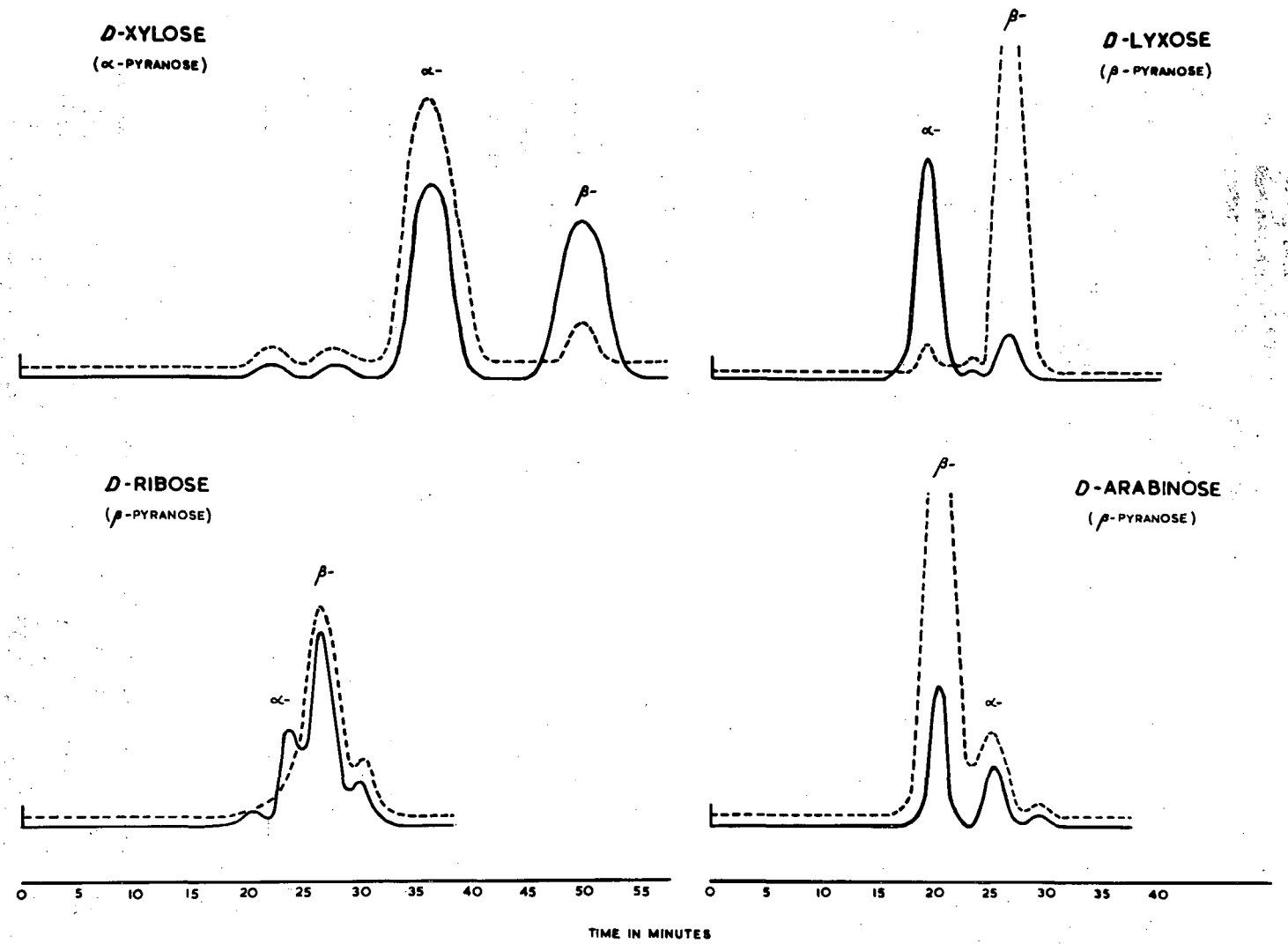


MUB-1284

Fig. 4-1. Separations of the trimethylsilyl ethers of the pentose. Products from crystalline sugars --------; products from mutarotated mixtures ———. The ring structures of the crystalline aldoses are in parentheses, and the peaks assigned to the pyranose derivatives are indicated.

The relative retention times of the trisilylated methyl pentopyranosides are also given in Table 4-I. Methyl β-lyxoside and the ribosides were not available, but their retention times were determined by indirect methods. D-lyxose was reacted under reflux with methanolic hydrogen chloride until equilibrium was established; at this point the ratio of the α- and β-pyranosides (assuming no contribution to the total optical rotation by furanosides) was determined polarimetrically to be 89:11. Trisylation of the mixture gave two chromatographically resolvable compounds present in the ratio 9:1. The major product corresponded in retention time to methyl tri-O-trimethylsilyl-α-D-lyxopyranoside, and the minor was assumed to be the anomer. From its optical rotation and reaction with periodate the equilbrium mixture of methyl-ribosides was shown to contain predominantly the β-pyranoside. The major peak in the chromatogram obtained from the ethers of this mixture was assumed, therefore, to correspond with this isomer, and the second peak (poorly resolved) was thought to be the α-pyranoside. The possible error involved in this last assumption is indicated in Table 4-I. The relative retention times of the penta-O-trimethylsilylpentitols were determined and are given in Table 4-II. The following points emerge from Tables 4-I and 4-II. (The regularities noted in the acetate series have been discussed in Section 2 of this Quarterly Report.)

1. (a) The order of elution of the pentitol ethers is the opposite of that of the corresponding acetates, and (b) the separation between xylitol and arabitol is greater than that between ribitol and arabitol in both series.

2. In the tetra trimethylsilylpentose ether series the derivatives of β-lxyose (C1), β-ribose (C1), and α-arabinose (1C) -- each of which has one bulky axial grouping [C(2), C(3), and C(4), respectively] in the indicated conformations -- have strikingly similar retention times ($R_T$ 0.53, 0.52, 0.49) that are much lower than that of the all-equatorial β-xylose ether (1.00) but greater than those of their anomers (0.39, 0.48, 0.41). These last three have two axial groupings in either chair conformation. The α-xylopyranose compound has a retention time (0.73) quite different from, and higher than, those of the other ethers with one axial substituent.

Table 4-II. Relative retention times of pentitol derivatives.

| Pentitol | Penta-acetate[3] (relative to penta-O-acetyl arabitol) | Penta trimethylsilyl ethers (Relative to penta-O-trimethylsilyl arabitol) | Penta trimethylsilyl ethers (Relative to tetra-O-trimethylsilyl β-xylose) |
|---|---|---|---|
| Ribitol | 0.92 | 1.06 | 0.57 |
| Arabitol | 1.00 | 1.00 | 0.54 |
| Xylitol | 1.18 | 0.91 | 0.49 |

3. The tri-O-trimethylsilyl glycosides can be similarly classified into (a) the all-equatorial β-xylose derivative ($R_T$ 0.77), (b) the ethers with one trimethylsilyl group axial at C(2), C(3), or C(4) (0.42, 0.43, 0.40), (c) compounds having two axial groupings (0.37, 0.39, 0.38), and (d) methyl tri-O-trimethylsilyl-α-D-xylopyranoside (0.69).

4. Differences between the retention times of anomers is significantly smaller in the glycoside ether series than in the fully trisylated ethers, so that inversion of the methoxy substituent at C(1) has, as would be expected, less effect on retention times than inversion of the larger trimethylsilyloxy group.

With the cyclic compounds, attention has been confined to the pentopyranoses, since these were most likely to reveal regularities. In derivatives of β-xylopyranose, since the lone pairs of electrons on the ring oxygen have approximately the steric requirements of two protons, one might expect that changing any one of the four equatorial substituents to an axial position would have the same effect on retention times. (In particular, similar effects would be expected by change of configuration at C(1) or C(4) and at C(2) or C(3), since the line joining the midpoints of the C(2)-C(3) and C(5)-O ring bonds (see sketch) approximates a geometrical twofold axis

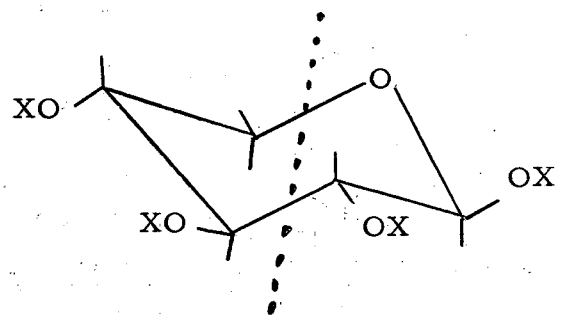


of symmetry, and therefore, corresponding substituents on these pairs of carbon atoms have similar steric environments.) In fact, equatorial-to-axial inversions at C(2), C(3), or C(4) have very similar effects both in the acetate and the tetra-O-trimethylsilyl series, although (for reasons unknown) these operate in opposite directions in the two classes. The presence of the ring oxygen atom is assumed to be responsible for the anomaly that arises when a similar change takes place at C(1), but it is not clear whether its effect is a direct electronic one that influences the character of the C(1) grouping or whether dipolar interaction between this grouping and dipole of the ring oxygen is the cause.

Because of the symmetry element mentioned above, the measured effect of equatorial-to-axial inversion at C(1) can be resolved into two factors: (a) a factor A resulting from the group's resultant axial nature (and equal to that found for the other axial substituents, see Table 4-III and (b) a modifying factor B due to the proximity of the ring oxygen atom. In the tetra-O-acetates factor B opposes and is greater than factor A, while in the tetra-O-trisyl series, where electronic factors would be expected to have relatively less influence, B again opposes but now is less than A.

Table 4-III. Stereochemical relationships and chromatographic behavior

| Relationship of substituents | Effects on retention times: Acetyl esters | Effects on retention times: Tetra trimethylsilyl ethers |
|---|---|---|
| Staggered on either side of zig-zag polyol chain | Decrease[a] | Increase[a] |
| One axial group at C(2), C(3), or C(4) in pyranose ring | Increase[b] | Decrease[b] |
| One axial group at C(1) in pyranose ring | Decrease[b] [Increase due to axial nature of C(1) substituent (factor A); decrease due to effect of neighboring ring oxygen (factor B)] | Modified decrease[b] (decrease due to A > increase due to B) |
| Two axial groupings in pyranose ring | Dependent on conformation[b] (whether C(1)-OAc is axial or equational) | Greater decrease[b] than that caused by one axial group |

[a]Relative to compounds with substituents together on one side of the chain.
[b]Relative to the corresponding all-equatorial compounds.

There exists therefore the anomalous situation in which the same changes in the steric interrelationships between the acetoxy and trimethylsilyloxy groups in substituted polyols and pyranose rings influence gas-liquid chromatographic behavior in entirely opposite ways. This is most likely to be resultant upon the largely different polarities of these two groupings. Similar detailed comparisons between the relative chromatographic properties of trisylated isomers and methylated sugars have not been carried out, but marked differences would be expected, since Bishop and Cooper[7] find that the order of elution of the methyl tri-O-methylxylosides is β-pyranoside, α-pyranoside, β-furanoside, and α-furanoside, while, in the trimethylsilyl series, the β-pyranose ether has longest retention time, and the two minor products of the trimethylsilylation of xylose (believed to be the furanose derivatives) are eluted first (Fig. 4-1). The different effects noted are summarized in Table 4-III. The physical properties of the systems that relate stereochemical changes to differences in retention times are not understood at present, but experiments designed to help an understanding are in progress.

## Experimental Procedure

The gas-liquid chromatography was carried out by use of the "Aerograph" gas chromatograph (Wilkens Instrument and Research, Inc.) at 180° on a column (0.6 cm i. d.) packed with Apiezon L grease (20%) on firebrick. The flow rate (helium) was 45 ml per minute and the relative retention times were determined by using internal standards of mixed α- and β-tetra-O-trimethylsilylxylopyranoses or--where convenient--penta-O-trimethylsilylribitol. They were reproducible to ± 0.01.

The trimethylsilylation reactions were carried out as described in the preceding paper, and the ethers were injected into the chromatograph without the aid of a solvent.

[7]C. T. Bishop and F. P. Cooper, Can. J. Chem. 40, 224 (1962).

## 5. THE TRIMETHYLSILYLATION OF XYLOSE AND THE NUCLEAR MAGNETIC RESONANCE SPECTRA OF THE MAJOR PRODUCTS

Robert J. Ferrier* and Mary F. Singleton

Trimethylsilylation has been employed to render carbohydrates and other nonvolatile compounds hydrophobic and susceptible of purification by distillation or of treatment by gas-liquid partition chromatography. Hedgley and Overend[1] have described the preparation and vapor-phase chromatography of several products obtained on treating nonreducing carbohydrate derivatives with trimethylsily chloride in pyridine solution and, although all these compounds were shown to be chromatographically homogeneous, it was mentioned briefly that multiple peaks were obtained on similar treatment of free sugars. Trimethylsilyl ethers of monosaccharides[2, 3, 4, 5] have been reported elsewhere, but none has been studied in detail. We have examined the action of this reagent on pyridine solutions prepared from crystalline aldoses and also from dried syrupy mutarotated mixtures of isomers. The products were all submitted to gas-liquid partition chromatographic analysis, and with each sugar it was observed that the ethers obtained from the crystalline aldoses contained one main component with either two or three resolvable minor ones, whereas those derived from the mixed isomers contained the same products but in greatly different proportions. This led to the conclusion that the observed multiple peaks were due to resolved isomers and not to degradation during examination.[2] The ethers of xylose were most readily resolved and were therefore selected for further examination.

Crystalline α-D-xylopyranose was dissolved in pyridine, and trimethylsilyl chloride was slowly added with stirring. The products were purified by extraction and distillation, and four completely resolved components (I-IV) were detected by the analytical gas chromatograph. The relative retention times were 1.0, 0.73, 0.55, and 0.44, and the relative proportions of the products calculated by measuring the areas under the peaks were 8.5, 80, 5.5, and 6. The ethers obtained by trisylation of dried mutarotated syrupy xylose had the same relative retention times, but now the percentage composition of the mixtures was 47, 47, 3, and 3. By courtesy of Mr. T. Johns of Beckman Instruments, Inc., the two major

---

*Present address: Chemistry Department, Birkbeck College, University of London.

[1] E. J. Hedgley and W. G. Overend, Chem. & In. (London) 378 (1960).

[2] F. A. Henglein and K. Scheinost, Makromol. Chem. 21, 59 (1956).

[3] R. Schwarz, E. Baronetzky, and K. Schoeller, Angew. Chem. 68, 335 (1956).

[4] F. A. Henglein, G. Abelsnes, H. Henecka, K. Lienhard, P. Nakhre, and K. Scheinost, Makromel. Chem. 24, 1 (1957).

[5] Scheng-Lieh Liu and Chin-Hsia Ho, J. Chinese Chem. Soc. (Formosa) 6, 137 (1961).

components (I and II) of the mixture were obtained in chromatographically pure form. Compound I was a colorless mobile oil; II crystallized readily to a low-melting solid that was soluble in all the common organic solvents, including petroleum ether. Other related polytrimethylsilyl compounds that have been obtained crystalline during the course of this work are methyl tri-O-trimethylsilyl-α-L-arabinopyranoside and hexa-O-trimethylsilyl-myo-inositol (see Table 5-II). Chemical analysis indicated that the compounds were isomeric and fully substituted -- they were devoid of OH absorptions in the infrared region. The molecular rotations, $[M]_I$ - 158 ($CHCl_3$), $[M]_{II}$ + 213 ($CHCl_3$), $[M]_{\text{methyl tri-O-methyl-}\beta\text{-D-xylopyranoside}}$ -150($CHCl_3$) and $[M]_{\text{methyl tri-O-methyl-}\alpha\text{-D-xylopyranoside}}$ + 177 (MeOH), indicate that I and II had β- and α- configurations, respectively. The possibility that both had pyranose ring structures was further examined by nuclear magnetic resonance (NMR) spectroscopy.

In Figs. 5-1 and 5-2 the spectra obtained for compounds I and II in chloroform solution are compared with those of tetra-O-acetyl-β- and -α-D-xylopyranose measured in the same solvent by Lemieux, Kullnig, Bernstein, and Schneider,[6] who were able to assign the four groups of signals obtained in their spectra to the four different kinds of hydrogen atoms in the molecules. Lenz and Heeschen have reported the NMR spectra of α- and β-glucopyranose and of an equilibrated mixture of xyloses measured in deuterium oxide.[7] Their xylose spectrum is included in Fig. 5-1.

The doublets of unit intensity that occur at lowest fields (5.17 and 5.65 τ) in the spectra of the two trisyl compounds are assigned to the anomeric (i.e., the least shielded) hydrogens. Their observed coupling constants, 2.5 and 7 cps (cycles per second), are consistent with those to be expected for α- and β-pyranose derivatives, since these, in perfect chair conformations, have angles between the C(2)-C(1)-H(1) and C(1)-C(2)-H(2) planes close to 60° and 180°. The Karplus calculations predict, for the corresponding coupling constants, 1.7 and 9.2 cps,[8] and those found for the α- and β-xylopyranoses and their derived acetates are 2.2 and 7.2 cps and 2 and 6 cps, respectively. If it could be assumed that furanose rings were planar, this evidence alone would suffice to prove ring size, since the α- and β-xylofuranose compounds would be expected to have $J_{1-2}$ near 8.2 and 2.2 cps. Accumulating thermodynamic,[9] spectroscopic,[10] crystallographic,[11] and

[6] R. U. Lemieux, R. K. Kullnig, H. J. Bernstein, and W. G. Schneider, J. Am. Chem. Soc. 80, 6098 (1958).

[7] R. W. Lenz and J. P. Heeschen, J. Polymer Sci. 51, 247 (1961).

[8] M. Karplus, J. Chem. Phys. 30, 11 (1959).

[9] K. S. Pitzer and W. E. Donath, J. Am. Chem. Soc. 81, 3213 (1959).

[10] F. V. Brutcher, T. Roberts, S. J. Barr, and N. Pearson, J. Am. Chem. Soc. 81, 4915 (1959).

[11] M. Spencer, Acta Cryst. 12, 59 (1959).

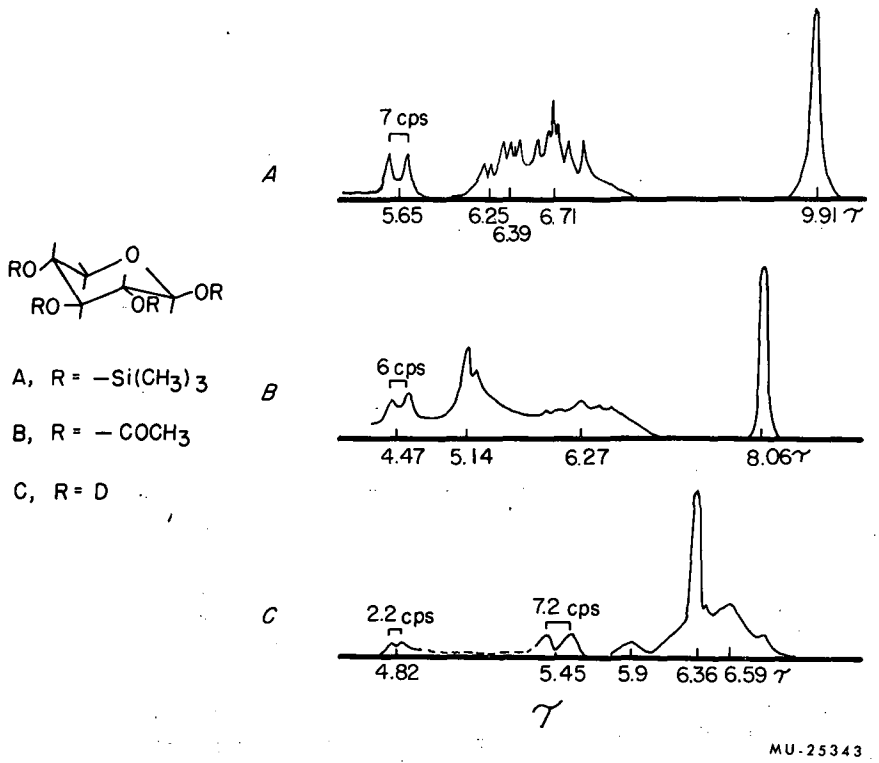


Fig. 5-1. The NMR spectra of β-D-xylopyranose derivatives: (A) trimethylsilyl ether in chloroform, (B) acetyl ester in chloroform (Ref. 6), (C) free sugar (with α isomers) in $D_2O$ (Ref. 7).

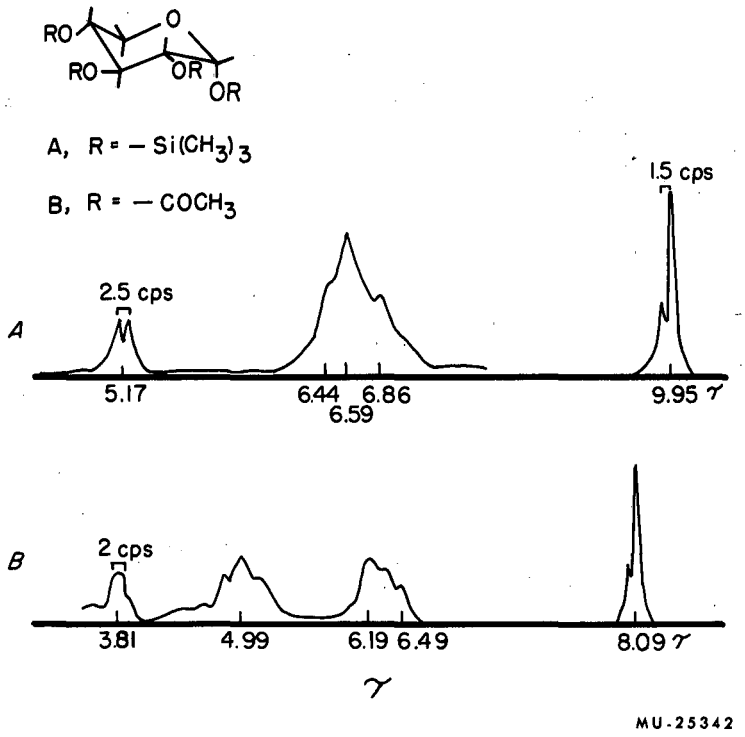


Fig. 5-2. The NMR spectra of α-D-xylopyranose derivatives in chloroform: (A) trimethylsilyl ether, (B) acetyl ester (Ref. 6).

NMR[12, 13, 14] evidence suggests that this assumption cannot be made. The difference in chemical shifts, 0.48 ppm (parts per million), of the two anomeric protons in the trisyl ethers is consistent with their being on six-membered rings, since the corresponding differences in shifts between the C(1) hydrogens in the xylopyranoses and their acetates are 0.63 and 0.65 ppm. The β- members of all three pairs resonate at higher fields. The information available on the chemical shifts of anomeric hydrogens on furanose rings [glycofuranosylamines,[13] 3.8 τ (both α and β); 1, 2-O-isopropylidene-α-furanose derivatives,[15] 4.1 τ], and the electronic effect of the trimethylsilyl group (see below) indicate that if either of the trisylated xyloses had a furanose structure, the τ value of the anomeric proton would be considerably smaller than the determined value. We conclude that both isomers are pyranose derivatives and note that the equatorial anomeric proton, as in the free sugars and acetates, resonates at lower fields than the axial. Finally, regarding the anomeric center, the signals from the axial and equatorial hydrogens in the trisylated derivatives occur at positions 1.18 and 1.36 ppm, respectively, up-field from the corresponding ones in the acetate spectra[6] and 0.20 and 0.35 ppm, respectively, up-field from the free xyloses.[7] Trisylation of simple alcohols also causes small shifts; the signals from the α protons in methanol, ethanol, and isopropanol before and after trisylation are: 6.62 and 6.76 τ; 6.44 and 6.39 τ; 6.15 and 6.16 τ.

The complex signals at 6.1 to 7.3 τ must be assigned to the ring methylene protons together with those at C(2), C(3), and C(4). Therefore, replacement of acetoxy by trimethylsilyloxy groupings at these carbon atoms also causes a shift in the signals of the α-hydrogens by + 1.4 ± 0.3 ppm. The multiplet at 6.25 τ in the spectrum of the β- compound is tentatively assigned to the equatorial proton of the C(5) methylene group following the finding that this proton in tetra-O-acetyl-β-D-xylopyranose resonates 0.6 ppm down-field from the axial one on the same carbon atom.[6] It is clear (see Figs. 5-1 and 5.2) that introduction of the bulky axial trimethylsilyloxy grouping at C(1) in the α- isomer affects not only the signal of the hydrogen at that position but also those from the other hydrogens on the ring. The result is that the equatorial proton absorbs at higher fields whereas the axial protons apparently suffer a shift in the other direction. (Lack of resolution in the spectrum of the α- isomer makes definite assignments difficult.) This could be explained most readily in two ways: (a) by the flattening of the pyranose chair as a result of the steric repulsions introduced between the large axial group and the hydrogens at C(3) and C(5), which causes all the "purely axial" protons to assume some equatorial character, and vice-versa--thus diminishing the difference between their chemical shifts -- or (b) by the effect of the magnetic anisotropy of the axial C-O bond.[14]

---

[12] C. D. Jardetzky, J. Am. Chem. Soc. 84, 62 (1962).

[13] R. U. Lemieux, Canad. J. Chem. 39, 116 (1961).

[14] R. J. Abraham, K. A. McLauchlan, L. D. Hall, and L. Hough, Chem. & Ind. 213 (1962).

[15] L. N. Jackman, Applications of Nuclear Magnetic Resonance Spectroscopy in Organic Chemistry (Pergamon Press, London, 1959), p. 112.

It can be noted from the detailed analyses of the spectra of the tetra-O-acetylpentopyranoses[16] measured by Lemieux et al. that inversions of equatorial acetoxy groupings in the all-equatorial β-xylose isomer invariably cause shifts of signals of all ring axial hydrogens to lower fields. Determination of the direction of the shifts resultant upon the introduction of an anisotropic axial group into a geometrically undisturbed ring would not give this result.[15] For example, in β-ribose tetraacetate the anisotropic effect of the axial C-O bond at C(3) would decrease the shielding of the axial protons at C(2) and C(4), but it would shield those at C(1) and C(5). Furthermore, Lenz and Heeschen found that in β-glucose the axial protons at C(2) to C(5) gave a single peak at 6.57 $\tau$, whereas in the anomer the signal from these protons occurred at 6.41 $\tau$ and overlapped with the C(6) proton signals.[7] Again, this is consistent with the concept of ring flattening in the α-isomer. The anisotropic effect of this axial hydroxyl group alone would not have given this result but would have decreased the proton shielding at C(2) by 0.18 ppm[17] and shielded those at C(3) and C(5) by 0.16 ppm and 0.22 ppm,[17] respectively. Therefore on this evidence, it becomes attractive to suggest that introduction of axial substituents into a pyranose ring results in generalized flattening, with loss by the other ring substituents of some of their axial or equatorial nature. This is more in keeping with the accepted ideas of conformational aspects of substituted cyclohexane chemistry than Lenz and Heeschens' conclusion -- derived (after many assumptions) from coupling constants of the anomeric protons -- that β-glucose shows more distortion from a perfect C1 chair than does the α-isomer.[7]

Finally, it is noted that the signals (9.9 $\tau$) from the hydrogens on the trimethylsilyl groupings in the case of tetra-O-trimethylsilyl-α-D-xylopyranose have been resolved; whereas those from the axial groupings appear at lower fields. This is consistent with the findings of Lemieux et al.[6] that axial acetoxy groupings produce signals at lower fields than do equatorial acetoxy groupings.

The NMR spectra of several other trimethylsilyl ethers were measured and compared with those of the corresponding acetates to determine whether or not the signals derived from hydrogen atoms on similar carbons bearing trimethylsilyloxy and acetoxy groupings generally differ as in the pyranose compounds. In Table 5-I the positions of the signals assigned to these hydrogens are noted together with the differences between the pairs of chemical shifts. Clearly, the effect on protons on secondary carbon atoms is general, and attributable to the stronger electron-withdrawing influence of the acetoxy group. Going from secondary to primary carbons, the differences decrease.

---

[16] J. A. Pople, W. G. Schneider, and H. J. Bernstein, High Resolution Nuclear Magnetic Resonance (McGraw-Hill Book Co., Inc., New York 1959), p. 397.

[17] Calculated from the equation $\sigma = (1-3\cos^2\theta/3r^3)\Delta x$; $\theta$ and r were measured from Dreiding molecular models. The Lenz and Heeschen[7] value $\Delta x_{c-o} = 10.8 \times 10^{-30}$ cm$^3$/molecule was used.

Table 5-I. The position of resonance of protons on secondary carbon atoms bearing (a) acetoxy groupings, (b) trimethylsilyloxy groups. (Measurements are made from the mid-points of the signals.)

| Derivative of | Proton(s) under examination | Position of resonance ($\tau$ values) (a) Acetate | (b) Trisyl ether | Change in position of resonance (ppm) |
|---|---|---|---|---|
| Methanol | C(1) | 6.76 | 6.76 | 0.00 |
| Ethanol | C(1) | 6.19 | 6.39 | 0.20 |
| Isopropanol | C(2) | 5.37 | 6.16 | 0.79 |
| Cyclohexanol | C(1) | 5.55 | 6.49 | 0.94 |
| myo-Inositol[b] | C(1), C(6) | 4.77 | 6.5[a] | 1.73 |
| α-xylopyranose[b] | C(1) | 3.81 | 5.17 | 1.36 |
| β-xylopyranose[b] | C(1) | 4.47 | 5.65 | 1.18 |
| α-, β-xylopyranose[b] | C(2), C(4) | 5.2 | 6.6 | 1.4 |

(a) complex multiplet

(b) fully substituted derivatives

There is a progressive increase in the difference in chemical shifts between the pairs of the series $CH_3$-X (X = OAc, O-trisyl), $C_2H_5$-X (X = OAc, O-trisyl), and $(CH_3)_2$-CHX (X = OAc, O-trisyl). Similar effects have been noted before and have been illustrated by Jackman.[15]

## Experimental

### Trimethylsilation of xylose

The method of Hedgley and Overend[1] was adapted; the sugar was dissolved in pyridine, and the reagent was added slowly with stirring. Immediate work-up by evaporation to dryness under reduced pressure, extraction of the residue with ether, removal of the ether, and vacuum distillation of the ether-soluble material gave good yields of colorless mobile oils. Analytical gas-liquid chromatography was performed by using the "Aerograph" gas chromatograph (Wilkens Instrument and Research, Inc.) at 180° on a column (5 ft, 1/4 in. i.d.) packed with Apiezon L grease (20%) on firebrick. Convenient retention times were achieved with flow rates of 50 to 75 ml per minute of helium. The preparative separation was carried out by use of the Beckman "Megachrom" instrument and silicone elastomer columns.

The fraction (I) with the highest retention time on the columns, characterized as tetra-O-trimethylsilyl-β-D-xylopyranose, was a colorless mobile oil $[\alpha]_D$ - 36° (1.5 g per 100 ml $CHCl_3$). (Found: C, 46.0%; H, 9.5%; part lost on complete hydrolysis in 50% aqueous ethanol: 64.8%. $C_{14}H_{42}O_5Si_4$ required C, 46.5%; H, 9.6%; part removed on hydrolysis, 65.8%). It was free from hydroxyl absorptions in the infrared region. Fraction II, tetra-O-trimethylsilyl-α-D-xylopyranose, had a retention time on the silicone columns of 0.79 that of fraction I, and crystallized in the receiving vessel. The solid had mp 30–32° (without recrystallization), $[\alpha]_D$ + 48.5° (2.0 g per 100 ml $CHCl_3$). (Found: C, 46.4%; H, 9.3%; part removed on hydrolysis, 64.1%.) No absorptions from hydroxyl groupings were present in the infrared spectrum.

### Reference materials

Isopropyl and cyclohexyl acetates were obtained commercially. Hexa-O-acetyl myo-inositol was prepared from the commercially available cyclitol. The corresponding trimethylsilyl compounds (Table 5-II) were prepared by trisylation of the appropriate alcohols in cooled pyridine solutions to which suitable diluents were added.

### Spectral measurements

The spectra were obtained at room temperature by using a Varian V-4311 NMR spectrometer at 60 Mc. Solutions were 20% carbohydrate material in chloroform. Chemical shifts were determined by the audio-frequency side-band technique and were measured relative to the chloroform resonance. Values of $\tau$ were calculated by measuring the chemical shift of chloroform from tetramethylsilane independently, yielding $\tau_{CHCl_3}$ = 2.73. No correction was made for a small hydrogen bonding shift of the $CHCl_3$ resonance (approximately -0.05 unit) which would occur in our 20% carbohydrate solutions. The $\tau$ values for Lemieux's spectra were calculated by using $\tau_{CHCl_3}$ = 2.59 (Lemieux, private communication).

Table 5-II. New trimethylsilyl ethers.

| Trimethylsilyl ethers | bp (°C) | mp (°C) | $n_D^{25}$ | %C | | %H | | % removed on complete hydrolysis | |
|---|---|---|---|---|---|---|---|---|---|
| | | | | Found | Calc. | Found | Calc. | Found | Calc. |
| Isopropyl | 85–86 | | 1.3811 | 54.7 | 54.5 | 11.7 | 12.1 | - | - |
| Cyclohexyl | 169–170 | | 1.4289 | 62.9 | 62.8 | 11.5 | 11.6 | - | - |
| myo-Inositol | - | 117–118 from aqueous methanol | - | 47.4 | 47.1 | 9.8 | 9.8 | 68.0 | 78.6 |

## 6. LIGHT-DARK TRANSIENT CHANGES IN CONCENTRATION OF SUGAR PHOSPHATES OTHER THAN RIBULOSE DIPHOSPHATE IN CHLORELLA

James A. Bassham and Martha Kirk

Changes in concentration of photosynthetic intermediates in algae upon sudden onset of darkness have been studied many times in this Laboratory--beginning with the work of Massini[1] and later continued by Bassham et al.[2] In all these studies the algae were permitted to photosynthesize in the presence of $^{14}CO_2$ for some time (such as 20 minutes) sufficiently long to saturate the $C^{14}$ labeling of the intermediates of the carbon-reduction cycle (Calvin cycle), after which the light was turned off. When samples were taken before the light was turned off, chromatographic analysis of the radioactive products of photosynthesis gave a measure of the concentrations of the reservoirs of cycle intermediates that were actively turning over. Samples taken just after the light was turned off and analyzed in the same way showed variations in the concentrations of individual compounds resulting from this change in external conditions.

Massini observed that upon darkness the level of PGA rose rapidly while the diphosphate-area radioactivity dropped rapidly. Bassham[2] found that of the diphosphates, ribulose diphosphate concentration dropped from a 0.5 μM per cc of algae (Scendesmus) to below detectable limits (< 0.0005 μM) when the light was turned off. In the same experiment, the level of fructose diphosphate dropped from 0.004 μM to 0.001 μM, and sedoheptulose diphosphate remained unchanged at 0.006 μM. Of the monophosphates, pentose and triose monophosphates concentrations dropped about 50% while heptose and hexose monophosphates remained unchanged. The change in ribulose diphosphate concentration was the most striking and proved to be of great importance, since it led to the discovery of the carboxylation of ribulose diphosphate (confirmed by Wilson's study of the transient changes accompanying sudden $CO_2$ depletion[3]). Since the fructose diphosphate concentration was very small before the light was turned off, its light-dark transient change was not striking. In any event, since triose phosphate may be expected to decrease in concentration in the dark, and does, the decrease in fructose diphosphate formed from triose phosphate is easily explained.

In our studies of the dynamics of the photosynthesis of carbon compounds[4, 5] we have used Chlorella pyrenoidosa and have gone to ever-increasing pains to achieve truly steady-state conditions of photosynthesis before and during the exposure to $^{14}CO_2$. In some reported experiments we have worked just at light saturation, whereas more recently we have worked at

---

[1] M. Calvin and P. Massini, Experientia VIII/12, 445 (1952).

[2] J. A. Bassham, K. Shibata, K. Steenberg, J. Bourdon, and M. Calvin, J. Am. Chem. Soc. 78, 4120 (1956).

[3] A. T. Wilson and M. Calvin, J. Am. Chem. Soc. 77, 5948 (1955).

[4] J. A. Bassham and Martha Kirk, Biochim. Biophys. Acta 43, 447 (1960).

[5] D. C. Smith, J. A. Bassham, and Martha Kirk, Biochim. Biophys. Acta 48, 299 (1961).

subsaturating light intensities. In our most recent report[6] we noted that with light intensities that gave 5 μM of $CO_2$ uptake per min per cc of algae (vs about 20 μM per min at saturation intensities) the total concentration of all compounds in the cycle (as carbon atoms) was about 5 μM of carbon instead of 12 μM or more.

We have now performed light-dark transient studies beginning with these steady-state low-light-intensity conditions (but resulting in somewhat larger concentrations). The PGA concentration increases, just as it did in previous experiments, though not so much. No doubt the smallness of the PGA increase is accounted for by the small reservoir of ribulose diphosphate available for carboxylation when the light is turned off (only about 0.15 μM).

The light-dark transient changes in sugar diphosphates are shown in Fig. 6-1, those of sugar monophosphates in Fig. 6-2, and those of triose and pentose monophosphates in Fig. 6-3. Perhaps the most striking difference from previously reported experiments is the behavior of fructose diphosphate. Under these conditions, its concentration starts at 0.22 μM per cc of algae and drops in the dark almost to zero, coming back to about 0.01. In the same experiment, ribulose diphosphate has a steady-state concentration approaching 0.15 and drops to zero. "Glucose diphosphate" (whose chemical identity is not known) and sedoheptulose diphosphate also drop in concentration in the dark, but tend to come back.

Among the sugar monophosphates, fructose-6-phosphate drops rapidly in concentration from 2.4 μM of carbon per cc of algae to about 0.5 μM. Glucose-6-phosphate concentration rises and then falls.

As expected, the concentration of triose phosphate drops very rapidly from 0.2 to 0.04 μM of carbon. The concentrations of pentose phosphates, small to begin with, decline.

The changes observed in this experiment are quantitatively rather different from those reported previously. However, it appears to be easy enough to explain them in terms of the Calvin cycle and reactions leading from it. The primary effect of turning off the light is to stop the supply of the cofactors which drive the cycle -- thought to be ATP and TPNH. Without ATP the phosphorylation of ribulose monophosphate to give ribulose diphosphate stops, and the ribulose diphosphate is used up by the carboxylation reaction, i.e., making PGA. Without ATP and TPNH, PGA is no longer reduced to triose phosphate which, therefore, decreases rapidly in concentration.

The cyclic utilization of fructose-6-phosphate requires triose phosphate, and the 0.12 μM of carbon drop in triose may account for a 0.18 μM drop in fructose-6-phosphate (out of the total drop of 1.9 μM). The fructose diphosphate probably is converted both ways -- to fructose-6-phosphate and also back to triose phosphate. An additional large amount of fructose-6-phosphate probably is used in the synthesis of carbohydrates.

---

[6] Martha Kirk and J. A. Bassham, in Bio-Organic Chemistry Quarterly Report, UCRL-10032, Sept. 1961, p. 78.

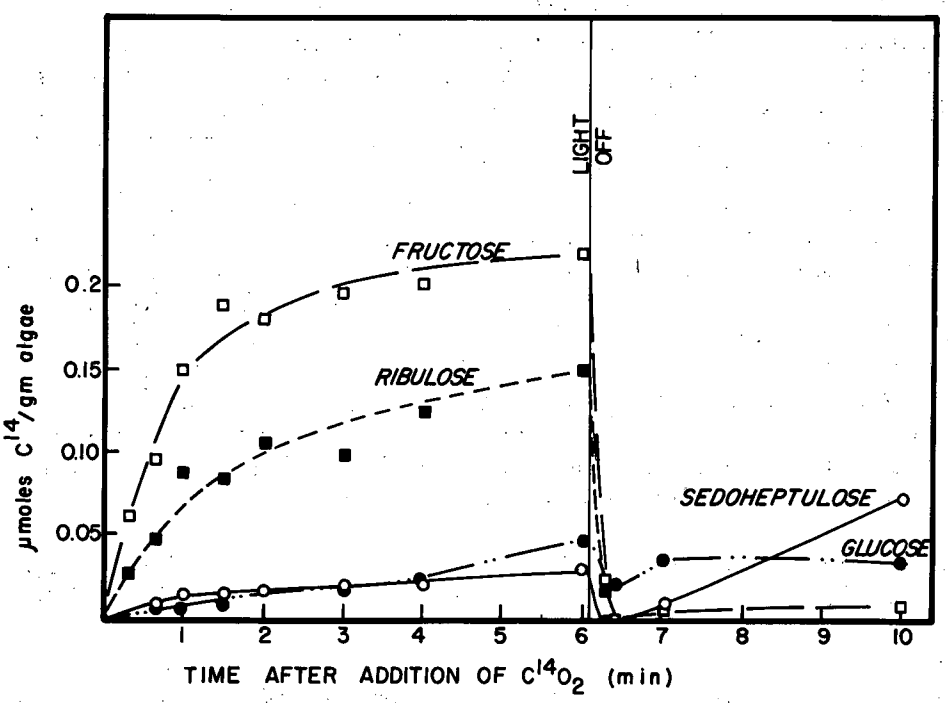


Fig. 6-1. Light-dark transients in concentrations of sugar diphosphates.

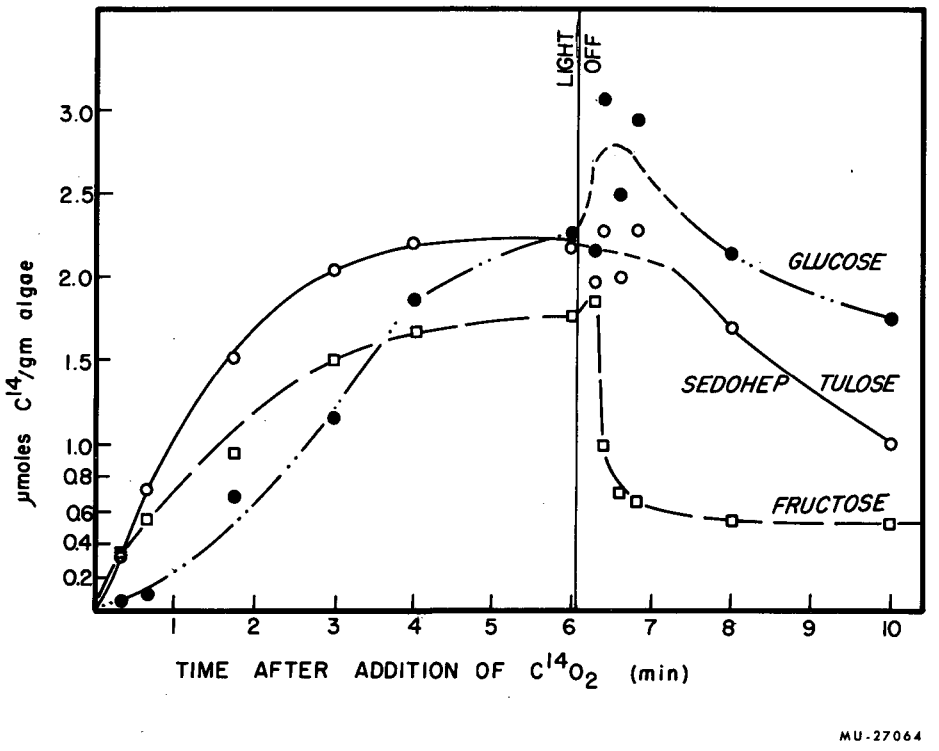


Fig. 6-2. Light-dark transients in concentrations of hexose and heptose monophosphates.

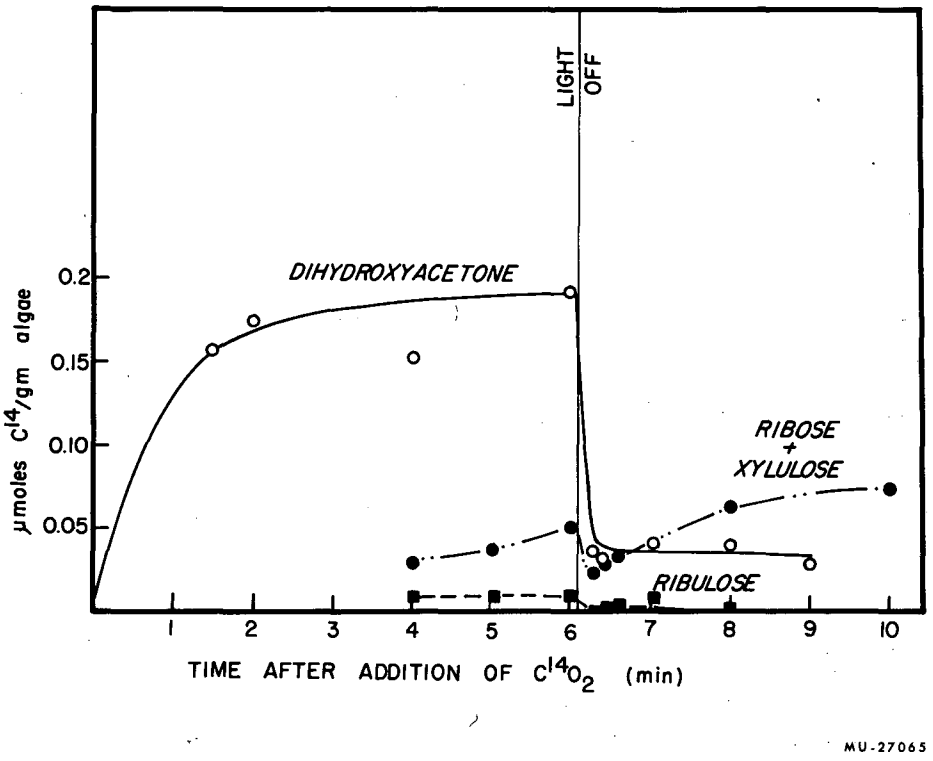


Fig. 6-3. Light-dark transients in concentrations of pentose and triose monophosphates.

The higher concentration of fructose diphosphate at low-light intensities,[6] when other sugar-phosphate concentrations (including those of triose phosphates) are lower, is hard to explain. Perhaps it is merely that higher-light intensities lower the inorganic phosphate concentration in the chloroplast by producing a high rate of photosynthetic phosphorylation and carbon-dioxide reduction. This lower inorganic phosphate concentration at high-light intensity might stimulate the phosphatasing of fructose diphosphate.

# 7. THE PREPARATION AND PARTIAL CHARACTERIZATION OF A PIGMENT-PROTEIN COMPLEX FROM THE LAMELLA OF HIGHER PLANT CHLOROPLASTS

John Biggins and Roderic B. Park

We have developed a technique for the preparation of a pigment-protein complex from spinach and barley chloroplasts. Preparations were found to be homogeneous in the ultracentrifuge and optically similar to quantasome aggregates. We are directing further work towards a full physical characterization of the macromolecule in order to ascertain whether it corresponds to the quantasome.

## Introduction

Photosynthetic pigments in higher plant chloroplasts are localized in a highly differentiated lamellar system. The lamellar system is embedded in a soluble protein matrix called the stroma. Quantum conversion has been demonstrated in isolated lamellae.

On the basis of electron microscope studies, Park and Pon[1] suggested a model for the substructure of the chloroplast lamellae and proposed that they consist of subunits that are 200- to 100-Å oblate spheroids. The spheroids are bound to a continuous unit membrane. The oblate spheroids have been termed quantasomes,[2] and it is possible that these structures may be the morphological expression of the physiological photosynthetic unit formulated by Emerson and Arnold.[3]

Sonic fragmentation of the chloroplast lamellae results in a heterogeneous system that can be partially resolved by differential ultracentrifugation. The smallest particles obtainable by this technique consist of aggregation of up to eight quantasomes, and their rates of quantum conversion are similar to unbroken lamellae.[1] Although these preparations are satisfactory for metabolic studies, their polydispersity impedes certain precise physical measurements.

This report describes a technique for the fragmentation of the chloroplast lamella that yields a monodisperse preparation of a pigment-protein complex.

## Materials and Methods

### 1. Chloroplast preparation

Chloroplasts were isolated from the leaves of spinach and barley by a procedure described by Park and Pon.[1] Barley was grown from germination in complete darkness, and 6-day-old seedlings were illuminated from 8 to 12 hours prior to chloroplast isolation.[4]

---

[1] R. B. Park and N. G. Pon, J. Mol. Biol. 3, 1 (1961).

[2] R. B. Park, J. Chem. Ed. (1962), in press.

[3] R. Emerson and A. Arnold, J. Gen. Physiol. 16, 191 (1932).

[4] John Biggins and Roderic B. Park, UCRL-10156, April 1962, p. 40.

2. Centrifugation

A Spinco Model L ultracentrifuge was used for preparative procedures and zone density gradients were used in an SW 39L rotor. Analytical ultracentrifugation was carried out on a Spinco Model E ultracentrifuge using a single-sector cell and schlieren optics.

3. Gel filtration

Gel filtration was used for the rapid removal of low-molecular-weight solutes from preparations. Sephadex G-25 columns, 1 by 20 cm, were equilibrated with appropriate buffers, and 1-ml samples of preparations, irrespective of concentration, were purified by elution with the same buffer. The holdup volume on these columns was between 3 and 4 ml.

4. Spectrophotometry

A Cary Model 14R recording spectrophotometer with 1-cm cuvettes was used to obtain the spectra.

A flow diagram of the preparative procedure is shown below:

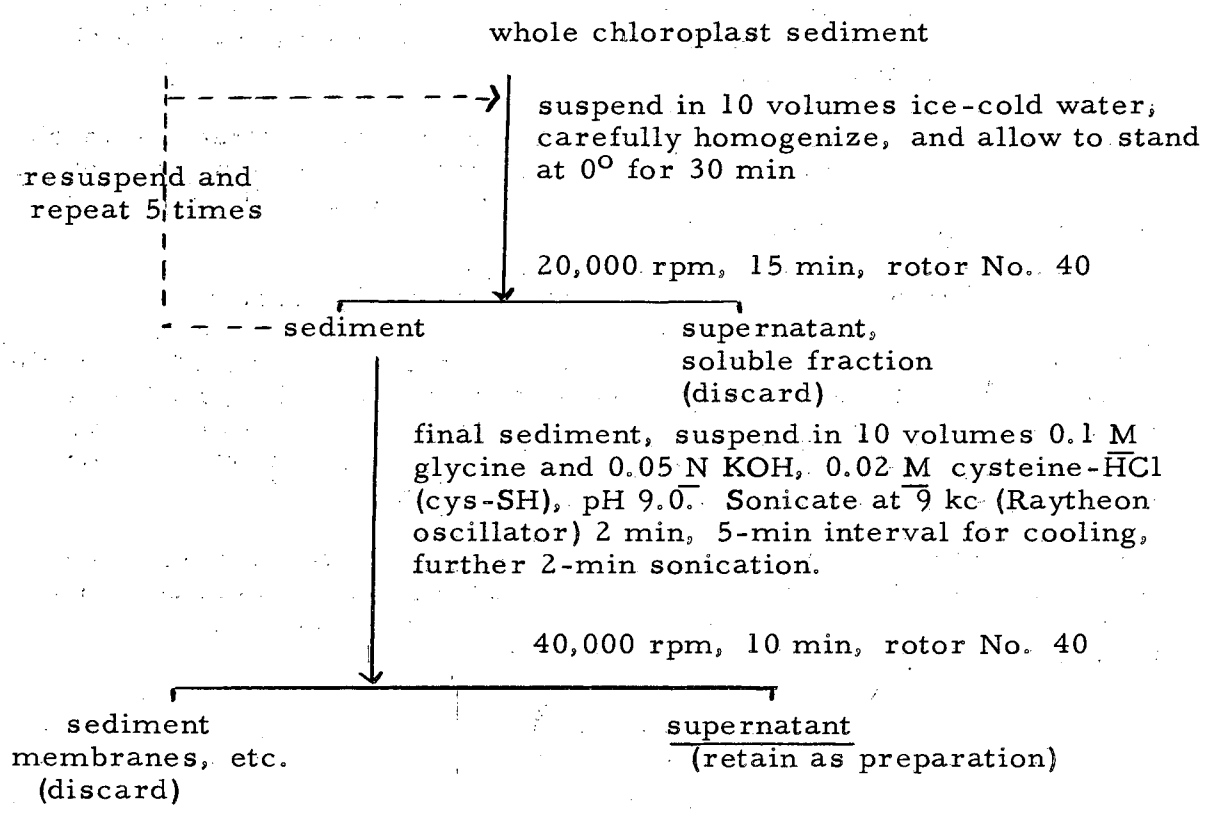

The final supernatant is allowed to stand at room temperature for 30 min or overnight at 0°. This preparation is concentrated by a zone density-gradient centrifugation using sucrose-buffer solutions. A 5-ml lusteroid tube (SW39L rotor) is layered with sucrose-buffer solutions of various densities to form a discontinuous density gradient as follows:

(a) 3-ml final supernatant in cys-SH buffer at pH 9.0
(b) 0.25 ml, d 1.14
(c) 0.25 ml, d 1.16
(d) 0.25 ml, d 1.19
(e) 0.25 ml, d 1.316

} 2.5 M sucrose-cys-SH buffer at pH 9.0 at indicated densities

This is centrifuged at 35,000 rpm for 3 h, using the SW39L rotor. A green fraction collects in the d-1.19 band and is removed by means of a syringe and hypodermic needle (by lateral entry through the lusteroid tube). The fractions from three tubes are combined, yielding approximately 1 ml, and placed on a Sephadex G-25 column equilibrated with the cys-SH buffer and eluted with the same buffer. The eluted preparations were shown to be free of sucrose after this treatment.

## Results and Discussion

Figure 7-1 shows a complete spectrum of a preparation from spinach chloroplasts. The spectrum is similar to that obtained by Sauer[5] for quantasome aggregates. The ultraviolet region is anomalous owing to absorption by cysteine in the buffer.

Figure 7-2 shows the sedimentation pattern of a concentrated spinach preparation taken 8 min after reaching 27,000 rpm. The pigment, visible in the sclieren optical system, is clearly associated with the boundary, and the preparation appears homogeneous.

Measurements on barley preparations yield similar results.

Preliminary data on the sedimentation behavior of the pigment-protein complex indicates that the sedimentation constant is approximately S = 86. The preparations were found to be entirely free of fraction I protein, the major protein constituent of green leaves, which has a sedimentation constant $S_{w,20}$ = 16 to 17.

As the preparation appears homogeneous in the ultracentrifuge, we are now attempting a full characterization of the pigment-protein complex in order to ascertain whether this macromolecule corresponds to the quantasome.

[5] K. H. Sauer, UCRL-10156, April 1962, p. 54.

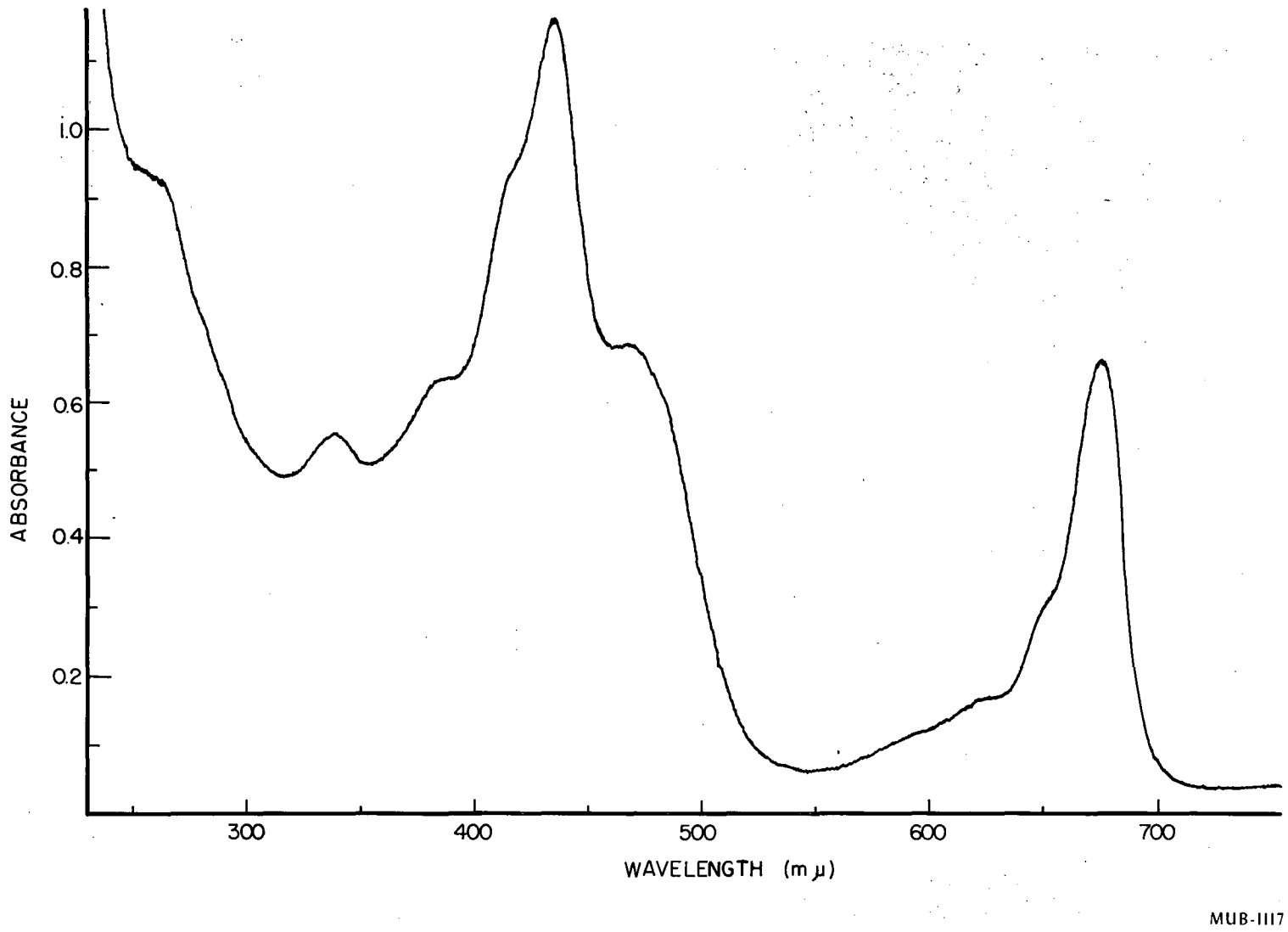


Fig. 7-1. Absorption spectrum of the pigment-protein complex in glycine-cysteine buffer at pH 9.0.

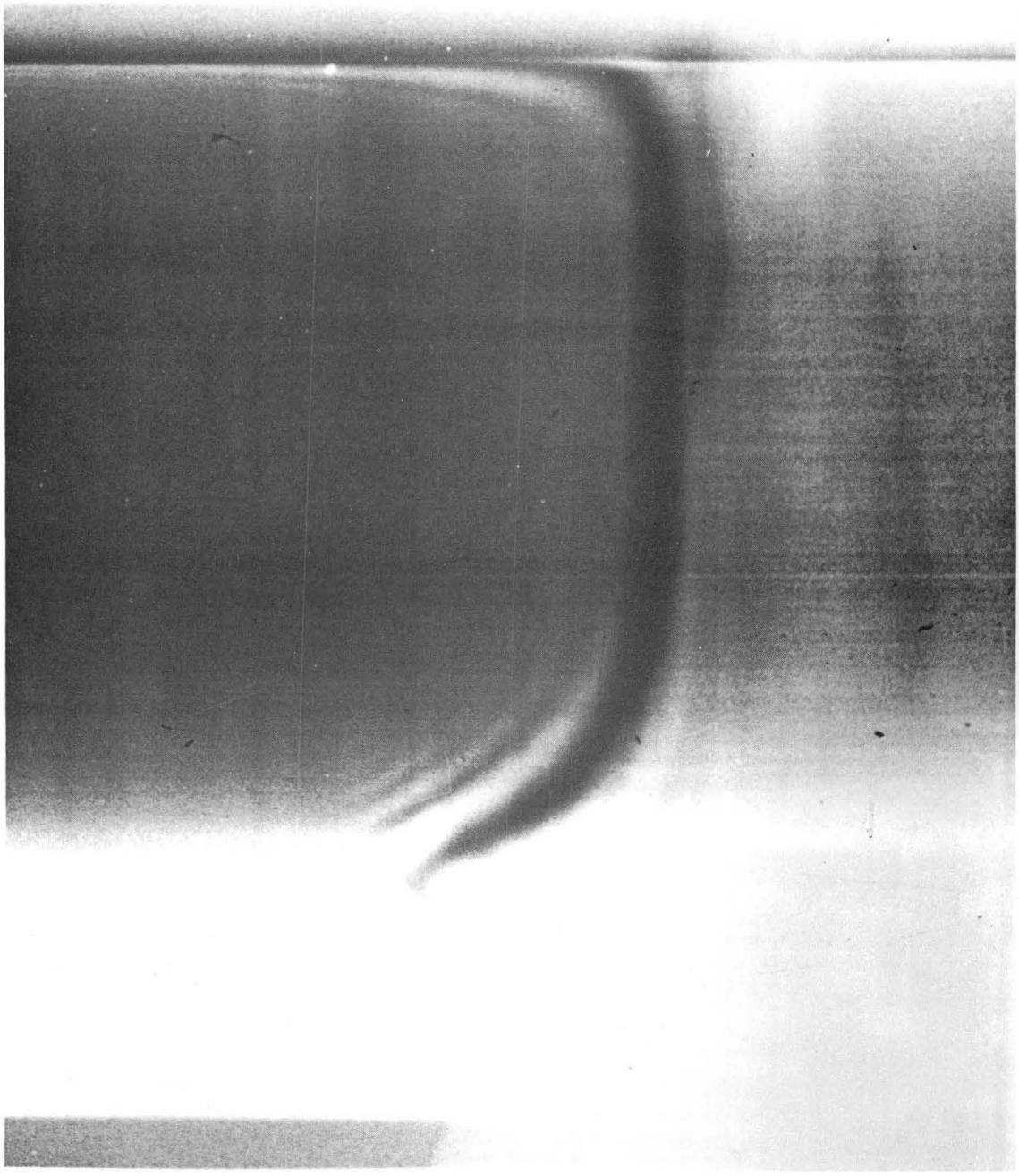

ZN-3234

Fig. 7-2. Sedimentation pattern of the pigment-protein from spinach chloroplasts in cys-SH buffer taken 8 min after reaching 27,000 rpm. Sedimentation is to the right.

# 8. CHEMICAL COMPOSITION AND SUBSTRUCTURE OF LAMELLAE ISOLATED FROM SPINACEA OLERACEA CHLOROPLASTS

Roderic B. Park and Ning G. Pon

Purified spinach chloroplast lamellae were active in the Hill reaction. Spectrochemical analysis showed that the lyophilized lamellae contained the transition elements iron, manganese, and copper. Wet chemical analyses established the ratios of protein, lipid chlorophyll, iron, manganese, and organic phosphorus in the lamellae. A minimum molecular weight on the basis of manganese content is 960,000. This minimum molecular weight is similar to the molecular weight calculated for the quantasome. Electron microscopy of whole and extracted lamellae shows that the lipid resides largely in the surface osmiophilic layer of the lamellae.

## Introduction

The photosynthetic reactions of green plant cells are localized within chloroplasts.[1] The chloroplasts contain both the photosynthetic pigments with their associated electron transport pathways and the enzymes responsible for carbon dioxide fixation.[2,3] Thin sections of chloroplasts when viewed in the electron microscope reveal a lamellar system embedded in a granular material called stroma. The chloroplast is surrounded by a double membrane.[4,5,6,7,8] Previous work on Spinacea oleracea chloroplasts shows that the light reactions and associated electron transport pathways of photosynthesis are localized in the lamellar structures.[3] The carbon dioxide fixation enzymes, on the other hand, are associated with the stroma portion of the chloroplast. Thus, the actual conversion of light energy into chemical energy during photosynthesis takes place in the chlorophyll-containing lamellar structures. Chloroplast lamellae as viewed in the electron microscope consist of two dark lines separated by about 150 Å (see a in Fig. 8-1). The structure may be regarded as a sandwich in which each half (100 Å thick) consists of an osmiophilic unit membrane attached to small particles about 200 Å in diameter. We have called these 200-Å units, with their attached membranes, quantasomes.[9,10] The quantasomes are illustrated in Fig. 8-1, and the ways in which these units

[1] D. I. Arnon, F. R. Whatley, and M. B. Allen, J. Am. Chem. Soc. 76, 6324 (1954).

[2] A. V. Trebst, H. Y. Tsujimoto, and D. I. Aron, Nature 182, 351 (1958).

[3] R. B. Park and N. G. Pon, J. Mol. Biol. 3, 1 (1961).

[4] E. Steinmann and F. S. Sjostrand, Exptl. Cell Res. 8, 15 (1955).

[5] A. J. Hodge, Rev. Mod. Phys. 31, 331 (1959).

[6] W. Menke, Experientia 16, 537 (1960).

[7] T. E. Wier, Am. J. Bot. 48, 615 (1961).

[8] S. P. Gibbs, J. Ultrastruct. Res. 4, 127 (1960).

[9] R. B. Park, J. Chem. Educ. (in press, 1962).

[10] M. Calvin, Science 135, 879 (1962).

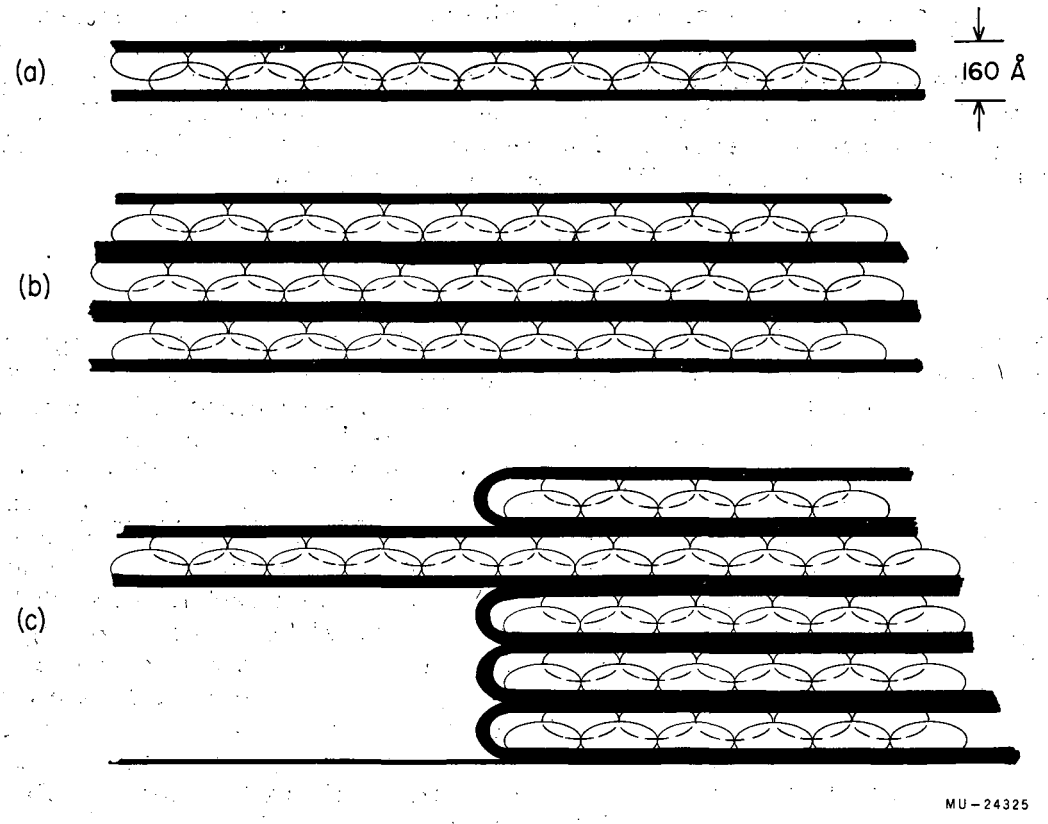


Fig. 8-1. Typical lamellar structures from (a) blue-green algae, (b) Euglena, (c) higher plants.

may combine to form various lamellar arrangements are indicated. The entire lamellar structure is not necessary to perform the light reactions of photosynthesis. Aggregates consisting of about 7 or 8 quantasomes are as effective in energy conversion as the whole chloroplast.[3] The possibility exists that the single quantasomes are the smallest units that can perform the light reactions of photosynthesis and thus are a morphological expression of the photosynthetic unit as formulated by Emerson and Arnold[11] and redetermined by Kok.[12]

Our recent work has been oriented toward formulating a more complete physical and chemical picture of the quantasome. Sauer and Calvin showed that the long-wavelength form (695 mμ) of chlorophyll is highly oriented within quantasome aggregates.[13] However, before an adequate molecular model of quantasome structure can be constructed, substances within the quantasome must be chemically analyzed and localized. This report presents data on the substructure and chemical composition within the quantasome aggregates isolated from spinach chloroplasts.

## Experimental Procedure

### (a) Isolation and purification of chloroplast lamellar structures

Spinach leaves were homogenized in a medium of sucrose, phosphate, and versenol, and filtered through cheesecloth as described previously.[3] The flow sheet for lamellar structure preparation is given in Fig. 8-2.

### (b) Lyophilization of chloroplast lamellar structures

The final precipitate (VI) obtained in the fractionation shown in Fig. 8-2 constitutes the purified chloroplast lamellar structures. This material was lyophilized by freezing to -190° and evacuating to dryness through a trap at -78°.

### (c) Spectrochemical analysis

One hundred forty-nine mg of lyophilized lamellae was ashed in a 5-ml weighed platinum crucible for 4 hours at 825°. A control consisted of an equivalent volume of the solutions used for the chloroplast preparation that had gone through the same grinding and centrifugation steps but without spinach leaves. The control was ashed in an identical way. The ash was weighed and dissolved in HCl (final volume 200 μl of 1 N HCl). Ten-microliter samples were used for the analysis. Spectrochemical analyses of the lipid and residue fractions were performed in similar fashion.

---

[11] R. Emerson and A. Arnold, J. Gen. Physiol. 16, 191 (1932).

[12] B. Kok and J. A. Businger, in Research in Photosynthesis, (Interscience Publishers, Inc., New York (1957), p. 357.

[13] K. Sauer and M. Calvin, J. Mol. Biol. (in press, 1962).

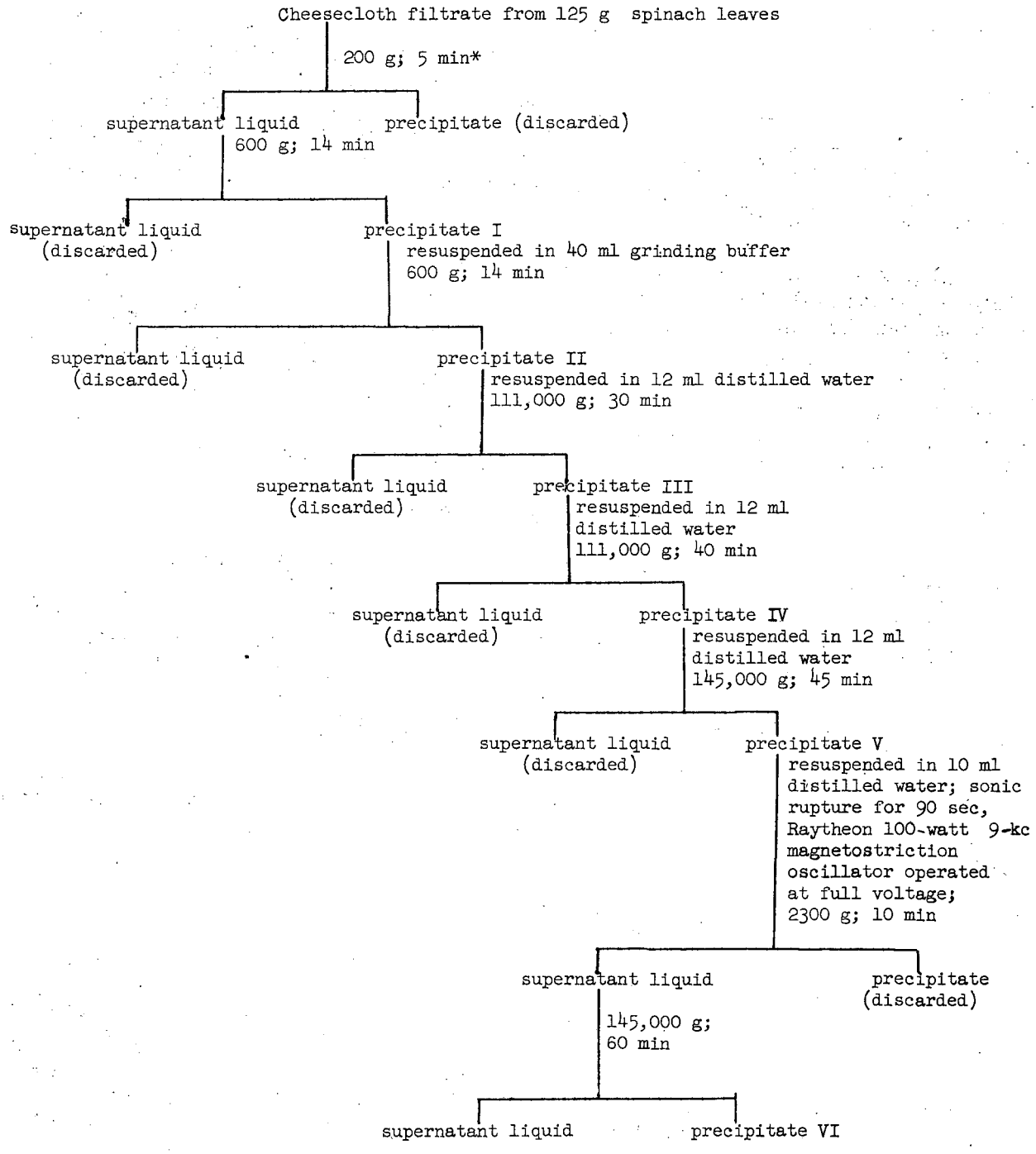


* The accelerations due to gravity (g) are maximum values. High-g runs were performed in a Spinco #40 centrifuge head.

MUB-1276

Fig. 8-2. Typical flow sheet for preparation of chloroplast lamellae.

(d) Nitrogen analysis

Nitrogen was analyzed by the Kjeldahl method as described previously.[3] This method gave results in close agreement (95 to 99%) with the theoretical values for a porphyrin ($Mn^{3+}$ hematoporphyrin IX dimethyl ester monochloride) and a phthalocyanine ($Mn^{2+}$phthalocyanine).

(e) Chlorophyll analysis

Chlorophyll concentrations were determined spectrophotometrically in 80% acetone according to the method of Arnon.[14]

(f) Manganese analysis

The method for the analysis of this element is essentially similar to that described elsewhere[15] but modified slightly to handle smaller volumes and concentrations of Mn. After digestion of the organic matter by a mixture of sulfuric and nitric acids, $Mn^{2+}$ is converted to $MnO_4^-$ by oxidation with excess $IO_4^-$. In a typical experiment, chloroplast lamellae containing between 25 and 50 mg of chlorophyll were digested in a 30-ml micro-Kjeldahl flask with 1 ml of concentrated sulfuric acid in the presence of concentrated nitric acid. The nitric acid was added in 0.2-ml portions. After each nitric acid addition the mixture was heated carefully until no more brown fumes were evolved. When the mixture became clear and nearly colorless, a few crystals of $NaHSO_3$ were added, and the mixture was heated until the fuming subsided. This step transforms any manganese in the form of $MnO_2$ and $MnO_4^-$ back to $Mn^{2+}$.

A control, for which the same solutions were used as for the chloroplast preparation and which had gone through the same grinding and centrifugation steps but without leaf material, was also digested in the above manner.

Each digested sample was transferred quantitatively to a 12-ml conical centrifuge tube and then diluted to 10 ml with especially deionized glass-distilled water. Eight ml of this solution was used for the Mn determination and the remainder for Fe determination (see below).

To the 8-ml sample for Mn determination were added concentrated (85%) $H_3PO_4$, 0.1 ml; concentrated $H_2SO_4$, 0.2 ml; and several crystals of $KIO_4$, approx 10 to 15 mg. The mixture was diluted to approx 10 ml and then heated in a hot water bath (90 to 100°) for 8 hours to develop the color fully. (A separate experiment showed that a minimum of 4 h was required to obtain maximum color yield under these conditions.) Each solution was diluted to 10 ml after it was cooled to room temperature; then, the insoluble material was spun down by use of a clinical centrifuge. The absorbance of

[14] D. I. Arnon, Plant Physiol. 24, 1 (1949).

[15] E. B. Sandell, in Colorimetric Determination of Traces of Metals, 2nd Ed. (Interscience Publishers, Inc., New York, 1950), p. 673.

the supernatant liquid from 400 mμ to 700 mμ was read in a Cary Recording Spectrophotometer (Model 14M) using a cuvette with a 2-cm light path and a slide wire of ranges 0 to 0.1 and 0 to 0.2.

A line was drawn from the absorbance at 430 mμ to the absorbance at 700 mμ. The difference between the absorbance of the sample and this connecting line at 525 mμ (a maximum absorbance for $MnO_4^-$) is the absorbance corrected for scattering and variations in the base line.

The optical density of the sample was compared with $MnO_4^-$ generated from a standard $Mn^{2+}$ solution (prepared by dissolving pure Mn metal in $H_2SO_4$). The procedure described above is valid for a range of Mn concentration between 0 and 0.25 μM. $Fe^{2+}$ at ten times the concentration of $Mn^{2+}$ did not interfere with the $MnO_4^-$ color, as shown by a separate test.

(g) Iron analysis

This test is based on the color formed by the iron-phenanthroline complex. Samples for this determination were prepared as described in the Mn determination above. Between 0.25 and 0.50 ml of the diluted digest was used for this analysis. To each sample were added an aqueous saturated solution of O-phenanthroline monohydrage, 0.4 ml; 1% (w/v) hydroquinone, 0.4 ml; 25% (w/v) sodium citrate, 2 ml; and then the required amount of a blank sulfuric-nitric acid digest to adjust the pH to 3.5 to 4.0. The last operation was done separately on an equivalent aliquot of sample plus all the reagents required for this determination. The blank sulfuric-nitric acid digest consisted of all ingredients for digestion except for the sample. Finally, the volume of the test solution was adjusted to 10 ml. The optical density of the solution was measured at 510 mμ by using a cell with a 2-cm light path. A curve of $Fe^{2+}$ concentration (0 to 0.5 μM) vs optical densities was determined by using $FeSO_4 \cdot (NH_4)SO_4 \cdot 6H_2O$ to prepare a standard solution. The presence of manganese ion had no effect on the Fe-phenathroline color. Furthermore, the digested sample itself has no interfering substances, as shown by addition of an internal standard.

(h) Phosphate analysis

This assay depends on the formation of the blue color of the reduced phosphomolybdate complex and is a modification of the classical Fiske-Subbarow method.[16] For the determination of total phosphates the samples from chloroplast material containing approx 1 mg chlorophyll were first digested by boiling with 0.4 ml of 70% $HClO_4$ until clear and colorless. After the samples were cooled to room temperature, they were transferred quantitatively to 12-ml conical centrifuge tubes with approx 5 ml of $H_2O$; 0.5 ml of 2.5% ammonium molybdate and 0.2 ml of the reducing reagent were added. (The reducing reagent was prepared by grinding 0.5 g of 1-amino-2-naphthol-4-sulfonic acid in a mortar and adding slowly 195 ml of 15% (w/v) $NaHSO_3$. Five ml of 20% (w/v) $Na_2SO_3$ was added; the vessel was stoppered, shaken, and finally filtered.) The mixture was diluted to 70 ml

[16] C. H. Fiske and Y. Subbarow, J. Biol. Chem. 66, 375 (1925).

with water, and the color was allowed to develop for at least 30 min before reading at 750 mμ by use of a 2-cm-light-path cuvette. A phosphate standard curve was set up by using the same digestion procedure and a phosphate concentration up to 0.5 μM per reaction mixture.

The content of inorganic phosphate in the original lyophilized spinach quantasome aggregates was determined by alternately washing and centrifuging the sample three times. The slightly green washings were combined. NaCl was added to make the solution 0.1 M, and the mixture was centrifuged at 40,000 rpm for 10 min (#40 head, Model L Spinco) to clarify the solution. The clear supernatant liquid was treated as above except for the digestion: $HClO_4$ was omitted. A control consisting of $H_2O$ plus NaCl was also treated similarly.

(i) Lipid extraction

The lyophilized lamallae were extracted subsequently with hexane, acetone, and methanol at 25° for lipid determination. In a typical experiment involving 15 mg of lyophilized lamellae, the lamellae were extracted four times with 2 ml of hexane, four times with 2 ml of acetone, and three times with 2 ml of methanol.

(j) Hill reaction

Hill-reaction activity was assayed manometrically by using $K_3Fe(CN)_6$ as the oxidant. The reaction mixtures contained 10 μM of $K_3Fe(CN)_6$ and enzyme (containing about 0.5 mg chlorophyll) in 3.0 ml of 0.01 M potassium phosphate buffer at pH 7.4. The reactions were run at 15° at a light intensity of 4,600 ft-c.

(k) Electron microscopy

Electron microscopy was performed on an Akashi TR-50 or a Siemens Elmiskop instrument. Techniques for sample preparation are described elsewhere.[3]

## Results

Chloroplast lamellar structures prepared according to the flow sheet in Fig. 8-2 were assayed for Hill reaction and photosynthetic phosphorylation by the methods described above. Controls consisted of precipitate II (washed whole chloroplasts) and a precipitate II fraction that was carried through the remainder of the procedure, but after precipitate II was initially resuspended in water, it was always thenceforth resuspended in its own supernatant rather than in fresh medium. Results of this experiment appear in Table 8-I. The data in Table 8-I show that the washed lamellar structures used for chemical analysis in later experiments are highly active in the Hill reaction, but lack the ability to perform photosynthetic phosphorylation. We have always observed increased Hill reaction rates in sonically ruptured chloroplasts, using $Fe(CN)_6^{3-}$ as the oxidant. This is apparently due to elimation of permeability barriers in the sonically ruptured system. A similar phenomenon may cause the increase in photosynthetic phosphorylation rate in the lamellae washed in their own supernatant. Washing in water,

Table 8-I. Enzymic activities of lamellae prepared according to the flow sheet in Fig. 8-2.

| Sample | Hill reaction ($O_2$ in μl/h per mg chlorophyll | Photophosphorylation* (μM $P_i$ esterified/h per mg chlorophyll) |
|---|---|---|
| Precipitate II (whole chloroplasts) | 379 | 4 |
| Unwashed lamellae | 840 | 18 |
| Washed lamellae | 830 | 0 |

*We wish to thank Mr. Charles Prevost for performing these studies.

on the other hand, is known to uncouple photosynthetic phosphorylation, and our results confirm this observation.[17]

It may be concluded that the purified lamellar structures analyzed in the subsequent experiments are highly active in the conversion of light energy into chemical energy as assayed by the Hill reaction.

Lamellae prepared according to the scheme in Fig. 8-2 were lyophilized by the method described above. The lyophilized preparations, when resuspended in 0.01 M potassium phosphate buffer, pH 7.4, retained 50 to 75% of their initial Hill reaction activity. These results are similar to those of French.[18]

One kilogram of leaves yielded 685 mg of lyophilized lamellae. The spectrochemical, chemical, and electron microscopic observations reported below were performed on this one preparation.

The results of spectrochemical analysis of lamellae and of lamellae separated into lipid-soluble (combined hexane, acetone, and methanol) extracts and lipid-insoluble fractions are given in Table 8-II. The spectrochemical data show that Mg is predominantly in the lipid extract of the lamellae, presumably largely associated with chlorophyll, whereas the transition elements Fe and Mn are predominantly associated with the non-lipid residue. These data are accurate only to a factor of 2, but they identified the elements that should be looked for by more accurate procedures. To obtain more accurate data, we applied the wet chemical procedures outlined under "Experimental Procedure" to the lyophilized lamellae. These data are presented in Table 8-III.

[17] A. T. Jagendorff and M. Smith, Plant Physiol. 37, 135 (1962).

[18] C. S. French, A. S. Holt, R. D. Powell, and A. C. Anson, Science 103, 505 (1946).

Table 8-II. Spectrochemical analysis of ashed lamellae and lamellar fractions. (Reliability: ± a factor of 2.)

| Element | Amount of element per 7.34 mg lamellae[a] | | |
|---|---|---|---|
| | Weight distribution of lamella (%) | Lipid (51%) (μg) | Residue (49%) (μg) |
| Mg | 50. | 30. | 3.5 |
| Fe | 5. | 0.5 | 3.5 |
| Cu | 1. | 1.7 | 1.1 |
| Mn | 0.3 | -- | 0.17 |
| Ca | 1.5 | 0.3 | 1.7 |
| Al | 0.6 | 0.07 | 1.2 |
| Si | 0.1 | 0.3 | 0.35 |

a. Not detected in sample: V < 0.01, Co < 0.05, Mo < 0.01, Ti < 0.01, Sn < 0.01, Cd < 0.5, Pb < 0.1, Sn < 0.1, Ni < 0.05, Bi < 0.05.

Table 8-III. Chemical analysis of lyophilized lamellae.

| Substance analyzed | Sampled analyzed (mg) | μM per g dry wt | Molar ratio of substance analyzed/Mn |
|---|---|---|---|
| Chlorophyll | 1.86 | 120. | 115 |
| Fe | 12.6 | 6.63 | 6.4 |
| Mn | 200.7 | 1.04 | 1.0 |
| Kjeldahl N | 11.26 | 5980. | 5750. |
| Total P | 10.3 | 77.7 | 74.7 |
| Inorganic P | 10.0 | 15.0 | 14.4 |
| Organic P[a] | -- | 62.7 | 60.3 |

a. Organic phosphorus equals total phosphorus minus inorganic phosphorus.

Lyophilized lamellae weighing 22.85 mg were separated into lipid-soluble and lipid-insoluble fractions according to the procedure described earlier under "Experimental Procedure." The weights and the phosphorus and nitrogen contents of the various fractions are given in Table 8-IV, and the spectra of these fractions are presented in Fig. 8-3.

Fifty-eight per cent of the mass of the lamellae is soluble in the lipid solvents. This number is higher than that reported by Menke[19] for whole chloroplasts and Bot[20] for isolated grana. This is probably because there is relatively less soluble protein in our washed lamellar preparation.

[19] W. Menke, Z. Physiol. Chem. 257, 43 (1938).

[20] G. M. Bot, Chronica Botan. 7, 66 (1942).

Table 8-IV. Weight, and phosphorus and nitrogen distribution, among various lipid extracts and the nonlipid residue of chloroplast lamellae.

| Fraction | Weight (mg) | Part of total weight (%) | Total P (μM per 10 mg dry weight) | μM P per mg of fraction | Part of total P (%) | Kjeldahl N (μM per 10 mg dry weight) | N* (%) |
|---|---|---|---|---|---|---|---|
| Total (orig.) | 22.85 | 100.0 | 0.777 | 0.077 | 100.0 | 59.8 | 100.0 |
| a. Hexane extr. | 2.40 | 10.5 | 0.069 | 0.066 | 8.9 | | |
| b. Acetone extr. | 8.21 | 35.9 | 0.319 | 0.089 | 41.00 | 8.72 | 14.6 |
| c. MeOH extr. | 1.97 | 8.6 | 0.163 | 0.189 | 21.00 | | |
| d. Residue | 9.53 | 41.7 | 0.210 | 0.050 | 27.00 | 55.0 | 92.0 |
| a + b + c + d | 22.11 | 97.0 | 0.761 | --- | 97.9 | 63.7 | 107.0 |

*Unextracted lamellae analyze 7.7% nonchlorophyll N by weight. The nonlipid residue analyzes 18% N by weight.

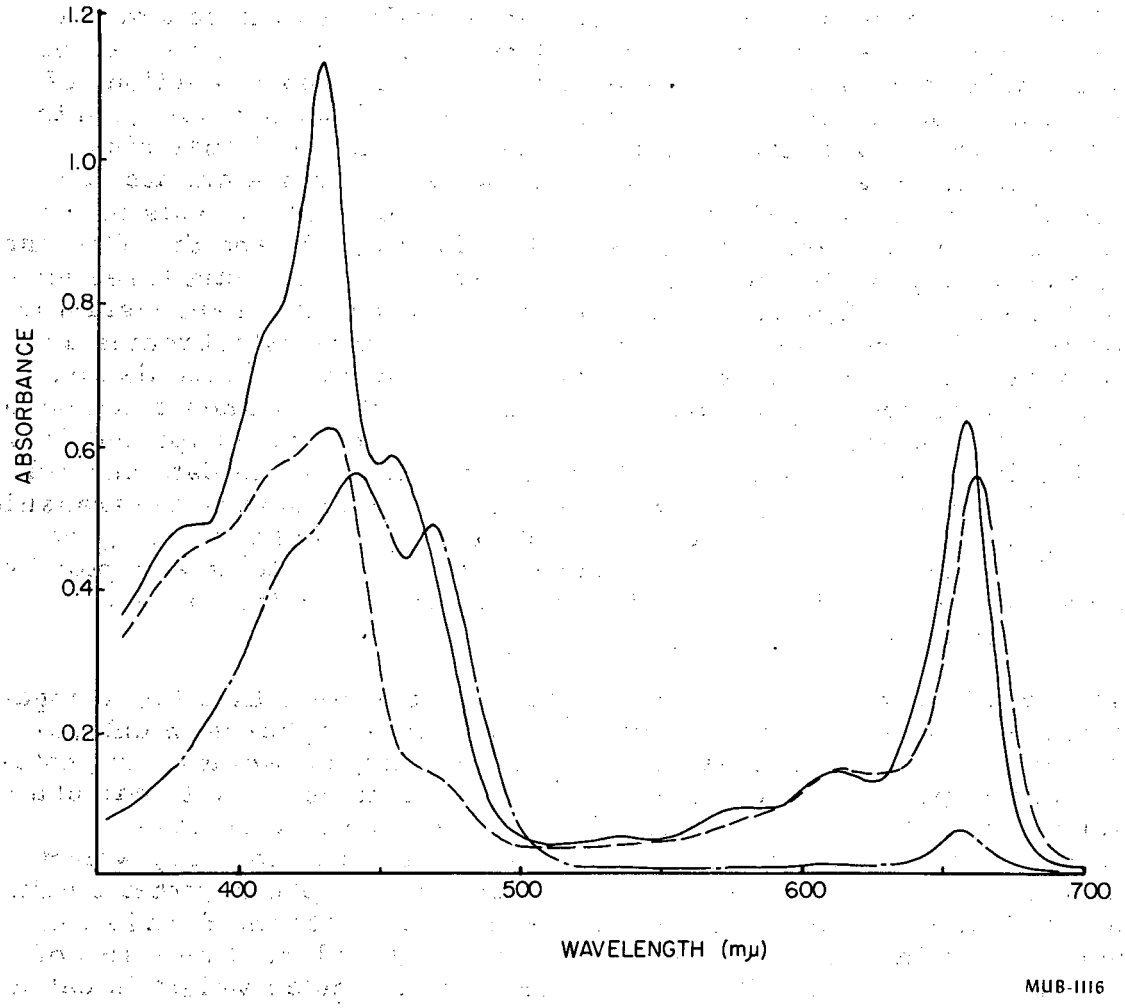


Fig. 8-3. Spectra of consecutive hexane (broken line), acetone (solid line, and methanol (dashed line) extracts of lyophilized chloroplast lamellae.

About 48% of the lamellae is soluble in hexane followed by acetone. Figure 8-4 is an electron microscopic comparison of shadowed lamellae before and after lipid removal. Spectrochemical analyses show that Fe and Mn remain in the residue and that the photosynthetic pigments are removed with the lipid. Apparently the residue consists of quantasome particles from which the "osmiophilic" lipid layer has been removed.

## Discussion

Purified chloroplast lamellae prepared by following the scheme in Fig. 8-2 are enzymically active in the Hill reaction. These lamellae performed the light reactions and associated electron transport reactions of photosynthesis. So far these are the only metabolic functions assigned to the lamellae. One hopes, then, that the results of chemical analysis of these lamellae will bear primarily on the lamellar structure and its performance of the photosynthetic process. Spectrochemical analysis of the lamellae shows the presence of Mg, Fe, Mn, Cu, Ca, Al, and Si. Calcium aluminum silicate probably accounts for the presence of the last three elements in the sample. Chlorophyll accounts for most of the mangnesium in the lamellae. The presence of iron was expected, since cytochromes are involved in photosynthetic electron transport.[21] Manganese was also expected, since it is required for oxygen evolution in photosynthesis and occurs in isolated chloroplasts.[22, 23] The existence of copper was suspected from work on localization of plastocyanin.[24] The spectrochemical data showed that these elements (Fe, Mn, Cu) were the only ones present in the transition-metal portion of the emission spectrum. Thus, any model for energy conversion and subsequent transport of electrons from water to an acceptor by washed chloroplast lamellae should involve only the transition metals observed spectrochemically.

The data in Table 8-III report the ratios of chlorophyll, iron, manganese, nitrogen, inorganic phosphorus, and organic phosphorus in chloroplast lamellae. Since manganese is required for oxygen evolution in photosynthesis and is present in lowest concentration, it is possible to calculate a minimum molecular weight for the photosynthetic unit in the lamellae. The manganese concentration of 1.04 μM manganese per gram dry weight, yields a minimum molecular weight of $9.6 \times 10^5$ for the photosynthetic unit. The data in Tables 8-II and 8-III may be used to calculate the distribution of substances within a unit of molecular weight of $9.6 \times 10^5$. Since 15% of the nitrogen exists as lipid nitrogen, the protein molecular weight is calculated on the basis of 4,890 nitrogen atoms, and an average molecular weight of 95 per amino acid residue. These data are summarized in Table 8-V.

---

[21] M. D. Kamen, in Research in Photosynthesis (Interscience Publishers, Inc., New York 1957), p. 149.

[22] E. Kessler, Planta 49, 435 (1957).

[23] J. V. Possingham and D. Spencer, Australian J. Biol. Sci. 15, 58 (1962).

[24] S. Katoh, S. Ikuko, I. Shiratori, and A. Takamiya, Arch. Biochem. Biophys. 94, 136 (1961).

a

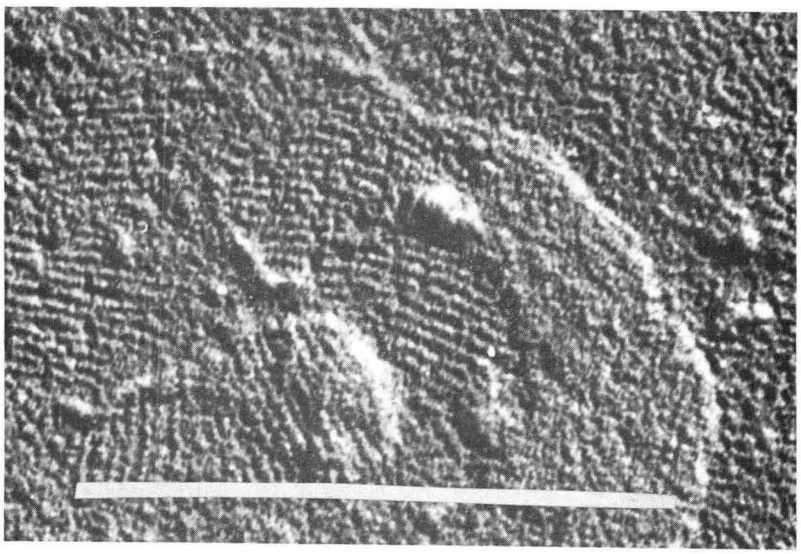

b

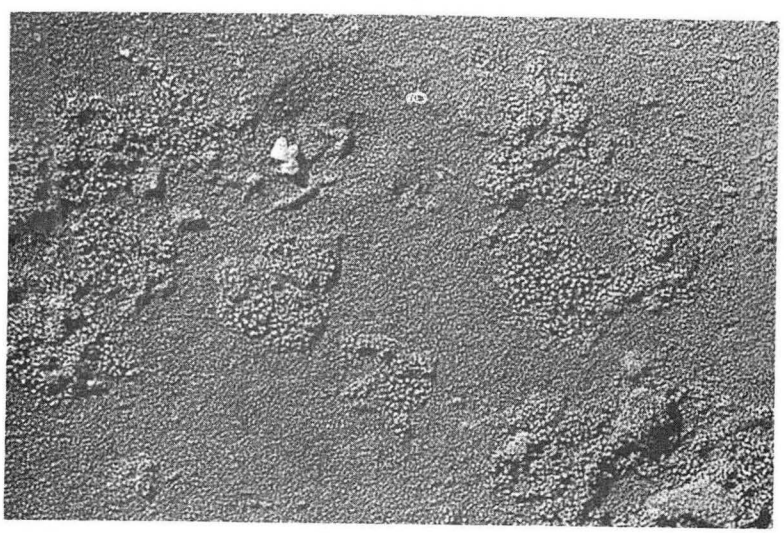

ZN-3235

Fig. 8-4. (a) Chloroplast lamella before lipid removal. (b) Chloroplast lamella after lipid removal. White line in (a) is 1 micron long. Magnification in (b) is the same as in (a).

Table 8-V. Distribution of substances in chloroplast lamellae on the basis of a minimum molecular weight of 960,000 for a chlorophyll-containing unit.

| Substance | Molecular weight | Calculated total weight (%) |
|---|---|---|
| Nonlipid portion | | |
| 6 Fe | 336 | |
| 1 Mn | 55 | |
| 3 Cu[a] | 189 | |
| 4,890 N atoms as protein | 464,000 | |
| | 465,000 | 48 |
| Lipid portion | | |
| 115 chlorophyll × 920 | 107,000 | |
| carotene | 25,000 | |
| Unidentified lipid by difference | 363,000 | |
| | 495,000 | 52 |

a. From spectrochemical analysis; reliability: ± a factor of 2.

The chlorophyll-to-nitrogen weight ratio in these experiments is 1.4. In previous experiments we have observed values ranging from 1.3 to 2.0, depending on the age of the spinach and the time of year.[3]

Data on the lipid components of the quantasomes (Table 8-III) show that these components make up 58% of the total mass of the quantasome. Chlorophylls and carotenoids in turn compose approximately 25% of the lipid-soluble material. Spectra of the three extracts show that -- with respect to the photosynthetic pigments -- hexane extracts primarily the carotenes, and that acetone and methanol remove the chlorophyll and xanthophylls. The phosphate analyses show that about 70% of the total phosphorus is in the lipid-soluble materials. Glycerol phosphates and phosphatides probably account for much of this phosphorus.[25] About 50% of the lipid nitrogen is accounted for by chlorophyll; the remainder of the lipid nitrogen is unidentified.

The electron micrographs in Fig. 8-4 show that the lipid components of the lamellae are largely associated with the surface osmiophilic layer. This observation is shown diagramatically in Fig. 8-5. The lamellae are photosynthetically active until after the hexane-acetone extraction. The total lipid extract in Fig. 8-5 is 48%, rather than 58%, because the hexane-acetone extractions were not followed by methanol extraction. Methanol extraction completely denatures the protein residue and is therefore excluded if the electron microscopy is used to observe the residue.

The mass of the 200-Å quantasome can be estimated from its density (assuming half protein and half lipid) and volume. Such a calculation yields a molecular weight between 1 and 2 times the minimum molecular weight reported in Table 8-V. On this basis the quantasome would contain several hundred chlorophyll molecules. Kok's recent data support the notion that the physiological photosynthetic unit consists of about 300 chlorophyll molecules.[12] Is the 200-Å quantasome a morphological expression of photosynthetic unit? It is appealing to think so. Further experiments will determine whether or not this hypothesis is correct.

---

[25] L. P. Zill and E. A. Harmon, Biochim. Biophys. Acta 57, 573 (1962).

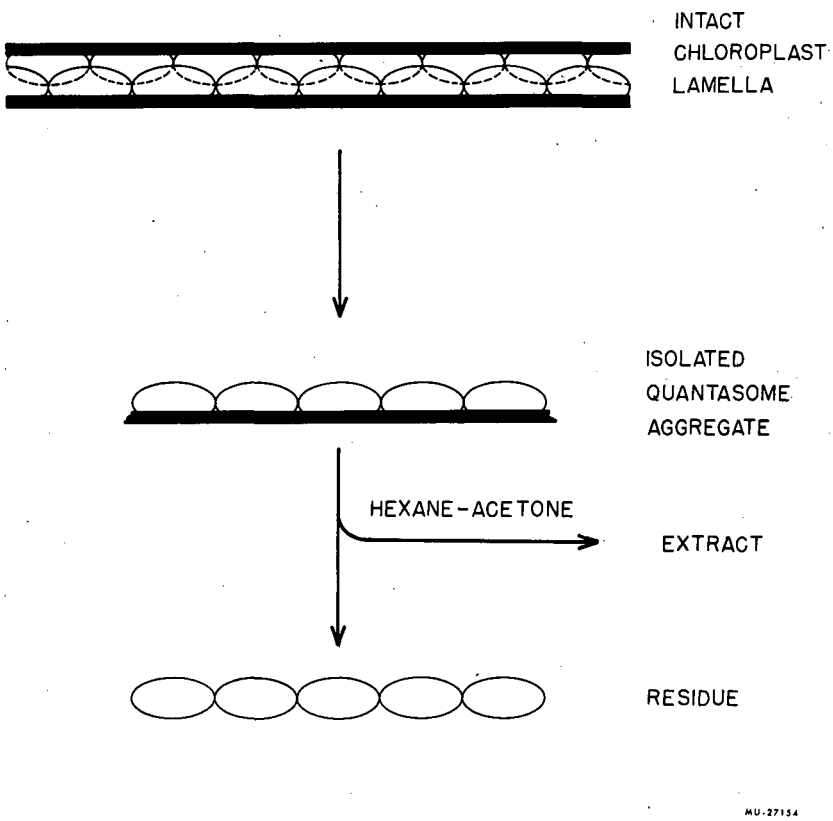


Fig. 8-5. Diagram of lipid localization within chloroplast lamellae.

# 9. CONCERNING THE OCCURRENCE AND THE ISOLATION OF A FAT-SOLUBLE FRAGRANT COMPOUND IN PETALS AND GREEN LEAVES OF MAGNOLIA SPECIES

Hartmut K. Lichtenthaler

While testing chlorophyll- and carotenoid-free tissues for the presence of quinones, a yellow fragrant oil was found in the petroleum ether extract of Magnolia petals. As this fragrant compound was detected in the green leaves too, it seems to be a characteristic substance of the metabolism of Magnolia species.

The fragrant compound has reducing properties and reacts with the α-α-dipyridyl-$FeCl_3$ reagents to give a pink color after 3 minutes. It also decolorizes potassium permanganate. The uv spectrum measured in absolute ethanol is shown in Fig. 9-1. Oxidation with potassium permanganate results in a shifting of the absorption spectra. The maximum and minimum wavelengths for both the oxidized and the reduced form in ethanol are presented in the table.

| | Reduced (mμ) | Oxidized form (mμ) |
|---|---|---|
| Maxima | 281 | 280 |
| | 227 | 234 |
| Minima | 268 | 255 |
| | 222 | 219 |

Irradiation of the oil with ultraviolet light for up to 4 hours did not change the absorption spectrum. This may indicate that the substance is a stable compound. However, when it is kept for a few days in the air, without solvent, the agreeable aroma of the fragrant oil changes to a rancid odor.

With an ethanolic solution of potassium hydroxide, a pale, unstable green color was formed. With concentrated sulfuric acid, a deep red color, stable for days, was obtained. The spectrum of this colored material is presented in Fig. 9-2. The red color formed with concentrated $H_2SO_4$ can be used for the detection of the compound on a paper chromatogram; a few micrograms give a positive reaction.

The ir spectrum (Fig. 9-3), showing a ketone bond and -CH= and $-CH_2-$ groups, indicates that the fragrant compound is a ketone with a long unsaturated carbon chain.

## Extraction

Magnolia petals (100 mg) were homogenized with 200 ml acetone in a blender at full speed for 1 minute. The homogenate was filtered through a glass-frit by permanent suction with an aspirator. The residue was washed, first with acetone, then with a mixture of acetone and petroleum ether (1:1), and finally with pure petroleum ether (see Fig. 9-4). To the combined extracts, placed in a separatory funnel, water was added, and by slight

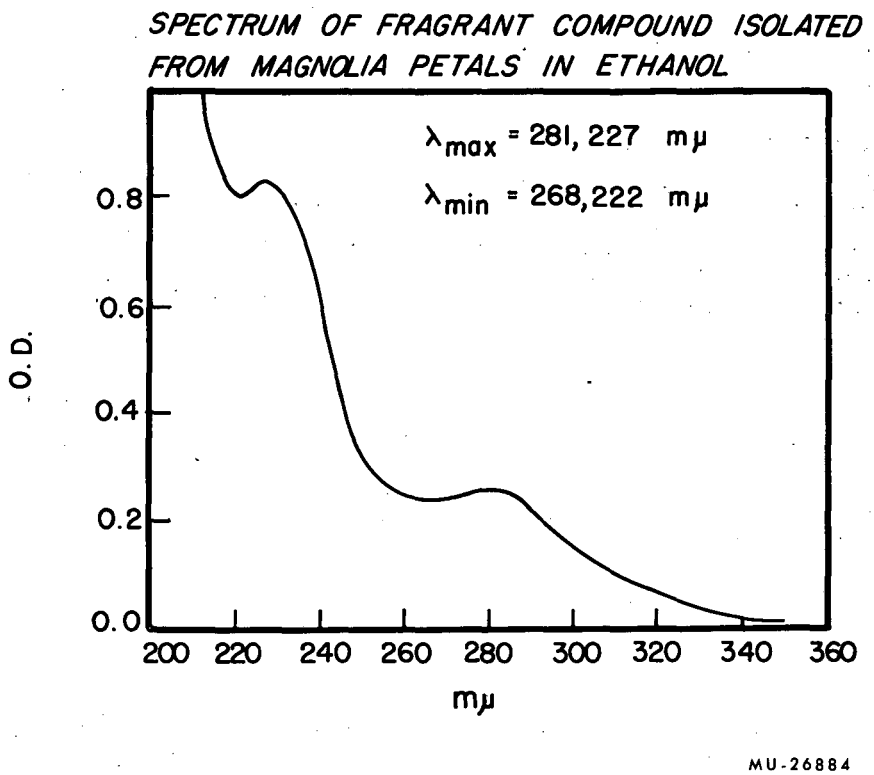


Fig. 9-1. Spectrum of a fragrant compound isolated from Magnolia petals in ethanol.

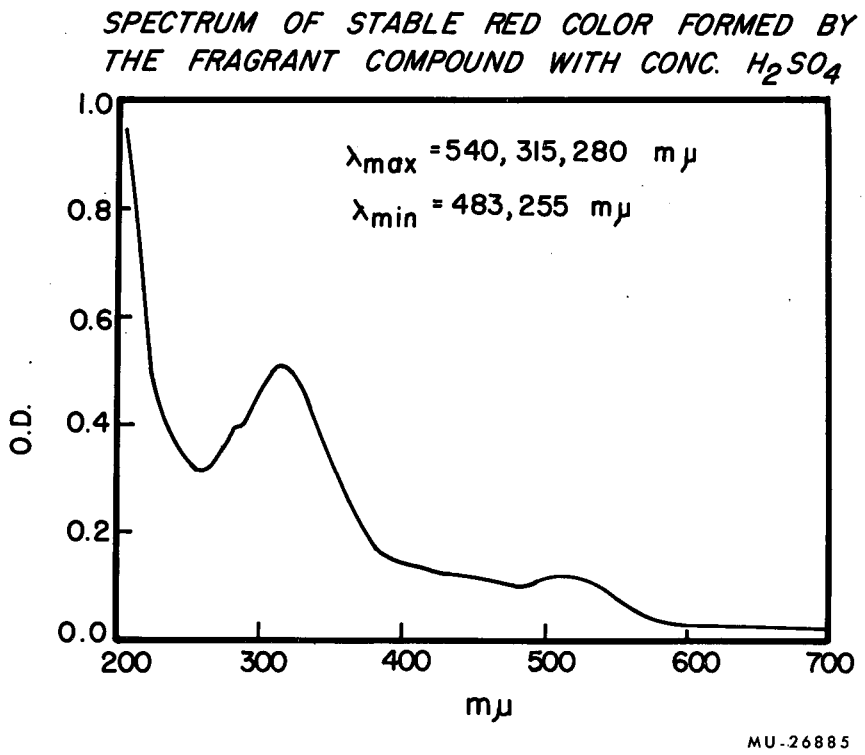


Fig. 9-2. Spectrum of the stable red color formed by the fragrant compound with concentrated $H_2SO_4$.

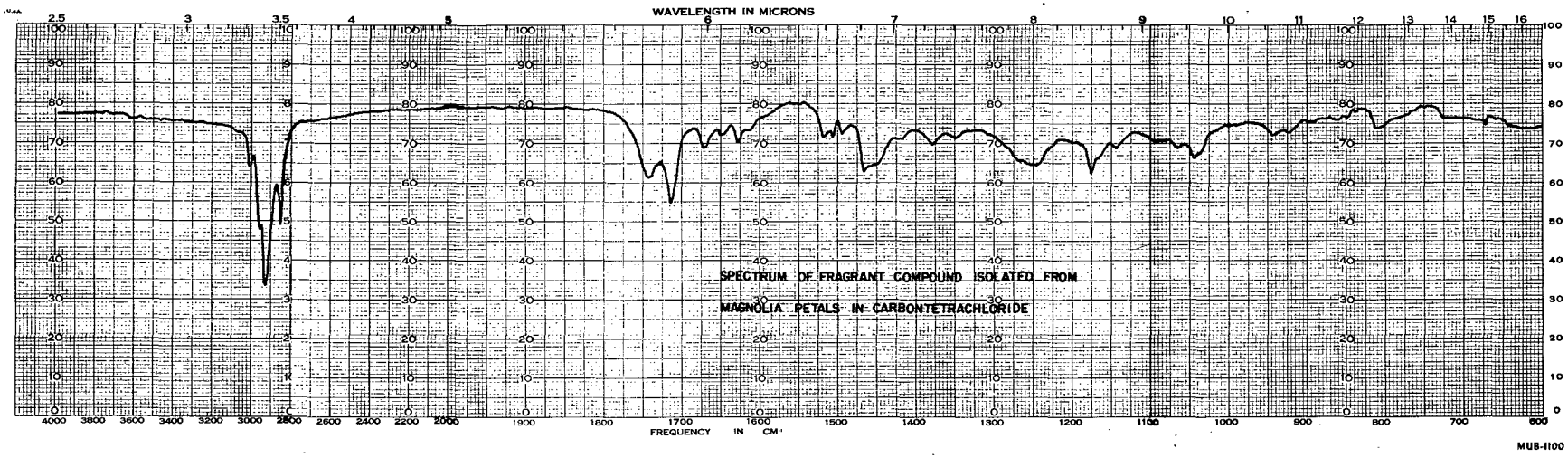


Fig. 9-3. Infrared spectrum of fragrant compound isolated from Magnolia petals.

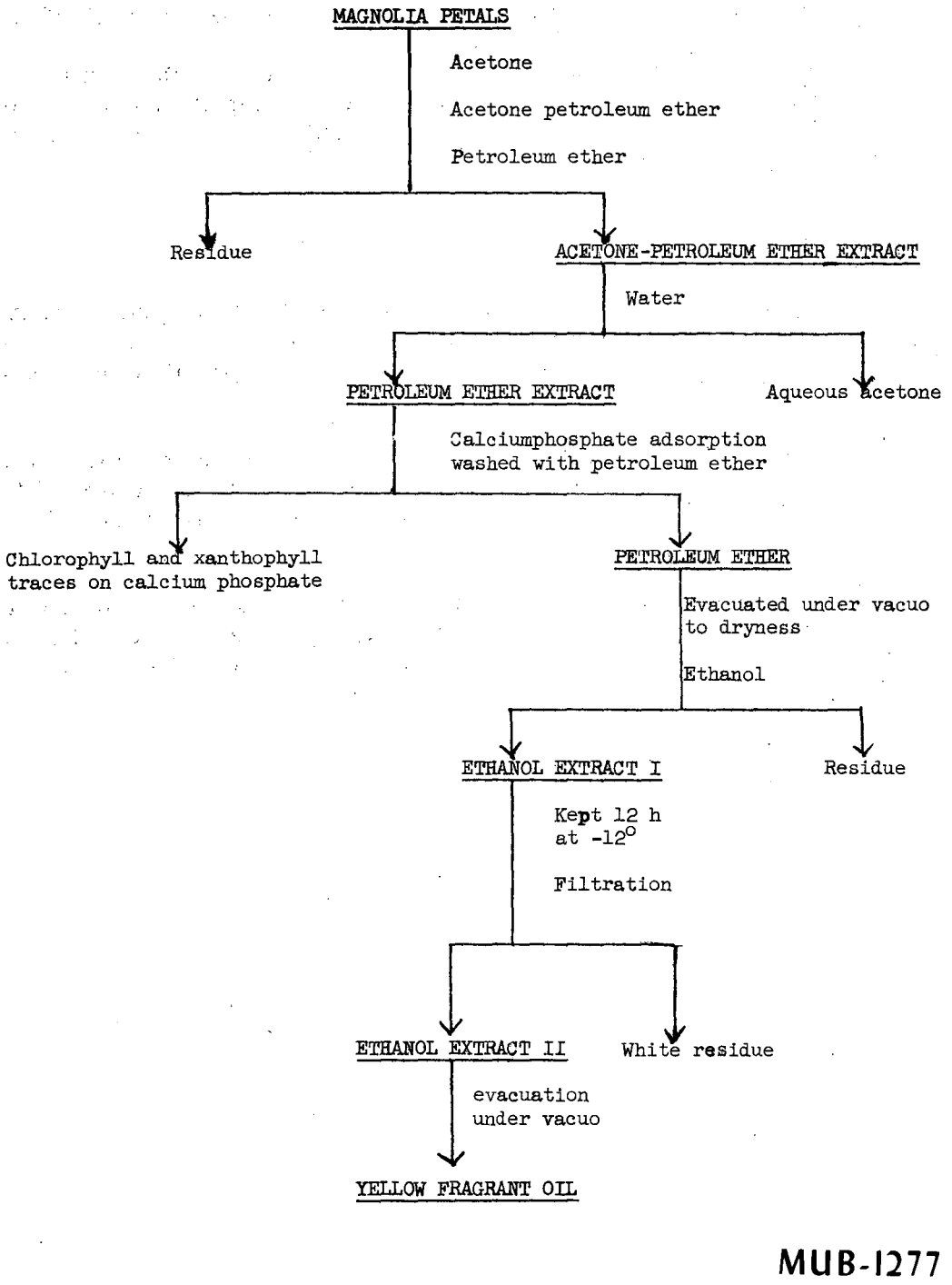


MUB-1277

Fig. 9-4. Isolation of a fragrant compound from Magnolia petals.

shaking, all fat-soluble compounds were dissolved in petroleum ether (about 200 ml). The hypophase (aqueous acetone) was discarded, and the epiphases was washed twice with water (25 ml) to remove traces of acetone. After the petroleum ether was dried with sodium sulfate, the extract was concentrated to 20 ml and then chromatographed on a column of dibasic calcium phosphate. Upon washing of the column with petroleum ether the fragrant compound was eluted, together with a very small amount of carotene.

After the solution was evacuated to dryness, the residue was taken up in 95% ethanol (2 ml), and this solution was kept overnight at -12°. The white precipitate was filtered off, and the purification process was repeated once more. The resulting yellowish ethanol extract was evaporated under vacuum to give a brownish-yellow fragrant oil.

Paper Chromatography

For further purification the fragrant oil was chromatographed on Whatman paper No. 3 MM (impregnated with 5% Dow-Corning silicone stopcock grease No. 59293) with the solvent mixture isopropanol–acetic acid–water (25:1:14).

The Rf value obtained for the compound is 0.80; 18 to 20 hours was required for the development of the chromatogram. The spectrum of the eluted spot (with EtOH) (Fig. 9-1) corresponds to that of the ethanolic extract II (see Fig. 9-4).

By the same extraction method as indicated in Fig. 9-4, an ethanolic extract of green Magnolia leaves was prepared. The separation of this extract by paper chromatography resulted in the detection of the same fragrant compound as was isolated from the petals.

# 10. EFFECT OF ENVIRONMENTAL COMPLEXITY AND TRAINING ON CHOLINESTERASE ACTIVITY, HEXOKINASE ACTIVITY, AND PROTEIN CONTENT OF RAT BRAIN

Edward L. Bennett, Marie Hebert, and Hiromi Morimoto
(in collaboration with David Krech and Mark R. Rosenzweig,
Department of Psychology, University of California, Berkeley)

## Introduction

Significant relations have been found between both acetylcholine concentration and cholinesterase (ChE) activity in rat brain and the learning ability of these animals.[1] These differences have also been correlated with both individual differences and strain differences among rats. In addition, we have found that differences in an animal's environment can cause changes in the specific activity (activity per mg wet tissue) and total activity (specific activity × total sample weight) of certain areas of a rat brain, as well as in the anatomy of the brain. This observation immediately raises the question of the specificity or generality of these effects. Thus, for example, a decrease in specific cholinesterase activity might be due to a selective deposition of an enzymatically inert substance such as lipid or water in the area studied -- with a resultant decrease in specific activity not merely of cholinesterase but also of other enzymes. A change in the proportion of cell types may be another result of differences in an animal's environment. Depending upon the relative activity of various enzymes in these different cell types, it might be expected that the activity of one enzyme would increase, that of another decrease, and that of a third enzyme remain constant as a result of cerebral stimulation.

To test the hypothesis that the differences in the biochemistry of the brain produced by environmental complexity and training (ECT) have a degree of specificity for the acetylcholine-cholinesterase-choline acetylase system, specific hexokinase activity, specific cholinesterase activity, and protein content have been determined in five areas of the brains of pairs of ECT rats and their isolated control (IC) littermates.

A second objective of this work was to determine if a colorimetric assay for cholinesterase activity, based upon the hydrolysis of acetylthiocholine in the presence of 5, 5'-dithio bis-(2-nitrobenzoic acid), would be sufficiently precise to determine the small difference in cholinesterase activity existing between ECT and IC rats.

The previously observed differences were found between ECT and IC rats in brain cortical weight and cholinesterase activity (specific and total), but corresponding differences were not found in protein content or hexokinase activity. The spectrophotometric assay for cholinesterase is sufficiently precise to differentiate between ECT and IC rats.

---

[1] D. Krech, M. R. Rosenzweig, and E. L. Bennett, Psychol. Bull. 57, 476 (1960).

## Experimental Procedure

### Subjects and Behavioral Conditions

Ten littermate pairs of male rats of the $S_1$ strain were weaned at 25 days of age and placed in the experimental conditions; these have been described in detail.[2] One animal of each pair, chosen at random, was assigned to the ECT conditions, and its littermate was assigned to the IC conditions. In brief, the ten ECT animals were housed in large hardware cloth cages and provided with wooden "toys." Every day they were put in a Hebb-Williams maze, and the pattern of barriers was changed daily. Beginning at about 55 days of age, they were trained successively in the Lashley III maze, the Dashiell maze, and the Krech Hypothesis Apparatus. The IC animals were housed individually in cages with solid walls, and they received a minimum of handling. All animals had food and water ad lib.

### Sacrifice and Dissection of Brain

All animals were sacrificed on the same day at about 105 days of age. The rats were delivered to the chemical laboratory with code numbers that did not reveal to which group they belonged. The killing order was arranged so that animals of a litter were taken in succession but randomized as to condition. Each animal was decapitated and the brain samples were removed by gross dissection. After removal of the calvarium, a specially designed miniature plastic T-square was placed on the brain to delimit the samples to be removed from the visual and somesthetic areas of the cortex. The boundaries of each cortical section were first circumscribed with a scalpel, and then the cortical tissue was carefully peeled free of the white matter. In rat brain, cortex can be separated cleanly from the underlying white matter in this way. After the Visual (V) and Somesthetic (S) samples had been taken, the remaining Dorsal Cortex (DC) was removed by going out to the temporal ridge of the skull. (The designations of the samples are capitalized throughout the report to make clear that we are referring to the special samples as defined here.) Next, a fourth sample was taken, including ventral cortex, hippocampus, and corpus callosum; this sample will be referred to as "Ventral Cortex" (VC). The remainder of the brain, including the olfactory lobes, the cerebellum, and medulla, was taken as the last sample. This sample will be referred to as "Subcortex" (SC).

As each sample was removed, it was rapidly weighed on a projection semimicro balance (Sartorius Selecta). After it was weighed, each sample was placed on dry ice. Dissection and weighing of all samples of a single brain took less than 10 minutes. The samples were stored in a deepfreeze until homogenized for analyses.

### Chemical Analyses

The samples were homogenized in 0.1 M $NaH_2PO_4$–$Na_2HPO_4$ buffer, pH 8.0, at $0^o$. The concentrations of the homogenates were V and S, 2.1 mg/ml; DC and VC, 5.0 mg/ml; and SC, 10.0 mg/ml. The three chemical measures were made on one brain area of all 20 rats in one day; this minimizes any possible daily variation.

[2] D. Krech, M. R. Rosenzweig, and E. L. Bennett, J. Comp. Physiol. Phychol. 53, 509 (1960).

Determination of Hexokinase Activity

The spectrophotometric assay used for the determination of hexokinase activity utilized the coupled reaction.

$$\text{I. Glucose + ATP} \xrightarrow[Mg^{2+}]{\text{hexokinase}} \text{glucose 6-phosphate + ADP;}$$

$$\text{II. Glucose 6-phosphate + TPN} \xrightarrow[Mg^{2+}]{\text{glucose 6-phosphate dehydrogenase}}$$

$$\text{6-phosphogluconate + 2TPNH + 2 } H^{+}.$$

The rate of reaction can be readily followed spectrophotometrically at 340 mμ. The only modification from the procedure that has been described in detail was the substitution of $NaH_2PO_4$–$Na_2HPO_4$ buffer for a $KH_2PO_4$–$K_2HPO_4$ buffer.[3] This was necessary for eliminating interference by potassium in the protein assay. Preliminary experiments showed that the substitution of the sodium phosphate buffer for a potassium phosphate buffer did not affect either the initial hexokinase activity of brain homogenates or the stability. All analyses were done in duplicate with two littermate pairs in each run of four simultaneous analyses. In the few cases in which duplicate analyses did not agree within 5%, a third analysis was made.

Hexokinase activity has been expressed in terms of mμM of glucose phosphorylated per mg wet tissue per minute.

Determination of Cholinesterase Activity

Cholinesterase activity was determined by a spectrophotometric assay recently described by Ellman et al.[4] The rate of hydrolysis of acetylthiocholine iodide (AcSCh, $6 \times 10^{-4}$ M) is determined in the presence of 5, 5'-dithio bis-(2-nitrobenzoic acid) (DTNB, $8 \times 10^{-5}$ M) in 0.1 M sodium phosphate buffer, pH 8.0, at 37°. The stock DTNB solution was prepared by dissolving 40 mg of DTNB in 10 ml of 0.1 M sodium phosphate buffer, pH 7.0, containing 15 mg of $NaHCO_3$. Twenty-five μl was used for each assay. The stock AcSCh solution was prepared by dissolving 270 mg of this compound in 25 ml of distilled water; 50 μl was used for each assay. Both solutions were stored in a deepfreeze. Thiocholine, formed by the hydrolysis of AcSCh, reacts extremely rapidly with DTNB to form the highly colored 2-nitro-5-thiobenzoate anion. This anion absorbs strongly in the visible spectrum with a maximum at 412 mμ. As in the hexokinase assays, two pairs of littermates were analyzed in one run using the Gilford automatic cell positioner and optical-density converter. The change in absorption at

[3] E. L. Bennett, J. B. Drori, D. Krech, M. R. Rosenzweig, and S. Abraham, J. Biol. Chem. 237, 1758 (1962).

[4] G. L. Ellman, K. D. Courtney, V. Androes, and R. M. Featherstone, Biochem. Pharmacol. 7, 88 (1961).

412 mμ was recorded on a Leeds and Northrup recorder. Aliquots of the homogenates containing the following weights of tissue were used: V and S, 2.10 mg; DC, 2.50 mg; VC, 2.00 mg; and SC, 0.75 mg. With these amounts of tissue an absorbance change of about 0.7 was obtained during the 10 minutes the reactions were recorded when the assay volume was 3 ml. The reagent blank in the absence of brain was about 6% of the reaction rate with brain.

The brain homogenate and sufficient phosphate buffer to make a total volume of 3 ml were prewarmed to 37° in the presence of DTNB during a 10-minute period, AcSCh was added, and the reaction rate was recorded for 10 minutes. All analyses were done in duplicate, and a third analysis was made in the few instances in which the first two analyses did not check within 5%. The results are expressed in terms of moles of AcSCh $\times 10^{10}$ hydrolyzed per min per mg wet tissue. The hydrolysis of AcSCh by cholinesterase is slightly more rapid than the hydrolysis of acetylcholine, so that the results are higher than we have previously reported.

## Determination of Protein Content

The protein content of the homogenates of the brain areas was determined by the Folin phenol reagent as previously described.[5,6] Aliquots of the homogenates containing about 1 mg of tissue were used; the resulting absorbance was about 0.4. Duplicate analyses were made on each sample. Eight standards with a protein content closely equivalent to that of the brain samples were run with each series of analyses. These standards were prepared from bovine albumin. The protein content of the brains is expressed in terms of mg equivalent albumin protein per mg wet tissue. The factor 6.25 has been used to convert from mg albumin nitrogen to mg protein nitrogen.

## Results

The differential effects of environmental conditions on weight, specific cholinesterase activity, specific hexokinase activity, and protein content are summarized in Table 10-I. Statistical analyses for the significance of the differences have not been completed yet. However, as we have found in previous experiments, the weight of the cortex of the ECT groups is larger than that of the IC group by about 5% for the entire cortex and in eight out of 10 pairs for each cortical area.

Specific cholinesterase activity decreased in the four cortical areas by about 4%, and this decrease was 8 or 9 out of 10 pairs in each cortical area analyzed. The specific hexokinase activity and percent protein showed no differences between ECT and IC animals. The largest difference in hexokinase content was 0.5%, and the largest difference in protein content was 1.1%. The other eight comparisons showed differences of 0.8% or less.

[5] O. H. Lowry, N. H. Rosenbrough, A. L. Farr, and R. J. Randall, J. Biol. Chem. 193, 265 (1951).

[6] E. L. Bennett, M. R. Rosenzweig, D. Krech, A. Ohlander, and H. Morimoto, J. Neurochem. 6, 210 (1961).

Table 10-I. Weight, specific cholinesterase activity, specific hexokinase activity, and protein content of five areas of ECT and IC rat brains.

| | Area | | | | |
|---|---|---|---|---|---|
| | Visual cortex | Somesthetic cortex | Remaining dorsal cortex | Ventral cortex | Sub-cortex |
| **Weight (mg)** | | | | | |
| ECT | 64.0 | 47.3 | 283.0 | 309.9 | 916.2 |
| IC | 59.2 | 46.6 | 274.4 | 293.0 | 923.0 |
| Ratio ECT/IC | 1.082 | 1.015 | 1.035 | 1.058 | 0.993 |
| No. of ECT > IC littermates | 8/10 | 8/10 | 8/10 | 8/10 | 5/10 |
| **Cholinesterase activity** (moles AcSch $\times 10^{10}$ hydrolyzed/min/mg) | | | | | |
| ECT | 60.2 | 71.9 | 69.1 | 101.8 | 182.8 |
| IC | 63.0 | 74.4 | 72.3 | 106.6 | 181.6 |
| Ratio ECT/IC | 0.955 | 0.967 | 0.955 | 0.954 | 1.007 |
| No. of ECT > IC littermates | 1/10 | 1/10 | 1/10 | 2/10 | 5/10 |
| **Hexokinase activity** (mμM glucose phosphorylated/min/mg) | | | | | |
| ECT | 1524.0 | 1402.0 | 1516.0 | 1252.0 | 1146.0 |
| IC | 1524.0 | 1406.0 | 1522.0 | 1249.0 | 1140.0 |
| Ratio ECT/IC | 1.000 | 0.998 | 0.996 | 1.003 | 1.005 |
| No. of ECT > IC littermates | 5.5/10 | 6.5/10 | 4.5/10 | 7.5/10 | 6/10 |
| **Protein content** (% of wet weight) | | | | | |
| ECT | 11.20 | 11.11 | 10.71 | 10.27 | 10.35 |
| IC | 11.17 | 10.99 | 10.70 | 10.20 | 10.33 |
| Ratio ECT/IC | 1.003 | 1.011 | 1.001 | 1.007 | 1.002 |
| No. of ECT > IC littermates | 5/10 | 8/10 | 5.5/10 | 6/10 | 5.5/10 |

We conclude, therefore, that the ECT affects the anatomy and specific cholinesterase activity of rat brain but produces little or no change in specific hexokinase activity or protein content.

In addition, the spectrophotometric assay for cholinesterase activity is sufficiently precise to determine differences of 5% in two groups of 10 rats. It is more rapid than the titrimetric method we have previously applied through the use of pH stats. The technique is simple, and it can be extended to small samples by suitable modification. In addition, it allows multiple assays to be made on a single area, as samples may be homogenized in buffer to retain the activity of certain enzymes. For example, hexokinase activity is much lower when the sample is homogenized in saline. On the other hand, when a sample is homogenized in a buffer, the titrimetric cholinesterase assays usually cannot be made.

## 11. G VALUES FOR THE RADIATION DECOMPOSITION OF NUCLEIC ACID CONSTITUENTS

Cyril A. Ponnamperuma and Richard M. Lemmon

In our studies of the radiation decomposition of nucleic acid constituents,[1,2] several reactions were examined. Of special interest are those which appear to be of biological significance. These observations may help us to understand the origin of a radiation mutation.

Among the reactions investigated may be listed the following.

1. Destruction of bases
2. Destruction of nucleosides
3. Destruction of nucleotides
4. Release of sugar from nucleosides and nucleotides
5. Release of sugar phosphate from nucleotides
6. Release of phosphate from nucleotides
7. Deamination of amino bases to hydroxy bases in the free bases, nucleosides, and nucleotides
8. Opening of the imidazole ring of purine bases
9. Formation of 8-hydroxy purines

The G values, or number of molecules destroyed, transformed, or produced per 100 electron volts, are presented in Tables 11-I through 11-IX. All the G values are reported for whatever total dose gave the maximum G value. All the irradiations in this study were done in the absence of oxygen. Literature reports of G values obtained in the absence of oxygen have been included for purposes of comparison.

The G values for destruction of bases (Table 11-I) show that there is no oxygen effect when the free bases are irradiated in aqueous solution. The purines are clearly more stable than the pyrimidines. This sensitivity of the pyrimidines arises from the ease with which the pyrimidines give rise to hydroperoxides when irradiated in water.[3,4] Guanine appears to be less sensitive to radiation than adenine although this apparent lower sensitivity may be due in part to the low concentration of the guanine -- a result of its low water solubility. Part 3 of Table 11-I shows a significant dependence of G values on concentration for both adenine and guanine (in the presence of oxygen).

All the nucleosides (Table 11-II) were irradiated at approximately the same concentration. The G values indicate that they are equally sensitive to radiation. Again, there is no apparent oxygen effect.

---

[1] C. Ponnamperuma and R. M. Lemmon, in Bio-Organic Chemistry Quarterly Report, UCRL-10156, April 1962, p. 6.

[2] C. Ponamperuma and R. M. Lemmon, in Bio-Organic Chemistry Quarterly Report, UCRL-10032, Jan. 1962, p. 90.

[3] G. Scholes, J. F. Ward, and J. Weiss, Science 133, 2016 (1961).

[4] B. Ekert and R. Monier, Nature 188, 309 (1960).

Table 11-I. Bases destroyed.

| Base | Concentration (moles per liter) | G |
|---|---|---|
| In the absence of $O_2$ | | |
| Adenine | $7.5 \times 10^{-3}$ | 0.9 |
| Guanine | $0.3 \times 10^{-3}$ | 0.1 |
| Cytosine | $9.0 \times 10^{-3}$ | 1.5 |
| Uracil | $8.9 \times 10^{-3}$ | 1.2 |
| Thymine | $7.9 \times 10^{-3}$ | 2.0 |
| In the presence of $O_2$[a] | | |
| Adenine | $2 \times 10^{-4}$ | 1.09 |
| Guanine | $2 \times 10^{-4}$ | - |
| Cytosine | $2 \times 10^{-4}$ | 2.05 |
| Uracil | $2 \times 10^{-4}$ | 1.93 |
| Thymine | $2 \times 10^{-4}$ | 1.89 |
| Concentration dependence of G values -- in the presence of $O_2$[a] | | |
| Thymine | $2 \times 10^{-3}$ | 2.76 |
| | $2 \times 10^{-4}$ | 1.89 |
| | $2 \times 10^{-5}$ | 1.23 |
| Adenine | $2 \times 10^{-3}$ | 1.10 |
| | $2 \times 10^{-4}$ | 1.09 |
| | $2 \times 10^{-5}$ | 0.65 |

a. G. Scholes, J. Ward, and J. Weiss, J. Mol. Biol. 2, 379 (1960).

Table 11-II. Nucleosides destroyed.

| Nucleoside | Concentration (moles per liter) | G |
|---|---|---|
| In the absence of $O_2$ | | |
| Adenosine | $3.8 \times 10^{-3}$ | 1.5 |
| Guanosine | $3.8 \times 10^{-3}$ | 1.3 |
| Cytidine | $4.1 \times 10^{-3}$ | 1.7 |
| Uridine | $4.1 \times 10^{-3}$ | 1.8 |
| Thymidine | $4.1 \times 10^{-3}$ | 1.7 |
| In the presence of $O_2$[a] | | |
| Adenosine | $2 \times 10^{-4}$ | 0.92 |
| Uridine | $2 \times 10^{-4}$ | 1.72 |
| Thymidine | $2 \times 10^{-4}$ | 1.75 |
| Inosine[b] | $2.5 \times 10^{-3}$ | 2.5 |

a. G. Scholes, J. Ward, and J. Weiss, J. Mol. Biol. 2, 379 (1960).
b. G. Hems, Radiation Res. 13, 777 (1960).

The sensitivity of the purine and pyrimidine nucleotides to radiation is about the same (Table 11-III). The G values for nucleotide destruction are not markedly different from those of the free bases and the nucleosides. Guanine is the only anomaly -- the free base is much more stable to radiation than the nucleoside or the nucleotide. Here, too, there seems to be no apparent oxygen effect.

We were not able to detect free sugar or sugar phosphate upon irradiation of either nucleosides or nucleotides (see Tables 11-IV and 11-V). Even the use of uniformly labeled ($^{14}C$) nucleosides and nucleotides produced no detectable radioactivity in the ribose and ribose phosphate areas. Apparently, attack upon the ribose part of the molecule is the initial event in the radiolysis of nucleosides or nucleotides. Scholes and Weiss[5] have also reported that they were unable to detect ribose or ribose phosphate in irradiated solutions of adenylic acid.

The release of phosphate (Table 11-VI) is the same for both purine and pyrimidine nucleotides. This is significantly lower than the value for nucleotides destroyed. The attack on the sugar and the base thus appears to be a major pathway in the destruction of the nucleotide molecule by free radicals generated in the irradiation of the aqueous solutions.[5]

Table 11-VII gives the G values for deamination or the conversion of the amino bases into the hydroxy bases. Adenine is converted into hypoxanthine, guanine into xanthine, and cytosine into uracil. At the nucleoside level, adenosine yields inosine, and uridine is formed from cytidine. No xanthosine, however, was detected from guanosine. Inosinic acid was formed from adenylic acid, and uridylic acid from cytidylic acid. The formation of xanthylic acid from guanylic acid was not investigated. The G value decreases from the base through the nucleoside to the nucleotide. Of the free bases, the pyrimidine cytosine appears most sensitive to this reaction.

In Tables 11-VIII and 11-IX are given the G values for two reactions of the purines -- the opening of the imidazole ring and the formation of the 8-hydroxypurines. The yield of 4, 6-diamino-5-formamidopyrimidine from adenine is considerably higher than the corresponding 2, 4-diamono-5-formamido-6-hydroxypyrimidine from guanine. Similarly, the yield of the 8-hydroxyadenine is considerably greater than that of the 8-hydroxyguanine. These results are consistent with the low G value for the destruction of guanine when the free base is irradiated.

All the reactions described here were studied at very high dose levels in order to obtain sufficient material for the identification of the products. However, if it were reasonable to extrapolate these results to low levels of radiations, they would probably have great significance in radiobiology, especially with reference to the origin of a radiation mutation.

Those reactions which would do gross damage to the replicating molecule, such as base destruction, release of sugar, etc., would no doubt be lethal. But a change that still allowed replication to take place would inevitably result in a mutation.

---

[5] G. Scholes and J. Weiss, Exptl. Cell. Res. Suppl. 2, 219 (1952).

Table 11-III. Nucleotides destroyed.

| Nucleotide | Concentration (moles per liter) | G |
|---|---|---|
| In the absence of $O_2$ | | |
| Adenylic | $2.9 \times 10^{-3}$ | 1.1 |
| Guanylic | $2.7 \times 10^{-3}$ | 1.2 |
| Cytidylic | $3.1 \times 10^{-3}$ | 1.3 |
| Uridylic | $3.1 \times 10^{-3}$ | 1.0 |
| In the presence of $O_2$[a] | | |
| Adenylic | $2 \times 10^{-4}$ | 0.75 |
| Uridylic | $2 \times 10^{-4}$ | 1.65 |

a. G. Scholes, J. Ward, and J. Weiss, J. Mol. Biol. 2, 379 (1960).

Table 11-IV. Sugar released from nucleosides and nucleotides.

| Nucleoside | Concentration (mole per liter) | G |
|---|---|---|
| Adenosine | $3.8 \times 10^{-3}$ | 0.0 |
| Guanosine | $3.8 \times 10^{-3}$ | 0.0 |
| Cytidine | $4.1 \times 10^{-3}$ | 0.0 |
| Uridine | $4.1 \times 10^{-3}$ | 0.0 |
| Thymidine | $4.1 \times 10^{-3}$ | 0.0 |
| Nucleotide | | |
| Adenylic acid | $2.9 \times 10^{-3}$ | 0.0 |
| Guanylic acid | $2.7 \times 10^{-3}$ | 0.0 |
| Cytidilic acid | $3.1 \times 10^{-3}$ | 0.0 |
| Uridylic acid | $3.1 \times 10^{-3}$ | 0.0 |

Table 11-V. Sugar phosphate released from nucleotides.

| Nucleotide | Concentration (moles per liter) | G |
|---|---|---|
| Adenylic acid | $2.9 \times 10^{-3}$ | 0.0 |
| Guanylic acid | $2.7 \times 10^{-3}$ | 0.0 |
| Cytidylic acid | $3.1 \times 10^{-3}$ | 0.0 |
| Uridylic acid | $3.1 \times 10^{-3}$ | 0.0 |

Table 11-VI. Phosphate released from nucleotides.

| Nucleotide | Concentration (moles per liter) | G |
|---|---|---|
| In the absence of $O_2$[a] | | |
| Adenosine-3'-phosphate | $2.9 \times 10^{-3}$ | 0.18 |
| Adenosine-5'-phosphate | $2.9 \times 10^{-3}$ | 0.25 |
| Cytidine-3'-phosphate | $3.1 \times 10^{-3}$ | 0.13 |
| In the presence of $O_2$[a] | | |
| Adenosine-3'-phosphate | $2.9 \times 10^{-3}$ | 0.34 |
| Adenosine-5'-phosphate | $2.9 \times 10^{-3}$ | 0.23 |
| Cytidine-3'-phosphate | $3.1 \times 10^{-3}$ | 0.36 |

a. M. Daniels, G. Scholes, and J. Weiss, J. Chem. Soc. (1956) 3771.

Table 11-VII. Deamination of amino bases to hydroxy bases in the free base, nucleoside, and nucleotide.

| | Concentration (moles per liter) | Product | G |
|---|---|---|---|
| Bases | | | |
| Adenine | $7.5 \times 10^{-3}$ | Hypoxanthine | 0.04 |
| Guanine | $0.3 \times 10^{-3}$ | Xanthine | 0.02 |
| Cytosine | $9.0 \times 10^{-3}$ | Uracil | 0.11 |
| Nucleosides | | | |
| Adenosine | $3.8 \times 10^{-3}$ | Inosine | 0.03 |
| Guanosine | $3.8 \times 10^{-3}$ | Xanthosine | 0.00 |
| Cytidine | $4.1 \times 10^{-3}$ | Uridine | 0.02 |
| Nucleotides | | | |
| Adenylic acid | $2.9 \times 10^{-3}$ | Inosinic acid | 0.01 |
| Cytidylic acid | $3.1 \times 10^{-3}$ | Uridylic acid | 0.02 |

Table 11-VIII. Opening of the imidazole ring of purine bases.

| Base | Concentration (moles per liter) | Product | G |
|---|---|---|---|
| Adenine | $7.5 \times 10^{-3}$ | 4, 6-diamino-5-formamidopyrimidine | 0.4 |
| Guanine | $0.3 \times 10^{-3}$ | 2, 4-diamino-5-formamido-6-hydroxypyrimidine | 0.002 |

Table 11-IX. Formation of 8-hydroxy purines.

| Base | Concentration (moles per liter) | Product | G |
|---|---|---|---|
| Adenine | $7.5 \times 10^{-3}$ | 8-hydroxy-adenine | 0.28 |
| Guanine | $0.3 \times 10^{-3}$ | 8-hydroxy-guanine | 0.001 |

## 12. RECOVERY OF CARBON-14 FROM THE ISOTOPE SEPARATOR (ION ACCELERATOR)

Fritz H. Woeller and Richard M. Lemmon

The isotope separator for the mass-spectral selection and acceleration of ions has been used successfully by Mullen[1] to bombard benzene with singly positive $^{14}C$ ions at energies up to 5 kV. Tracer-element projectiles or labeled targets permit submicro studies of reactions of this nature.

Carbon-14 beams near 1 μA are presently extracted from a capillary arc in which $^{14}CO_2$ is dissociated into ions. Figure 12-1 shows the vacuum system schematically. The feed gas (regulated for 11 to 13 mm pressure) enters the arc region through a fine valve. The pressure in the arc zone is of the order of 1 mm. Both beam and spent gas leave the arc section through a pinhole to enter the source with its assemblage of HV electrodes. The beam then goes through the trajectory tank to the target. A dual set of traps (T-1 and T-2 at -196°), oil diffusion pumps (DP), and forepumps (FP) maintain an operating pressure of $5 \times 10^{-6}$ to $5 \times 10^{-5}$ mm throughout source and trajectory tank. Under our usual conditiions, 0.3 mM (= 10 mCi) of 50% $^{14}CO_2$ (price, $70) per hour are fed into the system. The resulting 1-μA beam carries only $3.74 \times 10^{-8}$ mole $^{14}C$, equivalent to 2 μCi, per hour to the target. If this activity were incorporated completely and equally distributed over, say, five principal product compounds, something like a 1-h bombardment would be needed for a good quantitative evaluation. Consequently, a recovery of the isotope from the system is desirable both for economy and to minimize radioactive contamination. Very soon, however, it turned out that 80% or more of the $^{14}C$ leaves the source in the form of carbon monoxide, and its collection under the given conditions became quite a problem.

In general terms, the $^{14}CO$ must be removed from a high-speed vacuum system without restriction to the pumping capacity and also without dilution by carbon from cracked pump oils or nitrogen. As an alternative, one could economize by intermittent "static" operation through some kind of gas-feedback cycle. Mullen[1] had installed a CuO furnace at the forepump exhausts (see Fig. 12-1). He recovered 70% of the spent active material as $^{14}CO_2$, but its specific activity (sp act.) was diluted by factors of 6 or 8. Speculating that the dilution came mainly from forepump oil cracking, we tried using a CuO furnace and liquid nitrogen trap in the line between the diffusion pumps and forepumps; this part of the line is at a pressure of about 20 microns. The thin-wall stainless steel furnace had a diameter of 3 cm and an effective length of 15 cm of CuO (wire form) held at 700 to 900°. This arrangement retained 50% of the activity with a twofold dilution. In the cold trap between furnace and forepumps, liquid organic materials were condensed along with the $^{14}CO_2$. This was a sign of considerable back-diffusion from the forepumps. Another trap, facing the forepumps, might have reduced the dilution, but the recovery of 50% appeared unsatisfactory.

---

[1] Robert T. Mullen, The Chemical Interaction of Accelerated Carbon-14 Ions with Benzene, Thesis, UCRL-9603, March 14, 1961.

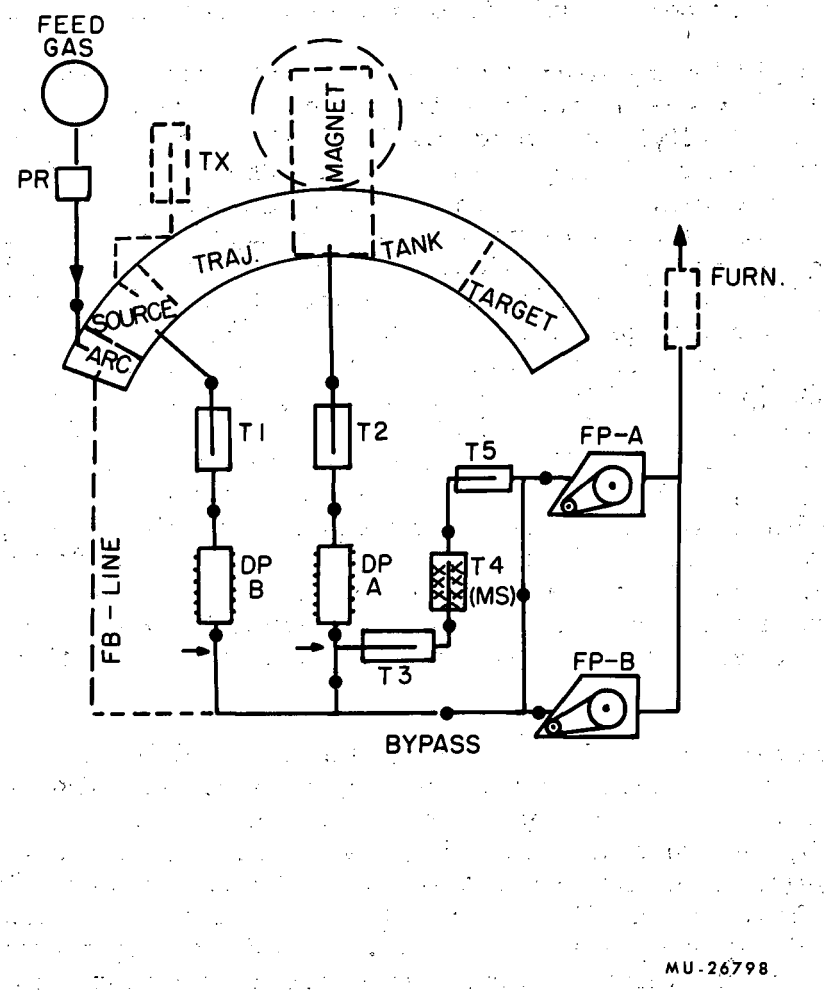


Fig. 12-1. Pumping system at isotope separator (schematic).

Undoubtedly, $^{14}CO$ was getting through the furnace. In addition, the pumping capacity of the system was reduced nearly to a critical point even by furnaces of the fairly wide diameter of 3 cm.

Then we tried two other approaches. One was a feedback line from the diffusion pump exhausts to the arc chamber (indicated by a dotted line). The proposed scheme was an intermittent pumping down of the system, followed by a cyclic operation in which the diffusion pumps would "crowd" the gas towards the arc. This method failed for two reasons. Firstly, the diffusion pump exhaust pressure of 20 μ was too low for maintenance of the capillary arc plasma. Secondly, the vacuum system was not built with a specific emphasis on static operation, and atmospheric leakage is too high with the current design.

We then decided to try a liquid-helium trap acting as a "pump" in a system of suitable size connected to the arc chamber. The trap was connected as shown in Fig. 12-1 by (TX) through a copper line of 2.5 $cm^2$ cross section. The pumping capacity of this combination turned out to be completely inadequate; our misconception was quickly realized after the following calculations were made. With 0.3 mM per hour of feed gas (disregarding any leakage from the outside), the quantities to be conducted through the system would be as shown.

| pressure (mm Hg) | liters/sec of $CO_2$, CO plus $O_2$ (at 80% conversion) |
|---|---|
| 760 | $3 \times 10^{-6}$ |
| $20 \times 10^{-3}$ (forepumps) | 0.1 |
| $10^{-5}$ (high vacuum side) | 200 |

[ The two diffusion pumps (DP) are rated at 1000 liters/sec total. ]

It happens that $10^{-5}$ mm is the upper limit at which a beam can be sustained without glow discharge and collapse of the HV system. Our liquid-helium trap arrangement was capable of conveying [2] only
(11.6 liters/$cm^2$/sec) × (2.5 $cm^2$) = 29 liters/sec.
To use a liquid helium "pump," one would have to insert a device offering a considerable surface area (say, 50 $cm^2$) directly into the trajectory tank.[3] Such a redesign would be exceedingly expensive, would be expensive to operate, and would present additional handling problems in collecting the condensed gas.

The best chance for a satisfactory compromise still appeared to be some sort of interception within the 20-μ pressure line between diffusion pumps and forepumps, even though this would mean a greater risk of dilution by $^{12}C$ and $^{14}N$. Before experimenting with liquid helium any further, we began to think in terms of molecular sieves held at -196°.

[2] A. Guthrie and R. K. Wakerling, Vacuum Equipment and Techniques (McGraw-Hill Book Co. Inc., New York, 1949), p. 20.

[3] A. Guthrie and R. K. Wakerling, op. cit.; Section 1.20 was used as a basis for this estimation.

A 15-in.-tall, three-stage trap of thin brass (represented by T-3, T-4, and T-5 in the figure) was constructed as a removable compact unit that could be immersed into one large Dewar. The trap sections T-3 and T-5 are concentric tubes, where each has an effective cross section of about 1.2 $cm^2$ throughout. The compartment T-4 has an outer tube of 7.5 cm diameter charged with 1/16 in. granules of Molecular Sieve 4-A and a 1/2 in. i.d. inner tube leading to the bottom. The three sections are separated by 1/2 in. Kerotest valves.

At 20 μ pressure, the only gases expected to reach T-4 from either side are CO, $CH_4$, $C_2H_6$, $N_2$, and $O_2$. The remaining question was how efficient the adsorption on molecular sieve would be in this highly dynamic system. The results of two experiments are shown in Table 12-I.

Table 12-I. Recovery experiments with Molecular Sieve 4-A.

| Test no.[a] | Grams of 1/16 in. m. s. | Percentage recovered[a] from traps T-1 and T-2 | from m. s. ($O_2$ wash) | retention on m. s. | Sp act. from m. s. (μCi/mg)[b] |
|---|---|---|---|---|---|
| 1 | 500 | 10 | 43 | -- | 9.1 |
| 2 | 1000 | 11 | 50 | 12 | 8.6 |

a. of total activity fed into the arc
b. starting material, sp act.: 10.4 μCi/mg

From traps T-1 and T-2 was recovered the carbon dioxide part of the spent gas. After the whole trap unit was taken off, the CO collected in T-4 was swept out by an $O_2$ stream for 16 hours while the trap was heated by infra-red lamps to above 100°. A tube furnace with CuO granules (600°) and two NaOH bubblers was checked for completeness of the conversion to carbonate. The retention on the adsorbent was estimated by scintillation counting of suspensions. The overall recovery in Test 2 was better than 60% of the activity (not counting the material retained on the molecular sieve) with only 20% dilution. There is reason to believe that this procedure can give even greater recoveries, while the dilution can probably be reduced even more if T-3 is also made a molecular sieve cell. Although the trap was made of brass for reasons of economy, liquid nitrogen evaporation was less than 1 gallon per hour. The trap arrangement was found to have no deleterious effect on pumping speeds.

The quantity of 1000 grams of molecular sieve, used in a stationary system, would be sufficient to adsorb on the order of 0.5 mole of diatomic gases, as estimated from a few isotherms available.[4] This is an amount of gas one thousand times as large as we are tyring to collect in one run of the accelerator. The retention then comes as no surprise; however, after the oxygen-sweep operation, no activation step (in which $C^{14}$ might be lost) is necessary to ready the trap. It remains to be seen, what the relative retention will be upon repeated use.

[4] Linde Company, Division of Union Carbide Corporation, New York 17 N. Y.: Molecular Sieve Isotherm data sheets Nos. 30, 51, 62, and 63 (1959) and direct communication, May 1962.

sa

This report was prepared as an account of Government sponsored work. Neither the United States, nor the Commission, nor any person acting on behalf of the Commission:

A. Makes any warranty or representation, expressed or implied, with respect to the accuracy, completeness, or usefulness of the information contained in this report, or that the use of any information, apparatus, method, or process disclosed in this report may not infringe privately owned rights; or

B. Assumes any liabilities with respect to the use of, or for damages resulting from the use of any information, apparatus, method, or process disclosed in this report.

As used in the above, "person acting on behalf of the Commission" includes any employee or contractor of the Commission, or employee of such contractor, to the extent that such employee or contractor of the Commission, or employee of such contractor prepares, disseminates, or provides access to, any information pursuant to his employment or contract with the Commission, or his employment with such contractor.